



**SINTEF** Petroleumsforskning AS  
SINTEF Petroleum Research

N-7465 Trondheim, Norway

Telephone: +47 73 59 11 00  
Fax: +47 73 59 11 02 (aut.)

Enterprise no.:  
NO 936 882 331 MVA

# REPORT

TITLE

**Reservoir geology of the storage units in the Sleipner CO<sub>2</sub>-injection case**  
– A contribution to the Saline Aquifer CO<sub>2</sub> Storage (SACS) project

AUTHOR(S)

Peter Zweigel, Ane E. Lothe, Rob Arts, Martin Hamborg

CLASSIFICATION

Confidential

CLIENT(S)

Den Norske Stats Oljeselskap (Statoil)  
Norges Forskningsråd, KLIMATEK Program  
SACS Consortium

REPORT NO.

23.4285.00/02/00

REG. NO.

2000.072

DATE

18 December, 2000

PROJECT MANAGER

Peter Zweigel

SIGN.

*Peter Zweigel*

NO. OF PAGES

79

NO. OF APPENDICES

3

LINE MANAGER

Grethe Schei

SIGN.

*Grethe Schei*

SUMMARY

The reservoir for the ongoing CO<sub>2</sub> injection in the Sleipner CO<sub>2</sub> storage project has been mapped and analysed in the area close to the injection facility based on seismics, well data, and rock samples. Two reservoir units have been identified, the Utsira Sand proper and a sand wedge within the lowermost part of the Nordland Shale. Maps are provided, which characterize the topography of these reservoir units.

The Utsira Sand contains thin shale layers that affect CO<sub>2</sub> migration. The net/gross ratio of the Utsira Sand ranges from 0.90 to 0.97. Porosity ranges from 27% to 41% with a dominance of values between 35% and 40%. Use of approx. 30% for worst-case scenarios is recommended. Reservoir parameters seem to be relatively constant within the sand, but there exist indirect indications for some reservoir heterogeneity, which may affect the CO<sub>2</sub> migration pattern.

Mud mobilisation at the base Utsira causes structuring of the intra Utsira shale layers and of the reservoir top. Anticlines and domes in the area of survey ST98M11 represent a total trap volume of 0.135 km<sup>3</sup>, corresponding to a theoretical storage efficiency of 0.3%.

Seismic amplitude anomalies at the top Utsira indicate probably the presence of some shallow gas in structural traps. The lack of abundance of these indicators may, however, signify the lack of a suitable retention capacity which may cause problems for CO<sub>2</sub> storage.

KEYWORDS ENGLISH

Carbon dioxide storage  
Reservoir geology  
Sleipner Field  
North Sea

KEYWORDS NORWEGIAN

Karbondioksyddeponering  
Reservoargeologi  
Sleipnerfeltet  
Nordsjøen

## **Authors, Institutes, and Addresses**

*Ane Lothe, Peter Zweigel*  
Seismics and Formation Physics Department

*Martin Hamborg*  
Basin Modelling Department

### **SINTEF Petroleum Research AS**

S.P. Andersens vei 15 B  
7465 Trondheim  
Norway

Tel.: (+47) 7359 1100

Fax: (+47) 7359 1102

<http://www.iku.sintef.no>

*Rob Arts*  
Department of Geo-Energy

### **Netherlands Institute of Applied Geoscience TNO - National Geological Survey**

Prins Hendriklaan 105  
P.O. Box 80015  
3508 TA Utrecht  
The Netherlands

Tel.: (+31) 30 256 46 38

Fax: (+31) 30 256 46 05

<http://www.nitg.tno.nl>

## Table of Contents

<b>1. Preface .....</b>	<b>4</b>
<b>2. Executive Summary .....</b>	<b>5</b>
<b>3. Project background and aim .....</b>	<b>7</b>
<b>4. Previous work and regional geological frame.....</b>	<b>9</b>
<b>5. Reservoir geometry .....</b>	<b>13</b>
5.1 Reservoir base / base Utsira Sand.....	15
5.2 Reservoir top / top Utsira Sand.....	26
5.3 Sand wedge in the cap rock.....	35
5.4 Reservoir internal barrier horizons .....	41
5.4.1 Geometry of reservoir-internal shale layers.....	41
5.4.2 Deformation of reservoir-internal shale layers .....	48
<b>6. Reservoir properties.....</b>	<b>50</b>
6.1 Reservoir parameters from logs and samples .....	50
6.1.1 Porosity .....	50
6.1.2 Net/Gross ratio.....	52
6.2 Observations on seismic data.....	54
6.2.1 Amplitude anomalies within and at the top of the sand units.....	54
6.2.2 Sand wedge heterogeneity .....	62
<b>7. Discussion .....</b>	<b>65</b>
7.1 Available storage volume.....	65
7.2 Sweep efficiency .....	67
7.3 Seal efficacy .....	68
<b>8. Outlook/ Open questions.....</b>	<b>70</b>
<b>9. Quoted references.....</b>	<b>71</b>
<b>Appendix 1 -- Determination of intra-Utsira shale layer thicknesses .....</b>	<b>74</b>
<b>Appendix 2 -- Amplitude anomalies in the Utsira Sand.....</b>	<b>76</b>
<b>Appendix 3 -- Horizon grids in 3D view .....</b>	<b>79</b>

## 1. Preface

This report documents results of work on the storage properties of the Utsira Sand in the Sleipner area, i.e. predominantly in block 15/9. This work is an integrated part of Work Area 1 'Reservoir Geology' of the Saline Aquifer CO<sub>2</sub> Storage project (SACS). Funding of the research documented here was provided by the industry- and EU-funded main SACS-project and - through an accompanying project – by the KLIMATEK program of the Norwegian Research Council.

We rate distribution of a documentation of our results to the project partners as desirable, because these results will be – and have already been - used as input for other activities within the SACS project. Documentation in a report will allow critical examination and correct application of the results by other project participants.

Documentation of our results is possible now because planned work on local aspects of the reservoir formation in the Sleipner CO<sub>2</sub> injection case has been nearly finished. We consider it unlikely that major improvements will take place within the ongoing SACS-projects, given the data situation and the agreed work plans. However, continuing interpretation of time-lapse seismic data may provide a refined picture of the reservoir geology in the direct neighbourhood of the injection site. Similarly, insights from regional geological investigations may allow further conclusions on local scale. These expected future results will be documented separately.

The present report covers only the probable storage units (the Utsira Sand and a sand wedge a few meters above). The assessment of the sealing efficacy of the cap rock sequence in the Sleipner area is going on and will be documented separately.

## 2. Executive Summary

The reservoir for the ongoing CO<sub>2</sub> injection in the Sleipner CO<sub>2</sub> storage project has been mapped and analysed in the area close to the injection facility. This work is based on selected regional 2D seismic lines, the 3D seismic cube ST98M11, wire-line log data from 22 wells, cuttings, and on the single existing core from the Utsira Sand.

The reservoir consists of two reservoir units: the Utsira Sand itself and an eastward thickening sand-wedge in the separated by a 5 m thick shale layer from the Utsira Sand. These units are overlain by the more than 100 m thick, shaly part of the Nordland Shale.

Top and base of the Utsira Sand and the top of the sand wedge have been mapped in 3D seismics (top and base Utsira in 2D seismics in a larger area, too), aided and constrained by information from wire-line logs. These three horizons have been depth converted in the 3D area and are, thus, available for volume calculations, migration and reservoir simulations etc.

Reflectors within the Utsira sand have been traced in selected lines in 3D seismics. These reflectors correspond probably to thin (approx. 1 m thick) shale layers that can be identified in wire-line log data. The reflectors approach base Utsira towards west, possibly reflecting sediment transport from east.

Porosity has been determined based on rock samples and wire-line log data (esp. density log) and ranges from 27 % to 41%. Values between 35 and 40 % may be representative for the overall porosity, but we recommend use of lower values (e.g. 30%) for 'worst case' calculations. The ratio of net sand thickness to gross unit thickness (Net/Gross ratio) ranges from 0.90 to 0.97. These values may, however, have low importance for the storage potential of the Utsira Sand, because gravity driven CO<sub>2</sub> accumulations will occupy the uppermost part of the unit only (Zweigel et al. 2000a) where the unit consists solely of sand.

Mud edifices at the base of the Utsira Sand have been investigated. They are partly mud volcanoes with mud outflows into the Utsira Sand, but the majority of them are pop-up structures, displacing the base Utsira Sand by up to 60 m (vertical component). Both, mud volcanoes and pop-ups, were generated synchronous to deposition of the lower part of the Utsira Sand. Pronounced compaction of the shales in the edifices led to local subsidence anomalies and an inverted topography already during deposition of the upper part of the Utsira Sand: local basins existed then above the mud edifices.

The subsidence anomalies caused a structuring of the top Utsira Sand with domes and anticlines linked by saddles. These structures provide now traps for CO<sub>2</sub>. The total trap volume in the area of survey ST98M11 is 0.135 km<sup>3</sup> (at 30% porosity and a storage efficiency of 85 %), which corresponds to a storage efficiency of 0.3%. However, only a fraction of this can be used for storage in a realistic injection scenario with a limited number of injection wells. The results confirm, thus, the previous general estimation of a total storage efficiency of traps of ca. 0.12% in Holloway et al. (1996).

Localised subsidence caused deformation of the reservoir-internal, thin shale-layers, too. Strain is small (usually below +1% longitudinal strain) and it is expected that the rocks were still ductile during deformation and, thus, could compensate this strain largely without brittle failure. However, migration of CO<sub>2</sub> through the shale layers as evident from time-lapse seismic data shows that they exhibit pathways.

The sand wedge in the lowermost part of the Nordland Shales contains probably a paleo-channel. This indicates that lithological heterogeneity - and thus heterogeneity of reservoir parameters - is likely within the sand wedge. Similar depositional features could be present in the Utsira Sand, but may be difficult to detect.

Analysis of wire-line log data suggests that the Utsira Sand may be very homogeneous within individual sand layers. Reservoir parameters (porosity, permeability, etc.) could, thus, be nearly homogeneous and the potential effect of their variability on the flow pattern could be small. However, if features such as channels were present (which may be difficult to identify both in wells and in seismics), reservoir heterogeneity would be expected. Seismic amplitude anomalies at the reservoir top may indicate some heterogeneity, because they are not always located at the crests of structural traps, which would be expected for gravity-driven accumulations of gas.

Some reservoir heterogeneity is caused by the fill of localised basins above compacted mud edifices. These basins are, however, in structural low positions (depressions of top Utsira) and the heterogeneity there will accordingly not much affect the migration of CO<sub>2</sub> through linked positive structural features.

The occurrence of seismic amplitude anomalies, which probably signify the presence of shallow gas, in some structural traps indicates a certain retention capacity of the overlying shales. The mapped anomalies cover, however, only a small fraction of the total trap surface. If abundant gas has been supplied from below (e.g. leaking from the Sleipner gas fields underneath), larger accumulations would be expected. The lack of these large accumulations may imply the lack of a suitable retention capacity, which may compromise CO<sub>2</sub>-storage safety.

### 3. Project background and aim

CO<sub>2</sub> separated from produced natural gas in the Sleipner Vest field (Norwegian block 15/9, Northern North Sea; Figure 3.1) is being injected into sands of the Utsira Formation - a shallow, saline aquifer in the direct neighbourhood of the production platform, above the Sleipner Øst field - to prohibit emission to the atmosphere (Baklid et al. 1996). Ongoing injection activities are accompanied by the 'Saline Aquifer CO<sub>2</sub> Storage' research project (SACS), which is mainly devoted to the prediction and monitoring of the distribution of injected CO<sub>2</sub>.

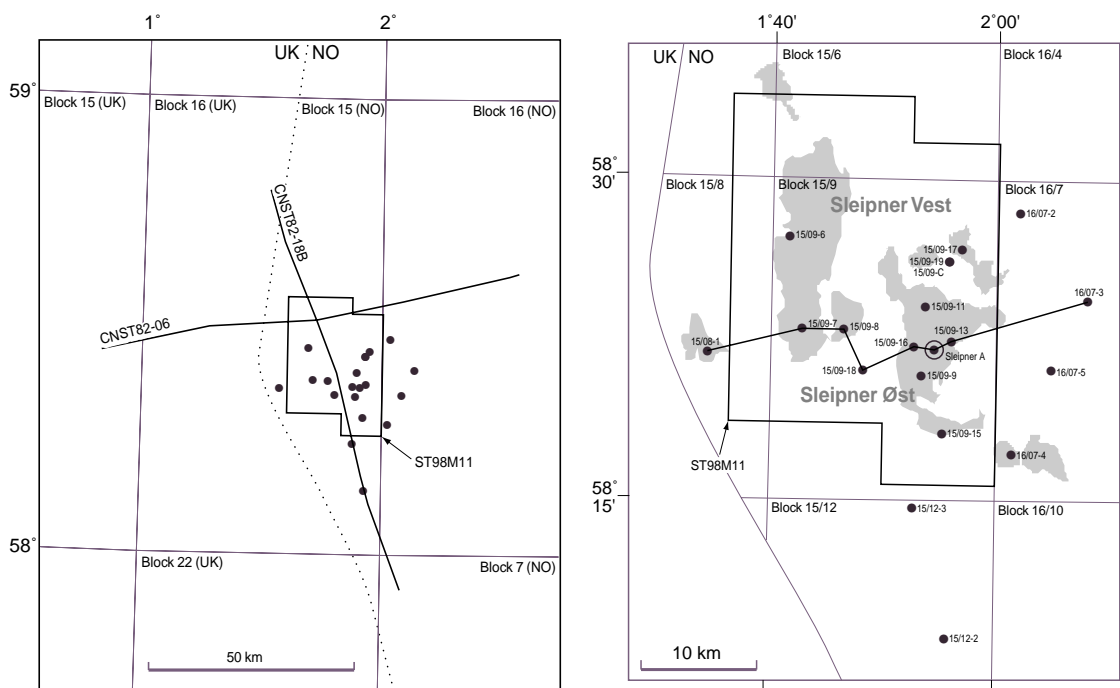


Figure 3.1 Left: overview map, showing position of 3D survey ST98M11, wells, and extent of the two 2D seismic lines shown in Figure 4.1. Right: Position of individual wells, the well section shown in Figure Figure 5.2, and the 3D seismic survey in relation to the Sleipner Vest and Sleipner Øst fields.

The results presented here are part of the efforts in the SACS project to characterise the CO<sub>2</sub> storage unit. We concentrated on the Sleipner area, and reservoir characterisation in this case has predominantly the purpose to improve the geological input for predictions of the future distribution of CO<sub>2</sub> and, thus, ultimately to aid an assessment of the safety of the storage site. Our results served already as input for reservoir modelling (partly documented in Lindeberg et al. 2000a) and for migration modelling by means of a secondary hydrocarbon migration modelling tool (Zweigel et al. 2000a). Further information about the reservoir geology is expected from ongoing work in SACS Work Area 5 'Geophysical Monitoring', where a detailed analysis of the time-lapse survey may yield an improved knowledge about the shape of reservoir-internal barriers and the spatial distribution of reservoir properties in the neighbourhood of the injection site.

Several reservoir properties will have an influence on the distribution of injected CO<sub>2</sub>. These are, *inter alia*:

- The topography of the reservoir top; this will guide buoyancy-driven migration below the seal and will define the shape and size of traps.
- The presence, permeability and topography of reservoir-internal migration barriers. These barriers will mainly affect vertical migration above the injection site, but they will also affect the filling pattern of traps and the conditions for potential Rayleigh convection (Lindeberg & Wessel-Berg 1997) and they may constitute minor traps.
- Reservoir porosity and its spatial variation, defining the space available for CO<sub>2</sub> during migration and trapping.
- Reservoir permeability and its spatial variation. Permeability strongly defines the migration velocity, and spatial differences in permeability may affect the migration pattern, e.g. high permeable zones will be preferred pathways leaving low permeable zones unpenetrated, thus reducing the available storage volume and increasing the maximum migration distance.
- The Net/Gross ratio and sweep efficiency, which define the available and accessible part of the pore space.
- Connections to other storage units in the neighbourhood, such as sand bodies within the cap rock.

Moreover, data from a detailed geological investigation on the local scale may allow inferences regarding the depositional environment of the Utsira Sand in general. These interpretations can then be used to predict reservoir properties in other areas where data coverage is less dense.

We do not address properties of the cap rock in the present report. It is being treated below as impermeable in general with the exception of the possibility of leakage into a sand body close to its base. The assessment of the integrity of the cap rock is the topic of a separate SINTEF report, which is in preparation.

SINTEF Petroleum Research's work in this NFR/KLIMATEK-funded project flanking the main SACS activities overlap thematically with activities in the main, EU- and industry-funded project, carried out by NITG-TNO and ourselves (local aspects) and BGS and GEUS (regional aspects). Some of the results reported below have, therefore, already been reported elsewhere within the SACS project (e.g. Gregersen et al. 1998, Lothe & Zweigel 1999, Holloway et al. 2000, Arts et al. 2000; Zweigel et al. 2000a).

#### 4. Previous work and regional geological frame

The Utsira Formation has been defined by Degan & Scull (1977) as the first thick sand unit below the Pliocene to recent deposits in the central parts of the Northern North Sea. Further definitions and subdivisions were mainly done by Isaksen & Tonstad (1989) and Gregersen et al. (1997). Eidvin et al. (1999) provided a recent age determination, assigning a (late) Middle Miocene age (ca. 10 Myr) to the base and an earliest Late Pliocene age (ca. 3 Myr) to the top.

The local geology of the Utsira Formation in the Sleipner area has been the topic of work within the SACS project, and results are documented in Gregersen et al. (1998), Lothe & Zweigel (1999), and Holloway et al. (2000).

A major conclusion of these works is that the Utsira Formation seems in the Sleipner area only to be represented by sands. It is, however, difficult to assess if the shales directly above the Utsira Sands in the Sleipner area are correlative to those shales that in the type well (16/1-1; Degan & Scull 1977, Isaksen & Tonstad 1989) were taken to constitute the upper part of the Utsira Formation. BGS and GEUS identified a 'regional shale drape' above the Utsira Sands in the Sleipner area (Holloway et al. 2000, Chadwick et al. 2000). This is a unit that is characterised on 2D seismics by reflectors parallel to the top Utsira Sand reflector, in contrast to the overlying shale package which has clinoformal geometries at the basin margins indicating progradation from the east and west (Figure 4.1). Further, Lothe & Zweigel (1999) report their interpretation of 2D seismic data that the uppermost part of Utsira Sands in the Sleipner area may correspond to a prograding shale unit in Norwegian block 25.

A clear depth localisation of the top Utsira Formation in the Sleipner area, keeping to the definition of the Utsira Formation in its type well, is thus difficult. Since the SACS project is predominantly concerned with the highly porous and highly permeable (i.e. sandy) part of the Utsira Formation, this stratigraphic question is here considered to be of subordinate importance. To avoid misinterpretations, we will in the following use the terminus *Utsira Sands*, which we define in the Sleipner area as the unit in the Mio-Pliocene that consists predominantly of sand. The top of the Utsira Sands is reached when shales occur above the sand package that can be correlated on a distance of a few km to the thick shale package of the Plio-Pleistocene. A sand wedge in the eastern part of the Sleipner area, which is underlain by shales that can be correlated to the base of the thick shale package in the west, is consequently not part of the Utsira Sands as defined here (see Lothe & Zweigel 1999). This definition is in line with our interest in hydrological units within the SACS project.

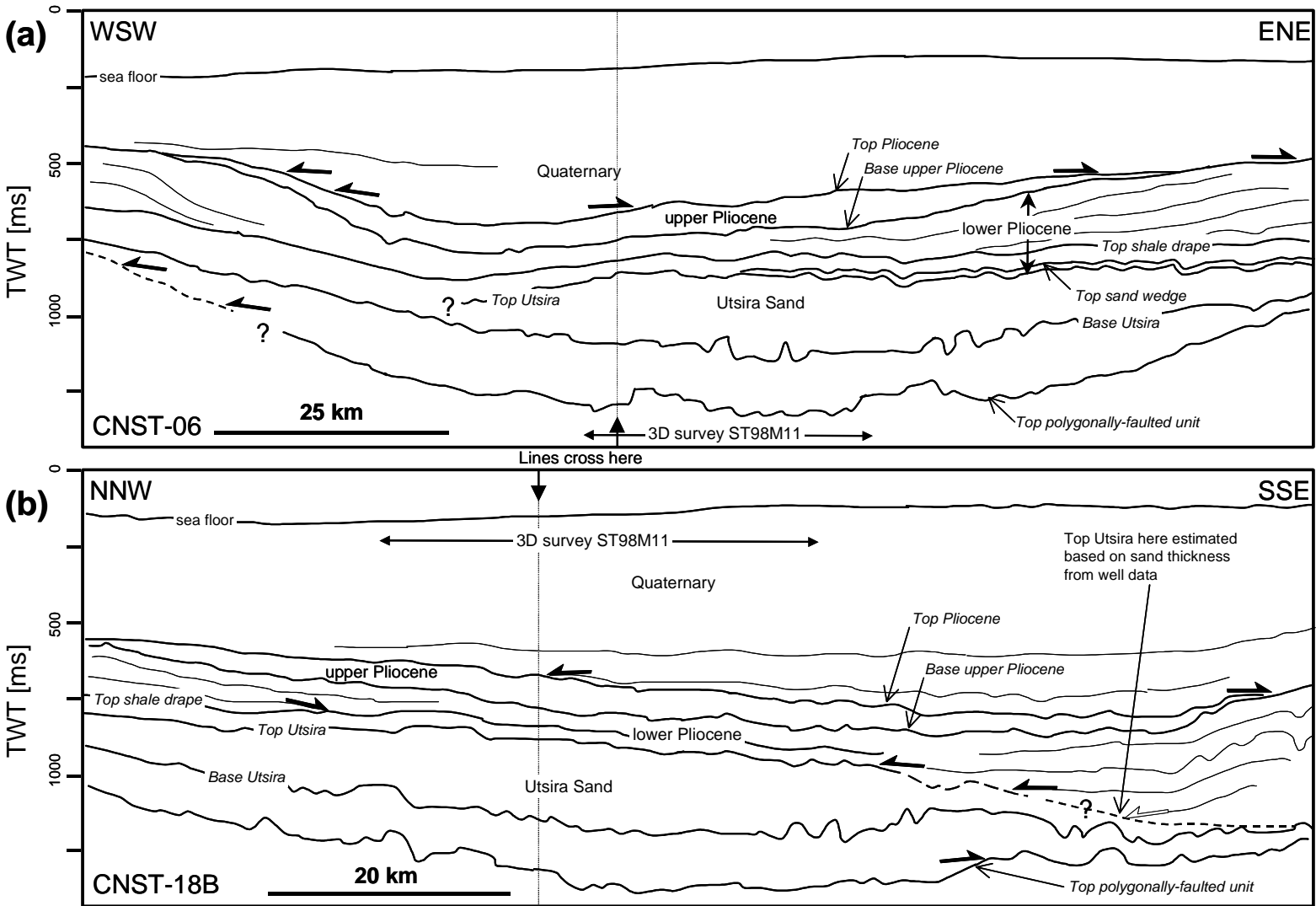


**Figure 4.1** Line-drawings of 2D regional sections covering the Sleipner area. (a) W-E section (CNST82-06) (b) N-S section (CNST82-18B). Position see Figure 3.1. Interpretations are by SINTEF and may differ in detail from the regional interpretations of BGS and GEUS.

The Sleipner area is the location of the depocentre of the Utsira Sand (Gregersen et al. 1997, Chadwick et al. 2000). Locally, the Utsira Sand reaches its maximum thickness (306 ms corresponding to ca. 315m) in the northern part of block 15/9 (Figure 4.2c). The top Utsira Sand has a general tendency of deepening towards south (Fig. Figure 4.2b; Lothe & Zweigel 1999, Holloway et al. 2000), whereas the base exhibits a slightly elongate, NE-SW-striking depression in the Sleipner area (Figure 4.2a; see also Lothe & Zweigel 1999). More details on the local topography will be provided in the next chapter.

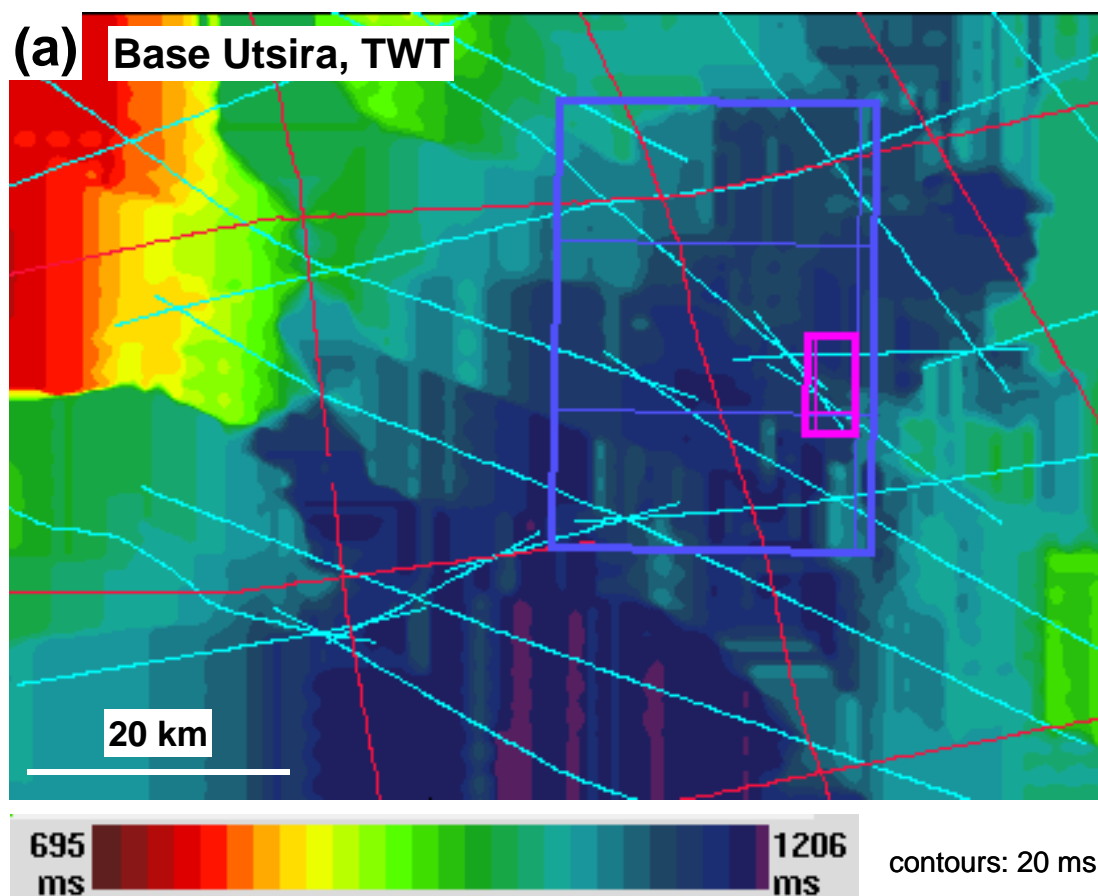


Figure 4.2 (a) TWT-map of base Utsira, NEXT PAGE: (b) TWT- map of top Utsira; and (c) TWT- map of the thickness of the Utsira Sand in the surrounding of block 15/9, based on interpretation of 2D seismic lines. Red and pale blue lines are seismic lines used in interpretation (red: survey CNST82, pale blue: survey VGST89). Large rectangle in right half of figures: area of 3D survey ST98M11; small rectangle: area of time-lapse survey ST9906.

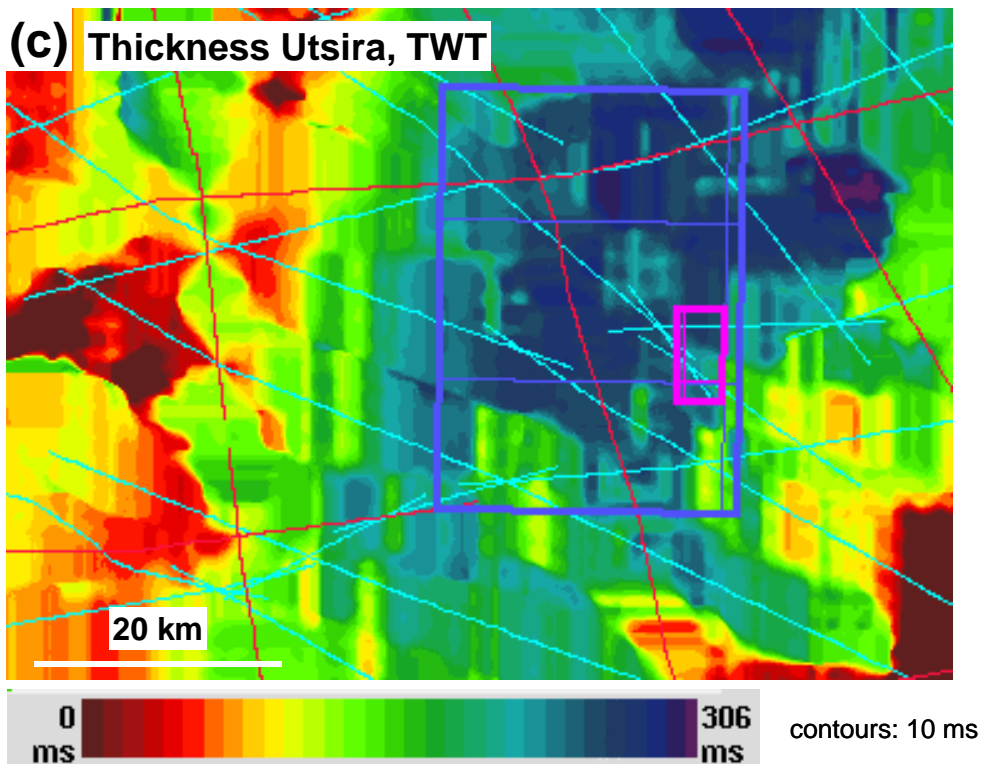
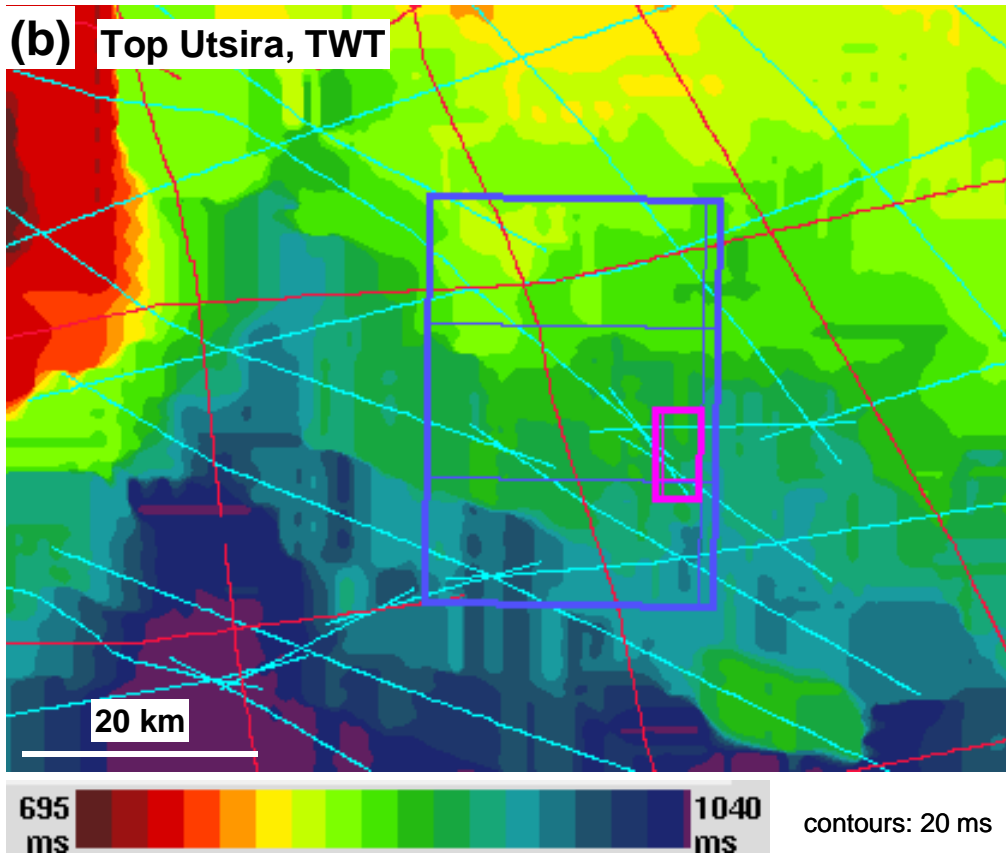
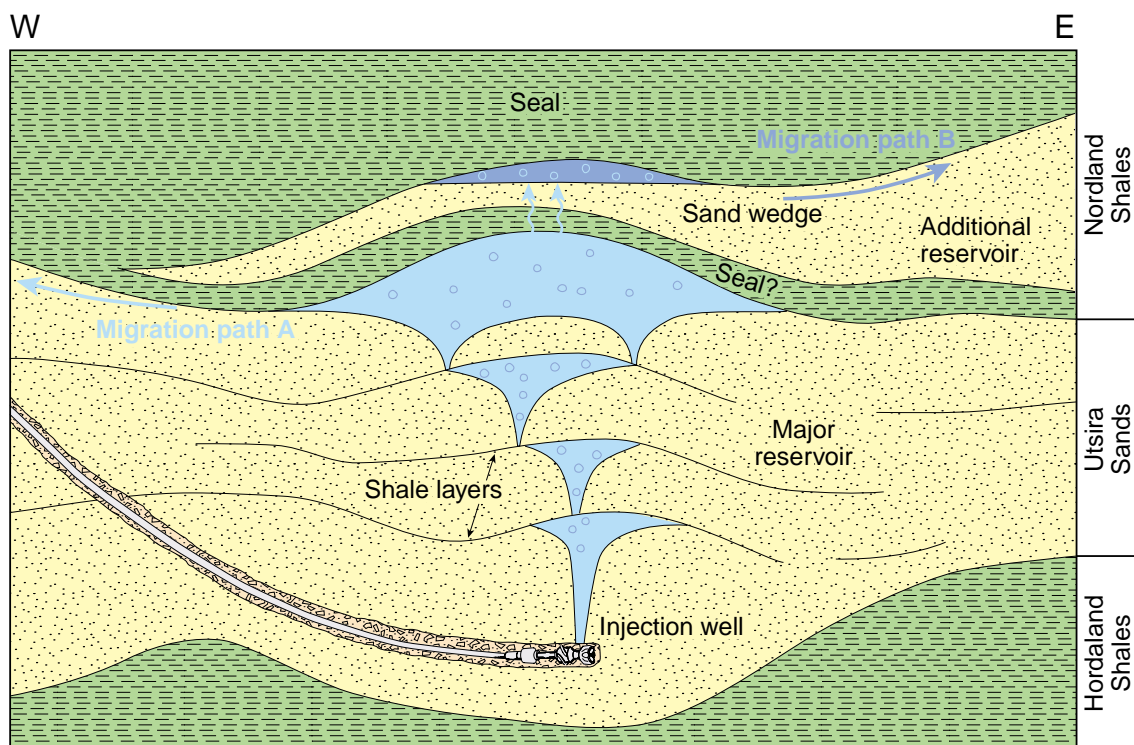


Figure 4.2 Continued from previous page.

## 5. Reservoir geometry

The CO<sub>2</sub> storage reservoir in the Sleipner case consists of the Utsira Sands and a sand-wedge within the lowermost parts of the Nordland Shales (Figure 5.1). The Utsira Sand is overlain by a unit (the Nordland Shales) that can be subdivided into several sub-units based on seismic facies, log characteristics, and depositional geometries (Gregersen et al. 1997, 1998, Lothe & Zweigel 1999, Holloway et al. 2000), but which for several hundred meters of thickness comprise almost exclusively pelitic sediments (Figure 5.2). In the eastern part of the study area, a pelitic layer of ca. 5 m thickness separates an eastward thickening sand wedge within the Nordland Shales from the Utsira Sands. Migration of CO<sub>2</sub> into this sand wedge is indicated by seismic anomalies in the 1999 time-lapse survey (Figure 5.30). The top and base of the Utsira Sands, and the geometry of the sand wedge will be described in detail below.



*Figure 5.1 Schematic representation of the storage system: CO<sub>2</sub> is injected close to the base of the Utsira Sand, in which it will migrate upwards, affected by thin intra-Utsira shale layers. The Utsira Sand is overlain by a thick shale package, the Nordland Shale, which is regarded to act as a seal. The CO<sub>2</sub> is, thus, expected to primarily accumulate below the top Utsira Sand, to fill structural traps, and to migrate laterally below that horizon, driven by buoyancy. Leakage into a sand wedge 5 m above the base of the Nordland Shale may be possible, with consequent accumulation and lateral migration below the top of that sand wedge. Heights and thicknesses are not at scale.*

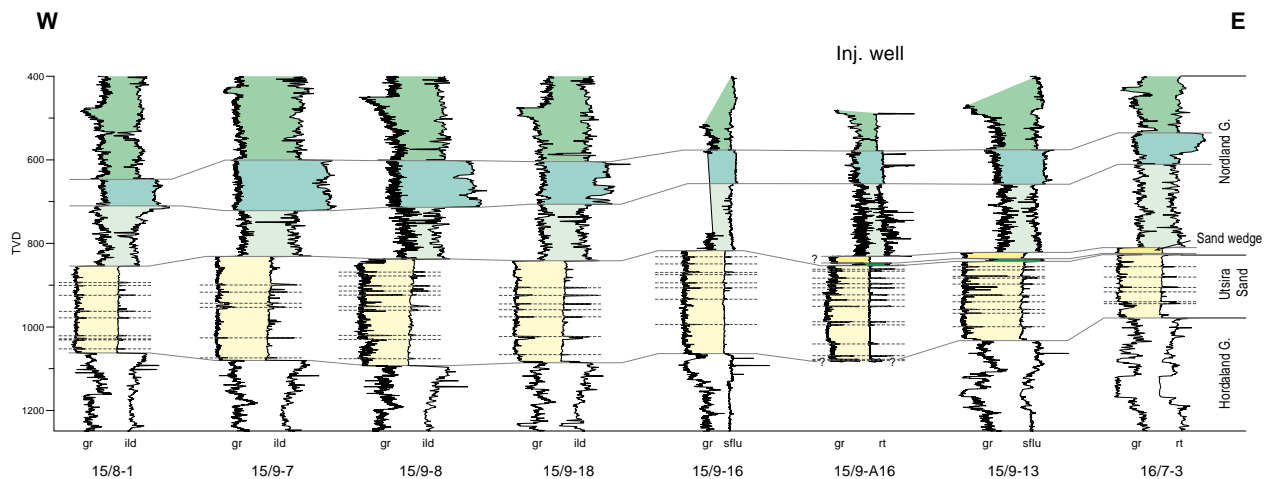


*Figure 5.2 W-E-oriented well profile through the Utsira Sand and its cap rock in the Sleipner area. Note the log peaks within the Utsira Sand, interpreted to indicate the presence of thin shale layers, and the occurrence of a westward disappearing sand wedge in the lowermost part of the cap rock sequence.*

CO<sub>2</sub> flow within the reservoir may be affected by reservoir-internal permeability heterogeneities, e.g. by the presence of flow barriers (low permeability zones). The Utsira Sands contain several thin shale layers, which probably have low permeability and which are likely the cause for CO<sub>2</sub> accumulations that led to reservoir-internal seismic anomalies in the 1999 time-lapse survey (Figure 5.30). Moreover, the sands may exhibit laterally changing reservoir properties. The shale layers are described and discussed below, as are the indications for layer parallel homogeneity versus heterogeneity of the sands.

Since this report is predominantly concerned with the storage reservoir itself, the cap rock (the Nordland Shales) will not be dealt with, with the exception of the potential storage unit within the lowermost cap rock sequence. For simplicity, it will be assumed below that the cap rock is impermeable for CO<sub>2</sub>, the only exception being that the possibility of migration of CO<sub>2</sub> into the sand wedge within the Nordland Shale will be considered. These assumptions will be discussed in a separate report, which addresses the cap rock integrity.

Much of the results presented below rest on interpretations reported in Lothe & Zweigel (1999) which was, however, of preliminary and rather descriptive character. Where necessary, work from that report will be included below - mostly without expressed reference.

The topography of mapped horizons is presented below mainly in two-way travel time (TWT). Depth values (in m) are slightly lower than the TWT values, because the overburden has in the mean an acoustic velocity below 2000 m/s (Table 5.1). Where depths are of special importance, converted values are given below. Note, however, that the relative topography of mapped horizons, e.g. the shape and size of traps, is not affected much by the time-depth conversion, because the pelitic sediments directly

above the Utsira Sand and the Utsira Sand itself have acoustic velocities of nearly 2000 m/s.

*Table 5.1 Interval acoustic velocities (p-wave) used in time-depth conversion (Arts 2000). <sup>(1)</sup> The high water velocity is due to tracking of a too shallow reflector, which had, however, the correct seismic signature. Note that the sand wedge was neglected during time-depth conversion; i.e. all the interval between top Utsira Sand and the Intra-Pliocene reflector was treated as having a uniform acoustic velocity of 2077 m/s.*

Unit name	Top of unit	Base of unit	Interval velocity (m/s)
Water	Mean sea level	Sea floor <sup>(1)</sup>	1659 <sup>(1)</sup>
Quaternary	Sea floor	Top upper Pliocene shales	1785
upper Pliocene shale unit	Top upper Pliocene shales	Intra-Pliocene reflector	2208
lower Pliocene shale unit	Intra-Pliocene reflector	Top Utsira Sand	2077
Utsira Sand	Top Utsira Sand	Base Utsira Sand	2056

<sup>(1)</sup> The high water velocity is due to tracking of a too shallow reflector, which had, however, the correct seismic signature.

## 5.1 Reservoir base / base Utsira Sand

The base of the Utsira Sand poses a definition problem: the base of the Utsira Sand – considered as a reservoir unit – is not always the base of the stratigraphic unit ‘Utsira Sand’ or ‘Utsira Formation’. In large areas of the occurrence of the Utsira Formation or the Utsira Sand, its base is a stratiform contact sand over shale. In some areas, however, this initial contact has been destroyed by diapirism and expulsion of muds from the underlying shale unit. Shale mounds formed there contemporaneously to deposition of sands in the surrounding (Lothe & Zweigel 1999). The base of the reservoir unit at these mounds is again the occurrence of sands above shales; this base is, however, often younger than the reservoir base away from the mounds, and it is of varying age on top of the mounds (Figure 5.3). We mapped the reservoir base instead of the stratigraphic base of the Utsira Sands because we are interested in the sands as a hydrological unit.

### *Boundary characteristics*

Both, outside and on top of the mud mounds, the base of the Utsira Sands is characterized in wire-line logs by a strong downward increase in gamma-ray, induction and resistivity, and sonic velocity (Figure 5.4). Density does also often show a small, punctuated increase towards the shales; it decreases then, however, often rapidly downhole within the shales. In some cases, gamma-ray log patterns are not unequivocal, e.g. exhibiting low GR-values below a layer of elevated GR-values (e.g. well 15/9-16 in Figure 5.2). Then, the induction and/or resistivity logs were used for determination of the base Utsira: values within the sand of the Utsira Sand are very constant and a marked deviation over more than a few meter depth was taken to signal presence of the Hordaland Shale. This interpretation is in line with mud logs from

production wells from Sleipner A, which show the depth of base Utsira always where we interpreted it based on the combination of gamma ray, induction, and resistivity logs.

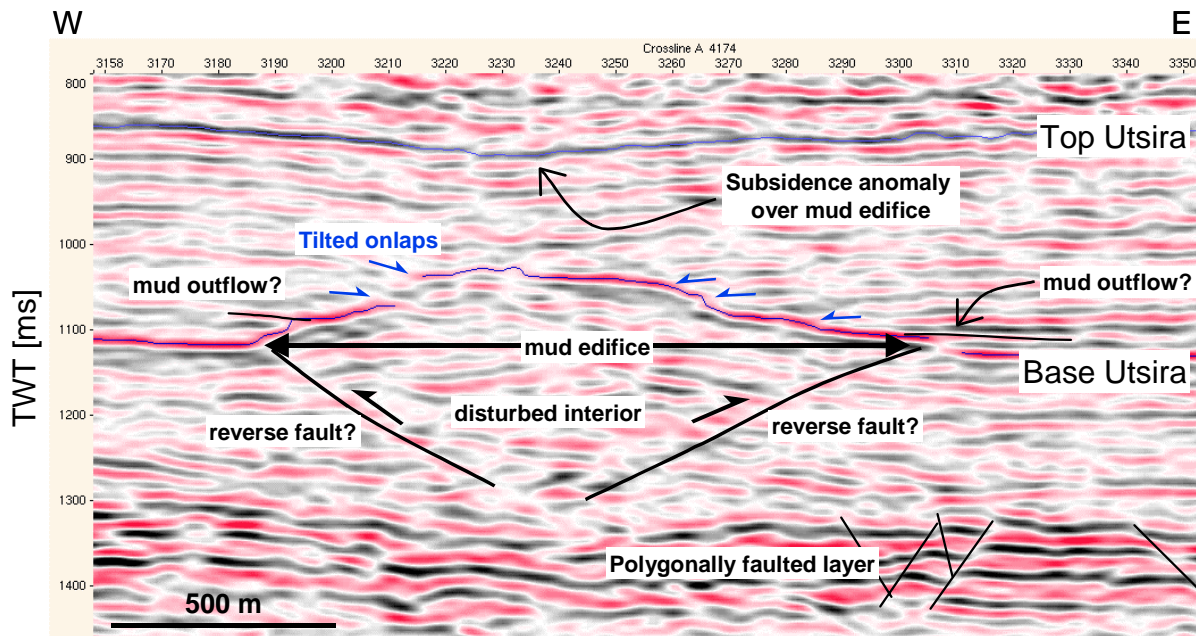
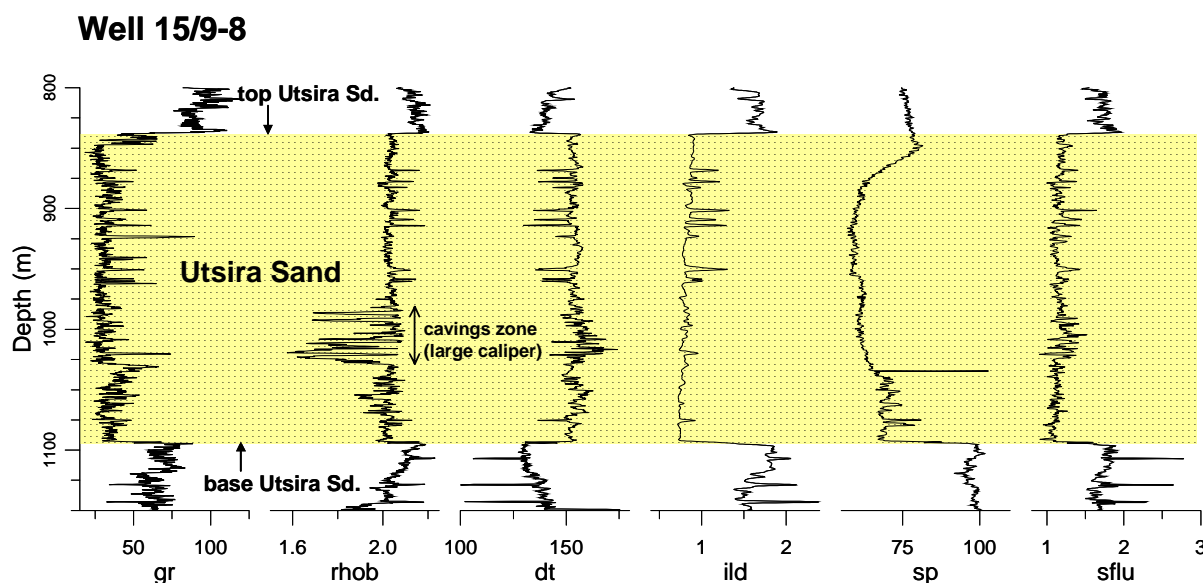


Figure 5.3 Piece of seismic crossline 4174 from survey ST98M11, showing a mound-shaped mud edifice at the base Utsira Sand. Indicated features such as tilted onlaps, marginal faults etc. are typical for most of the mud edifices and are discussed in the text.

The downward increase in acoustic velocity (and density) across the base Utsira Sand causes it to constitute a boundary with a positive reflection coefficient. The resulting reflector has an amplitude which is much above those of the surrounding (Figure 5.3). The 2D seismics inspected (surveys CNST-82 and VGST-89 in this region) are of minimum phase and normal SEG polarity. The base Utsira Sand corresponds, thus, to the zero crossing above an amplitude trough. For convenience, the maximum of the peak directly above this zero crossing was picked, yielding a slightly (ca. 10 ms) too high position of the interpreted boundary, resulting in a slightly too low thickness of the Utsira Sand. The 3D seismic survey ST98M11 is zero-phase and of normal SEG polarity, such that the base Utsira Sand corresponds to the maximum of a peak, which was traced.

For more details on the interpretation methodology, e.g. tracing of reflectors at mounds, refer to Lothe & Zweigel (1999).



*Figure 5.4 Wire-line logs from well 15/9-18. The Utsira Sand, its top and its base, are unequivocally identifiable from log data. Note also that many of the intra-Utsira high GR peaks have correspondences on many of the other logs, indicating that most of these peaks are due to the presence of shales (as opposed to glauconite-rich sands). GR: Gamma-ray, rhob: bulk density, dt: sonic log, ild: induction log, sp: self potential, sflu: spherically focused log (resistivity).*

The base Utsira Sand constitutes a reflector against which toplap of underlying reflectors occurs in the western part of the studied area (Figure 5.5). This shows truncation of previously deposited strata and may signify that the base Utsira is an unconformity at regional scale.

### *Horizon topography*

Semi-regional interpretation of 2D seismic lines shows that the base Utsira Sand in the Sleipner area forms a slightly elongate, NE-striking depression, being a bay-shaped extension of a larger depression in the south (Figure 4.2a). The 3D seismic survey ST98M11 (Figure 5.6a, [Appendix 3](#)) covers large parts of the deepest area of this bay, but contains in its northwestern part some of the slope of the bay, too. The base Utsira Sand in the 3D survey exhibits, thus, a general deepening from the northwestern corner (ca. 970 ms TWT, i.e. ca. 900 m) towards south (ca. 1180 ms TWT or 1120 m). Note, however, that the relatively steep gradient at the northwestern corner of the 3D area is not regionally representative, but is the combined effect of regional dip and the southeastern flank of a local elevation (possibly caused by mud mobilisation, see below; Figure 4.1a).

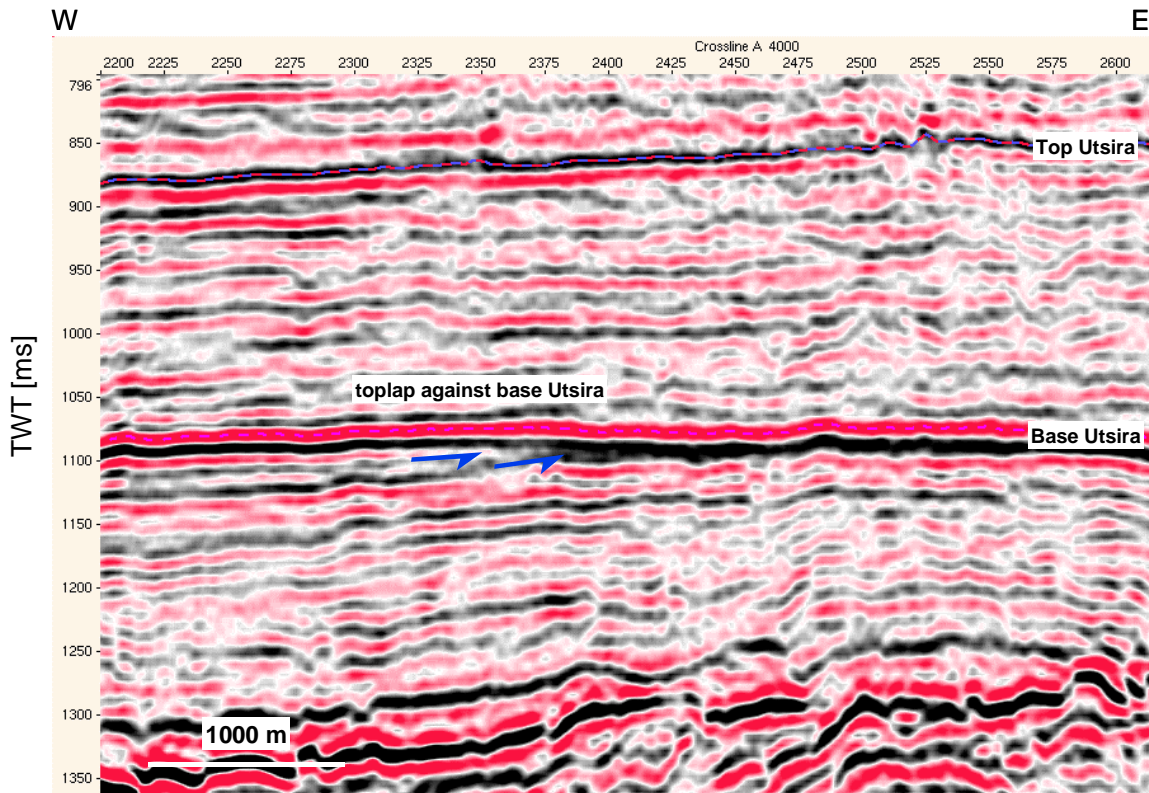


Figure 5.5 Reflectors beneath base Utsira tolap against this horizon. This section (crossline 4000) is from the western part of survey ST98M11.

On both, 2D and 3D seismic sections, the base Utsira Sand is characterised by the existence of mounds which modify the general dip of the surface locally. The height of these mounds is typically ca 100 ms TWT, corresponding to ca. 100 m (Figure 5.3). In map view (Figure 5.6a), these mounds constitute isolated, nearly circular domes or irregularly elongated bodies with varying orientations, and in one case observed they form a ring or polygon. This multitude of shapes, lacking a preferred orientation is in contrast to statements of Heggland (1997) and Gregersen et al. (1997) who reported and/or interpreted elongated bodies with their long axis striking NE or parallel to the basin axis (N to NE), respectively. The diameter of the mounds is usually ca. 1 to 2 km, and the length of elongated bodies is up to more than 10 km. Lothe & Zweigel (1999) provide a more detailed description of the mounds. Further work to characterize these structures is under way as a SINTEF project involving a diploma thesis at the Norwegian University of Science and Technology (NTNU).

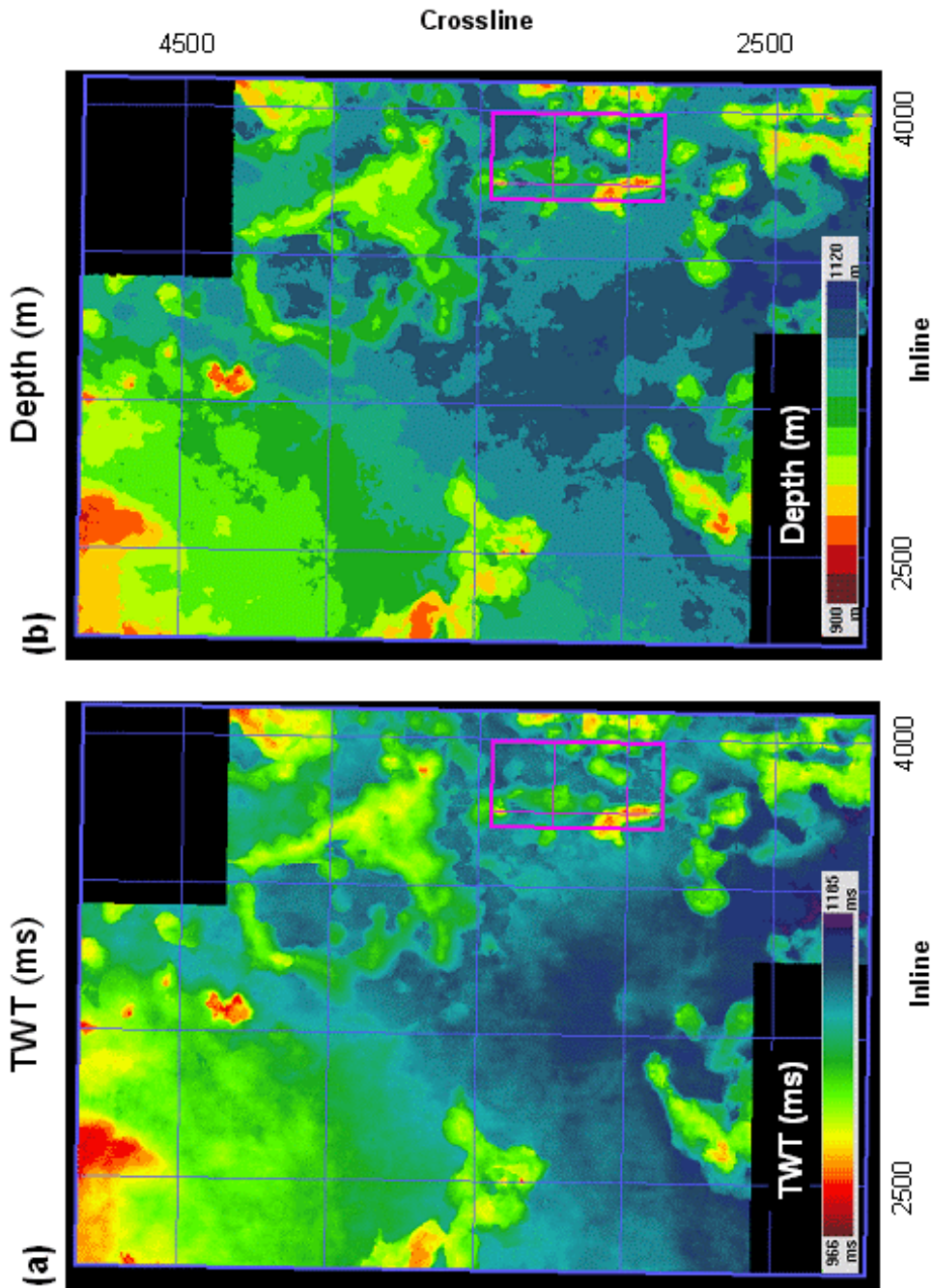
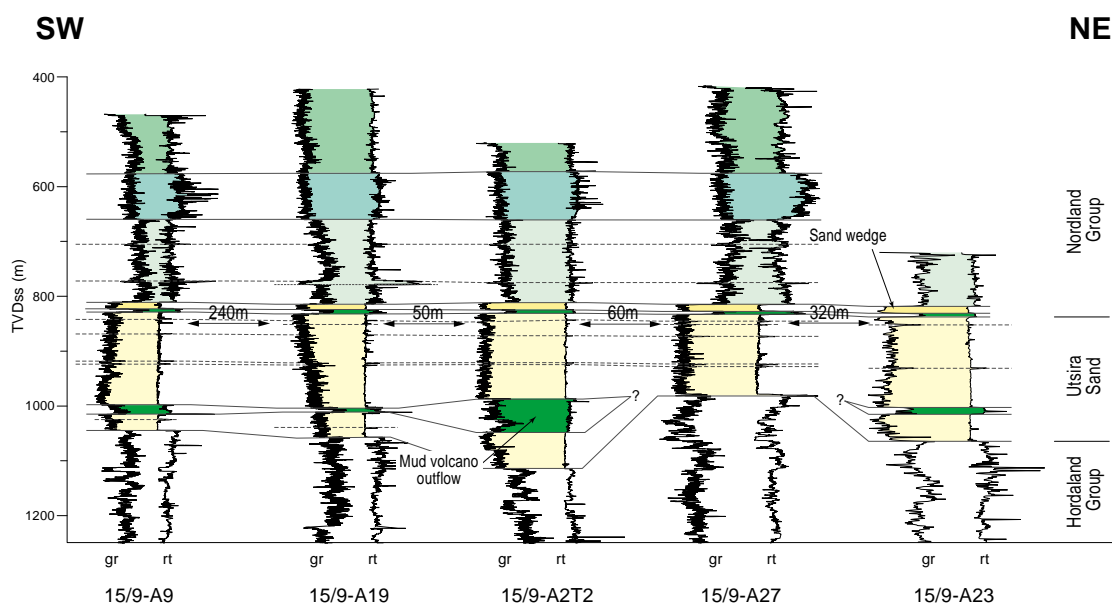


Figure 5.6 Topography of the base Utsira Sand reflector in the area of the 3D seismic survey ST98M11. (a) in two-way travel time, (b) in depth. The distance between 500 lines corresponds to 6.25 km. Colours change every 20 m on the depth figure. The violet rectangle in the centre at the right side is the area of the 1999 time-lapse survey (ST9906). The white rectangle denotes the outline of Figure 5.10b. Note the presence of variously shaped positive topographic features (mud edifices).

In accordance with Heggland (1997) do we interpret the mounds as mud diapirs and mud volcanoes, i.e. as sites where mobilisation of the underlying Hordaland shales locally uplifted the base Utsira Sand (diapirs) and/or led to ejection and localised deposition of fluidised mud at the base of, and interlayered with, the Utsira Sands (volcanoes). Post-depositional mobilisation of muddy sediments of this stratigraphic interval is a known feature from large parts of the northern North Sea (recent publications are, e.g., Jordt et al. 1996, Løseth et al. 1999, Rundberg & Nystuen 1999) but has not yet been described in much detail.

We interpret the continuation of reflectors at some of the mounds, from the top and the flanks of mounds (where they have high amplitudes) into the interior of the Utsira Sand (where they become soon as weak as 'normal' intra-Utsira reflectors) as indications of an extent of the sand-shale contact into the Utsira Sand (Figure 5.3). This entails the presence of mud-sheets in the surroundings of, and fed by, the mud volcanoes, a feature illustrated in wells situated at the margin of a mud volcano (Figure 5.7). Our interpretation implies, thus, activity of the volcanoes during deposition of the lower part of the Utsira Formation.



*Figure 5.7 Wire-line log section of closely spaced wells penetrating through the Utsira Sand in the neighbourhood of a mud edifice. Note the presence of a thick (up to 46 m) mud package surrounded by sand. The wire-line log based interpretation of the base Utsira in, e.g., well 15/9-A2T2 is in line with the mud log. We interpret the mud package as representing an outflow of a mud volcano.*

The present shape (total height) of the mounds does not correspond to their height as positive topographic features during Utsira Sand deposition. Topography then was likely much less. The present total height is interpreted to be due to superposition of several phases of mud rise and mud outflow. Attempts to reconstruct the mud edifice topography through time are part of an ongoing diploma project supervised by SINTEF personnel and results will be reported later.

We interpret downward flexure of strata overlying the mounds (Figure 5.3) as indication for stronger compaction of the mounds than of the surrounding (Figure 5.8). Such increased compaction can be explained as a consequence of the different lithology: disturbed, possibly gas-rich muds in the mounds versus regularly deposited, undisturbed sands in the surrounding. This anomalous compaction took place already during deposition of the (upper part of the) Utsira Sands (see Chapter 5.4) and continued until deposition of the lower parts of the overlying Nordland Shales (see Chapter 5.2)

Many of the mud edifices show evidence for faulting. Figure 5.9 illustrates one example where the whole mound seems to consist of an uplifted cone. There, seismics show that the top portion of the uplifted part has the same reflector pattern as the upper part of the Hordaland shales outside the edifice. In most other cases (e.g. Figure 5.3), the interior of the mounds is much more disturbed. However, in these cases, too, reverse faults often occur at the feet and the margins of the mud edifices. These faults dip towards the centre of the mounds with dip angles ranging from ca. 14° to 23° (Figure 5.3) and have vertical heaves of up to ca. 60 m (corresponding to displacements of up to ca. 155 m).

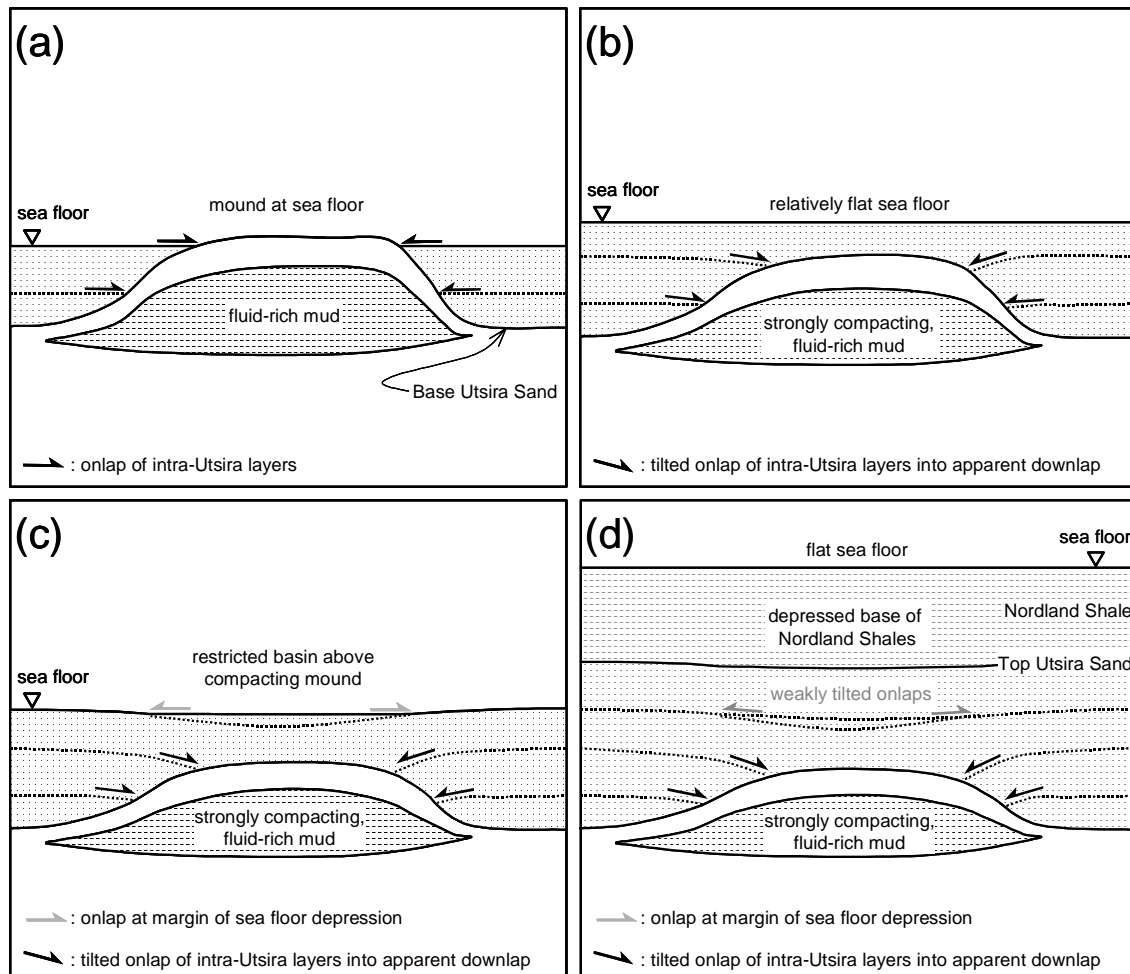
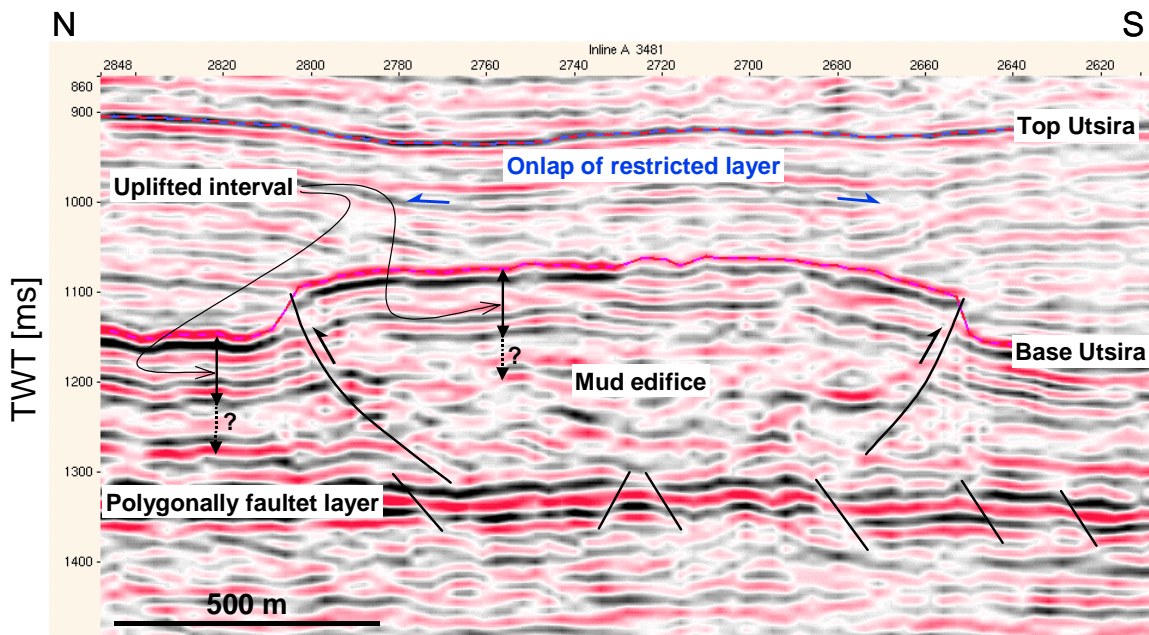


Figure 5.8 Schematic illustration of the effects on the overburden caused by pronounced compaction of mud mound material. (a) Disturbed, potentially gas-rich muds are present in the mounds. (b) Stronger compaction of the mud in the mounds compared to that of the mud and sand in the surroundings causes rotation of initially horizontal strata, a dip of the strata towards the centre of the mounds, and a rotation of horizontal onlaps into apparent downlaps. (c) Continued localised subsidence after termination of mud flow creates local depressions which are filled by deposits of laterally restricted occurrence. (d) Further localised subsidence after termination of Utsira Sand deposition causes deflection of the lower parts of the Nordland Shales.



*Figure 5.9 Piece of seismic inline 3481 illustrating a ‘pop-up’ mud edifice, being bounded by reverse faults which define a roughly conical base of the edifice. Note the identical seismic characteristics of the top part of the shales within and outside the mud edifice. Faults do not continue into the Utsira Sand above the top-level of the uplifted shales. The polygonally faulted high-amplitude layer has not been affected by the reverse faults.*

The reverse faults are evident from the presence of packages on both sides of the fault which have identical reflector patterns, but are displaced with respect to each other (Figure 5.3). These internally undisturbed packages are usually up ca. 80 m to 100 m thick and correspond to a layer of relatively high gamma ray values and relatively high, but often downward decreasing acoustic velocities. They are underlain by a unit that is mostly strongly disturbed within the mud edifices and that exhibits often lower gamma ray and lower acoustic velocities outside the mud edifices. We expect that the presence of a stronger rock package (strength indicated by higher acoustic velocity and by lacking internal disturbance) underlain by a weaker one played an important role during the process of mud mount generation (see, e.g. similarities in Davies et al. 1999).

Faulting of the base Utsira Sand outside the mud edifices has only rarely been observed and if, then only with small displacements of a few ms. The only major exception is a structure surrounded by the ring shaped mound assemblage in the north-eastern part of the study area. There, a circular piece of the base Utsira Sand has been tilted and uplifted along a cone-shaped, downward-closing reverse fault (system) (Figure 5.10). This may be an initial stadium of an edifice like the one shown in Figure 5.9.

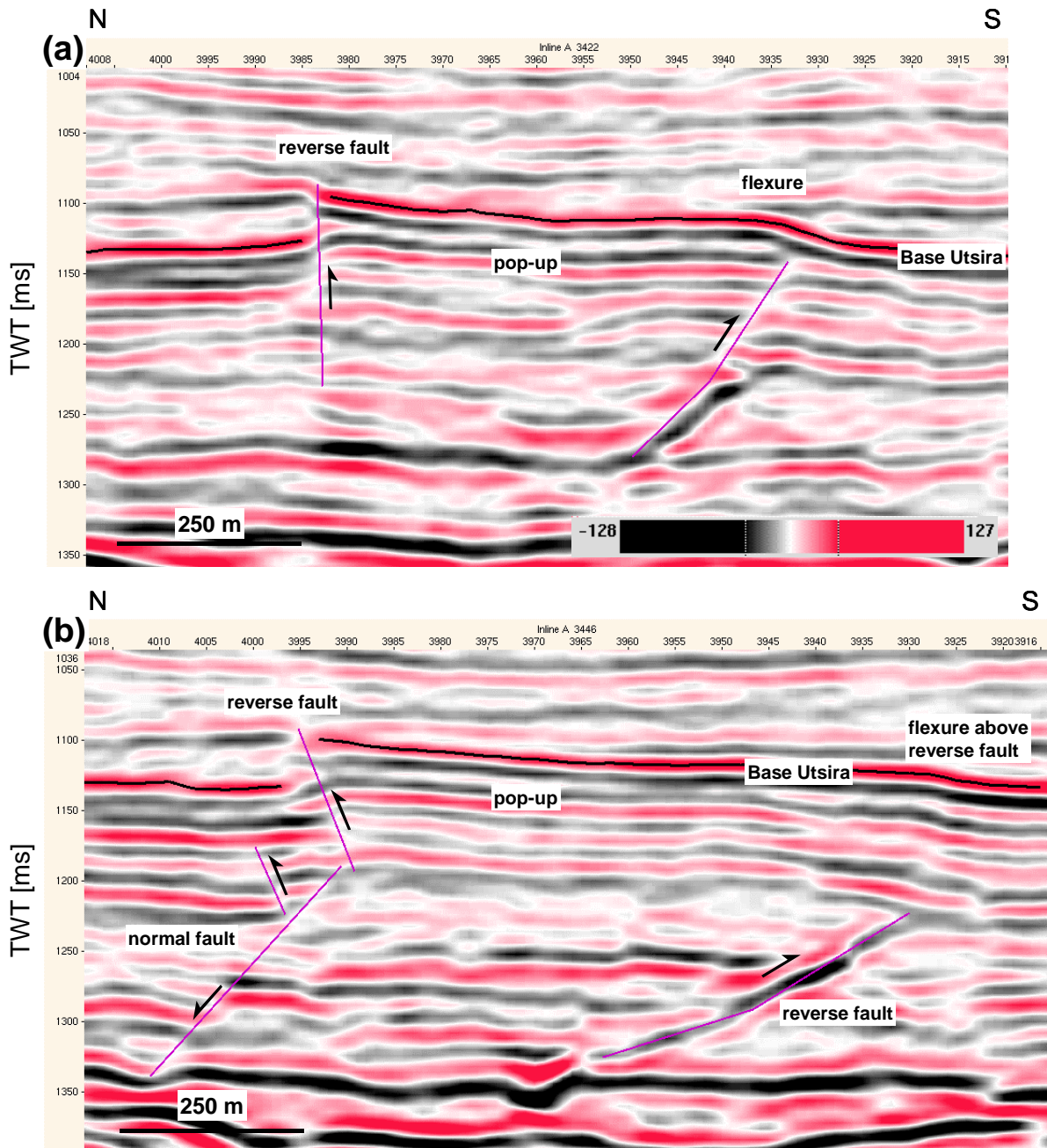


Figure 5.10 Small ‘pop-up’ mud edifice located in the centre of the ring-shaped mud mounds in the northern half of survey ST98M11 (for localisation see Figure 5.6). (a) and (b) Seismic sections through the structure. NEXT PAGE: (c) Map of the base Utsira Sand which is uplifted at a strongly bent, half-conically shaped reverse fault in the NW and flexed in the SE. Line A and Line B indicate positions of sections in figure parts (a) and (b), respectively.

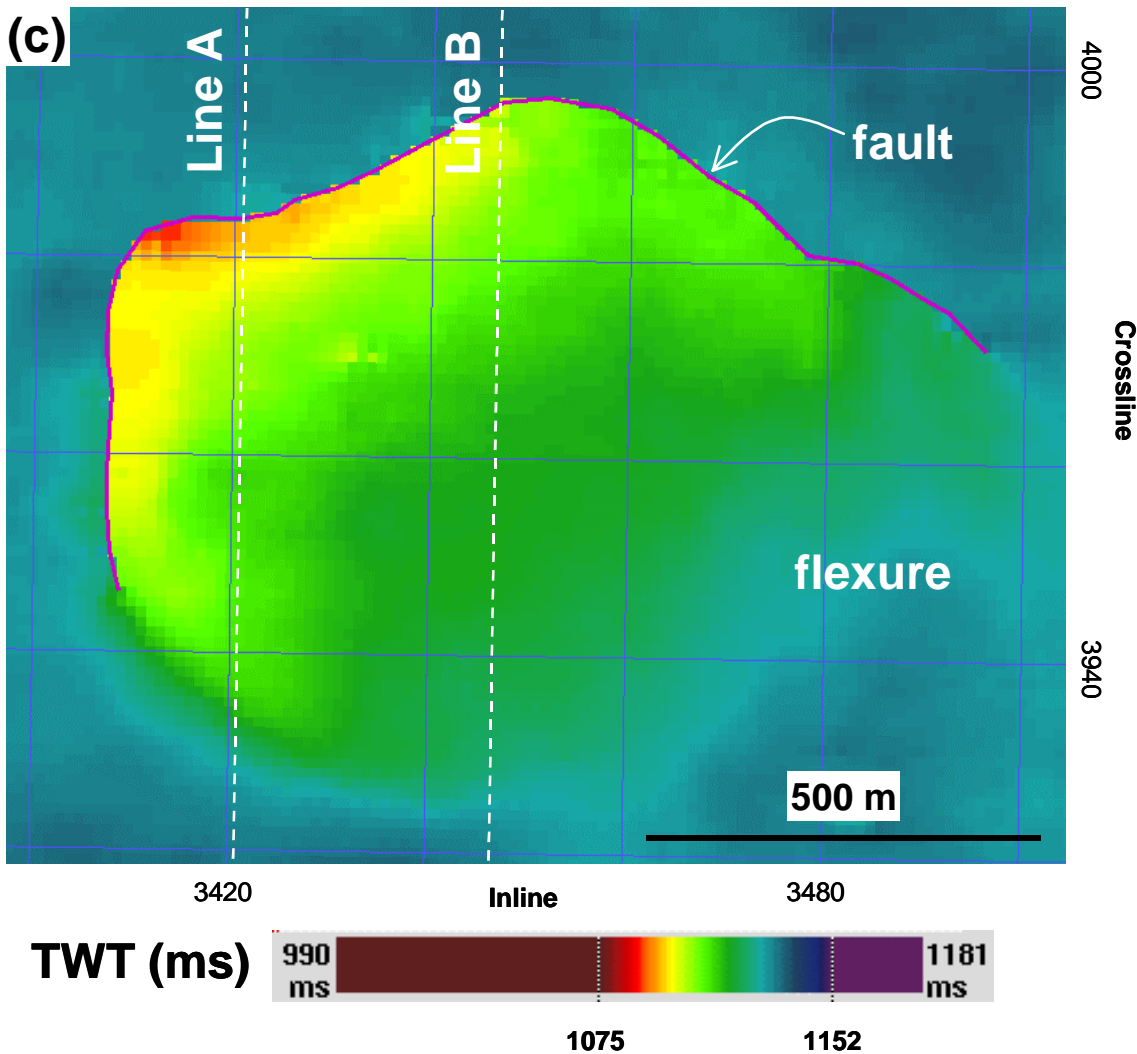


Figure 5.10 Continued from previous page.

All the observed faults affect mainly the Hordaland Shales up to the base Utsira Sand and if they rarely extend into the Utsira Sand themselves, they are limited to the lowermost part of the sands. They are, therefore, interpreted to have formed during the earliest stages of Utsira Sand deposition. Their spatial and temporal link to the mud mounds suggests a genetic relationship between the reverse faults and the mounds.

The occurrence of reverse faults indicates horizontal contraction. The cause for this contraction is not yet known. It could be due to tectonics, however, then the faults should exhibit preferred orientations, which they seem not to do. Other explanations could be volume-increase of the shales underlying the Utsira Sand (opposite to the processes leading to polygonal normal fault networks such as in Cartwright & Lonergan 1996, and visible in a layer ca. 200 ms below the base Utsira Sand, Figure 5.3), subsidence anomalies (see, e.g., Odonne et al. 1999), or as a response to material flow underneath (Figure 5.11).

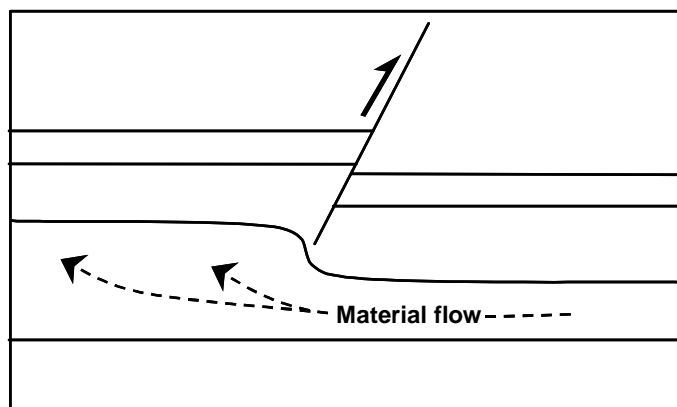


Figure 5.11 Schematic figure showing generation of reverse faults by material flow of, e.g., an underlying mud sequence.

## 5.2 Reservoir top / top Utsira Sand

### *Boundary characteristics*

The top of the Utsira Sand is characterized by a strong downward decrease in gamma-ray logs, induction and resistivity logs, sonic velocity and sometimes density (Figure 5.4). It is easily detectable in all studied wells.

The downward decrease in acoustic velocity (and density) across the top Utsira Sand causes it to constitute a boundary with a negative reflection coefficient. The resulting reflector has usually an amplitude that is stronger than those of the surroundings. The 2D seismics inspected (surveys CNST-82 and VGST-89 in this region) are of minimum phase and normal SEG polarity. The top Utsira Sand corresponds, thus, to the zero crossing above an amplitude peak, which was traced. The 3D seismic survey ST98M11 is zero-phase and of normal SEG polarity, such that the base Utsira Sand corresponds to the maximum of a trough (Figure 5.3), which was traced.

### *Horizon topography*

Semi-regional interpretation of 2D seismic lines reveals that the top Utsira Sand in the surrounding of the Sleipner area has a general dip towards S or SSE (Figure 4.2b). A ca. 10 km wide, north-striking depression of the top Utsira Sand exists directly west of the UK-Norwegian median line.

Within the area of the 3D seismic survey ST98M11, the top Utsira Sand follows the semi-regional trend of southward-deepening, with the exception of the northern part, where a local high causes a southeastward dip (Figure 5.12; [Appendix 3](#)). The general

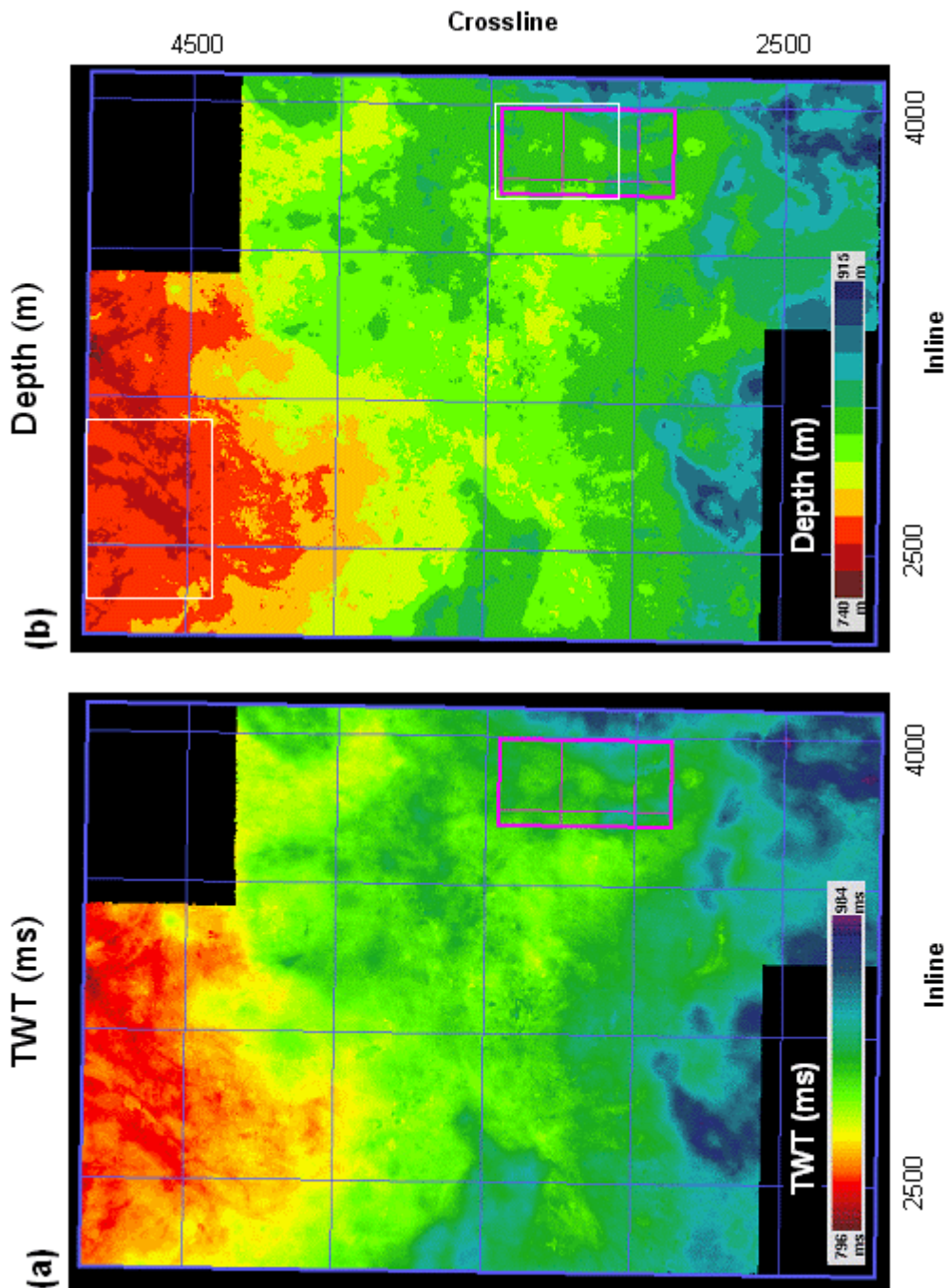


Figure 5.12 Topography of the top Utsira Sand reflector in the area of the 3D seismic survey ST98M11. (a) in two-way travel time, (b) in depth. The distance between 500 lines corresponds to 6.25 km. Colours change every 15 m on the depth figure. The violet rectangle in the centre at the right side is the area of the 1999 time-lapse survey (ST9906). The white rectangle in the north and the east are the outlines of Figure 6.3 and Figure 5.14, respectively.

trend is modified by depressions, domes, and anticlines. The domes and anticlines have typically diameters of a few km (ca. 2 to 5 km), heights of ca. 100 ms TWT (ca. 100 m), and are often linked to each other by saddle structures. The topography of the top Utsira Sand has a clear relationship to the topography of the base Utsira Sand, such that mounds at the base correspond to depressions at the top (Figure 5.3; for mechanism: see Figure 5.8). Linked depressions at the top form then the margins of domal or anticlinal structures. The wavelength of structures at the top is larger and their amplitude is smaller than those of structures at the base Utsira Sand, causing a much smoother topography at the top as compared to the base.

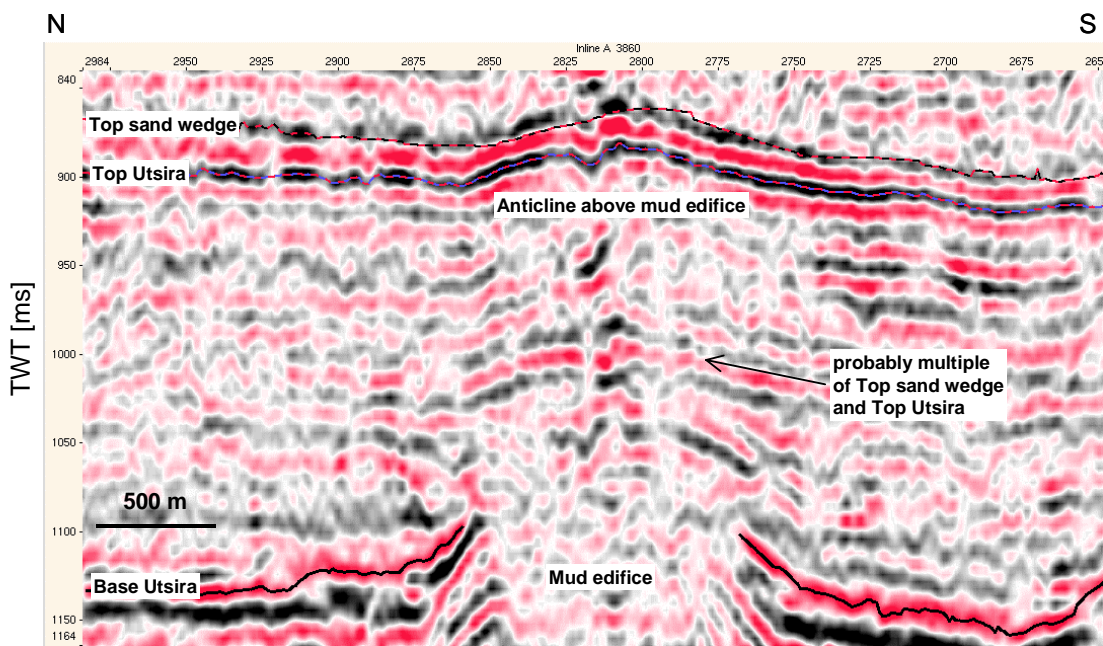


Figure 5.13 *Inline 3860 shows a positive topographic feature of the top Utsira and possibly of intra-Utsira reflectors above a mud edifice. This observation is the single exception of the rule that mounds at base Utsira correspond to depressions at top Utsira.*

Two major depressions of the top Utsira Sand, superimposed on the general southward dip, extend from the middle portions of the eastern and the western margin of the 3-D survey area towards the centre of the survey (Figure 5.12). They cause the presence of a large, roughly EW-striking anticlinal structure west of the injection site. This anticlinal structure is linked by a saddle with the generally shallower part of the top Utsira Sands in the north.

The CO<sub>2</sub> injection site is positioned close to the base of the reservoir below a domal structure of the top Utsira Sand (Figure 5.14). This dome has a diameter of ca. 1.2 km and a height above its spill point of ca. 12 m (Figure 5.15). Two saddle-shaped ‘channels’ provide outlets to other structures. A ‘channel’ towards north connects it to a second dome which is ca. 2.0 km in diameter and ca. 8 to 10 m high. The second channel leads towards west into a wide (ca. 3.0 km diameter), irregularly shaped dome

that is linked at its northwestern corner to the large, EW-striking anticlinal structure described before (Figure 5.12). The small dome north of the injection site possesses also a connection to this anticlinal structure.

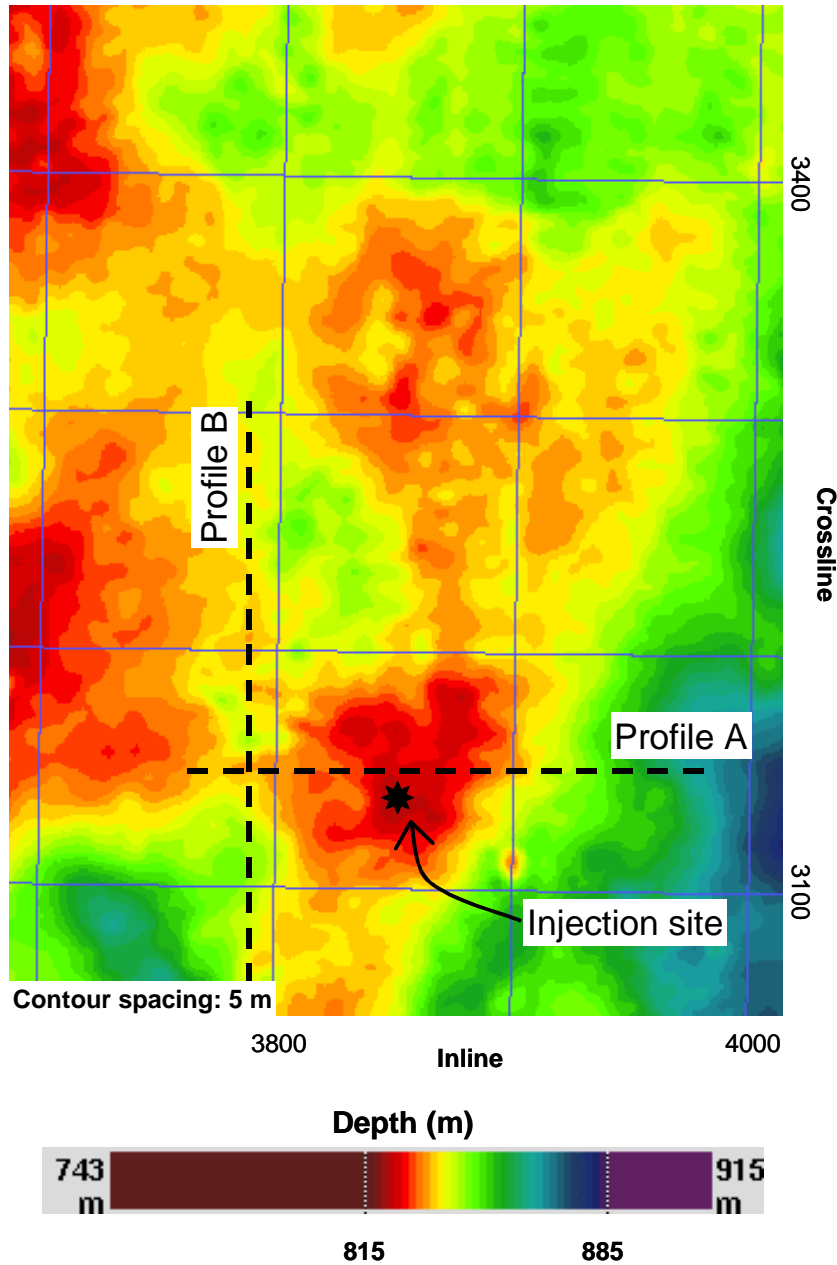


Figure 5.14 Topography of the top Utsira Sand reflector in the area around the CO<sub>2</sub> injection site (in m). Note the presence of two connected domes which both have saddle shaped 'channels' providing potential spill paths towards west. Profile A: Figure 5.15, Profile B: Figure 5.16.

The depth to the tops of the domal and anticlinal structures indicate the minimum depths up to which CO<sub>2</sub> will rise if it will be contained in the Utsira Sands. These depths are ca. 820 m in the dome above the injection site, ca 825 m in the dome to the

north of it (Figure 5.14), and ca. 800 m in the large dome and the E-W striking anticlinal structure in the west (Figure 5.12b).

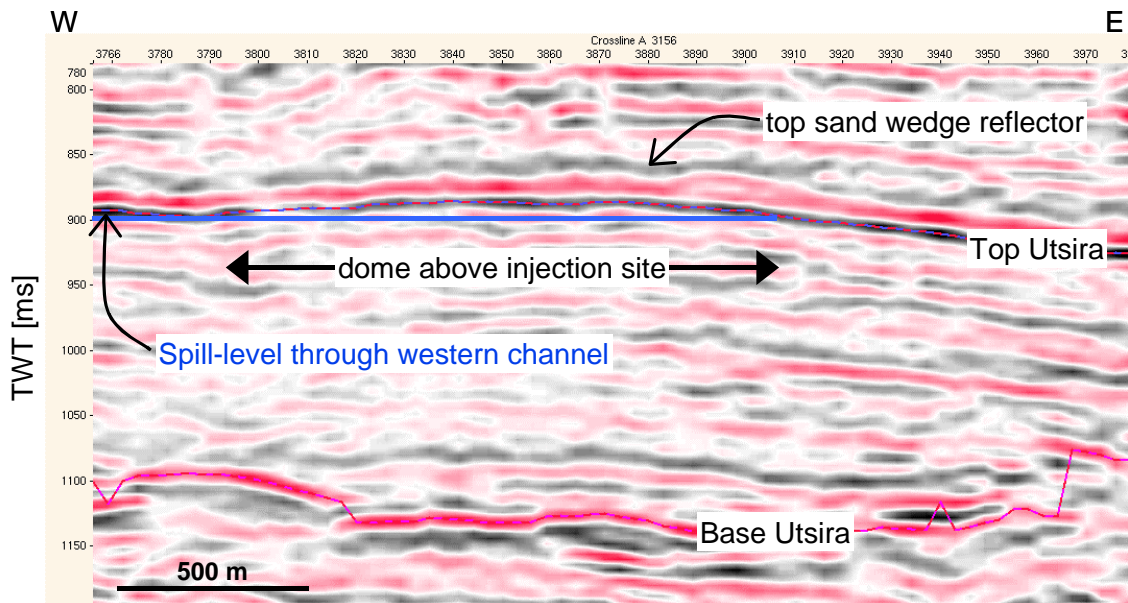


Figure 5.15 E-W section through the dome above the CO<sub>2</sub> injection site (seismic crossline 3156 of survey ST98M11). The section cuts along the westward channel which provides a potential spill path towards west. Position of line, see line on A Figure 5.14.

The depths of potential spill points, i.e. especially of the saddle shaped channels linking the traps, determine the migration pattern of CO<sub>2</sub>. Unfortunately, alternative spill points are often at very similar depths (Figure 5.14), with depth differences often below a metre (see Figure 7.3 in Zweigel et al. 2000a). Moreover, interpretation is in some cases hampered by low data quality due to signal disturbances (Figure 5.16). The resulting uncertainty will have effects on the modelling of CO<sub>2</sub> migration pathways, and such modelling must consequently include alternative scenarios (see Zweigel et al. 2000a for a discussion of these uncertainties).

Modelling of CO<sub>2</sub> migration below the top Utsira Sand has been carried out at SINTEF Petroleum Research, employing the in-house secondary hydrocarbon migration simulator SEMI. This modelling used several alternative versions of the top Utsira Sand. Results have been presented in a separate report (Zweigel et al. 2000a).

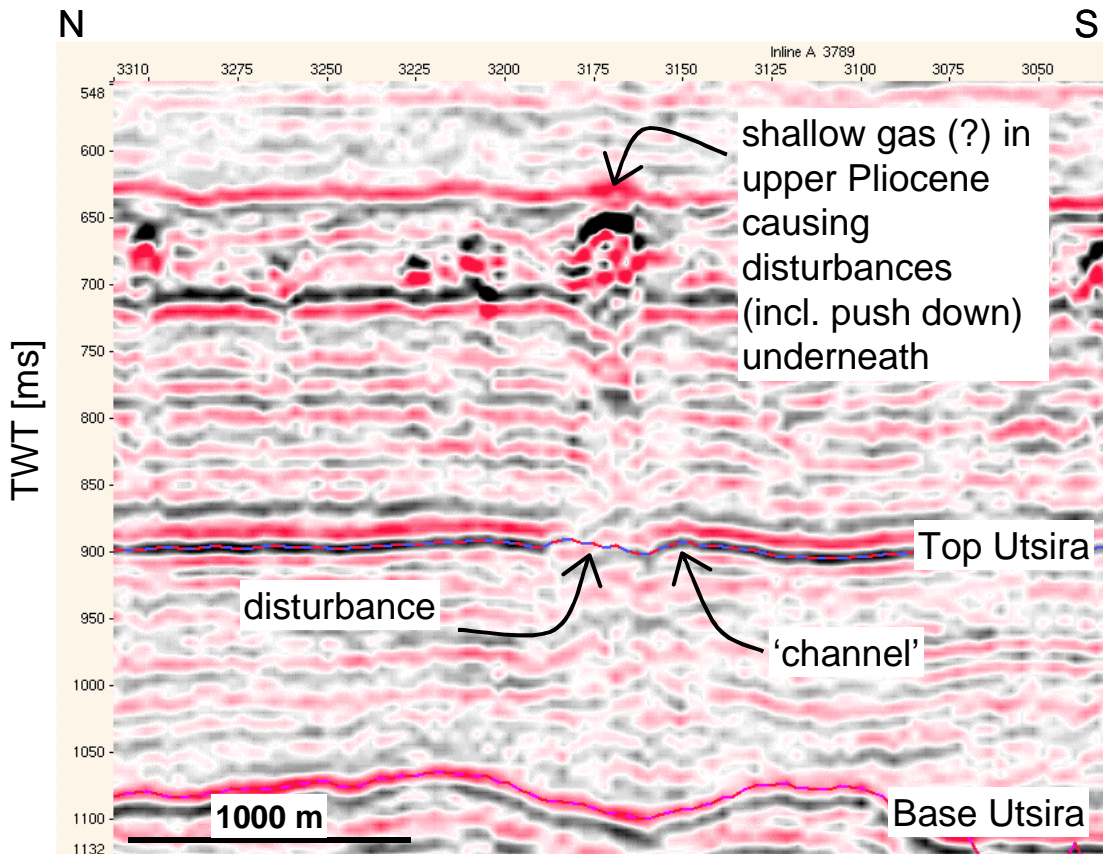
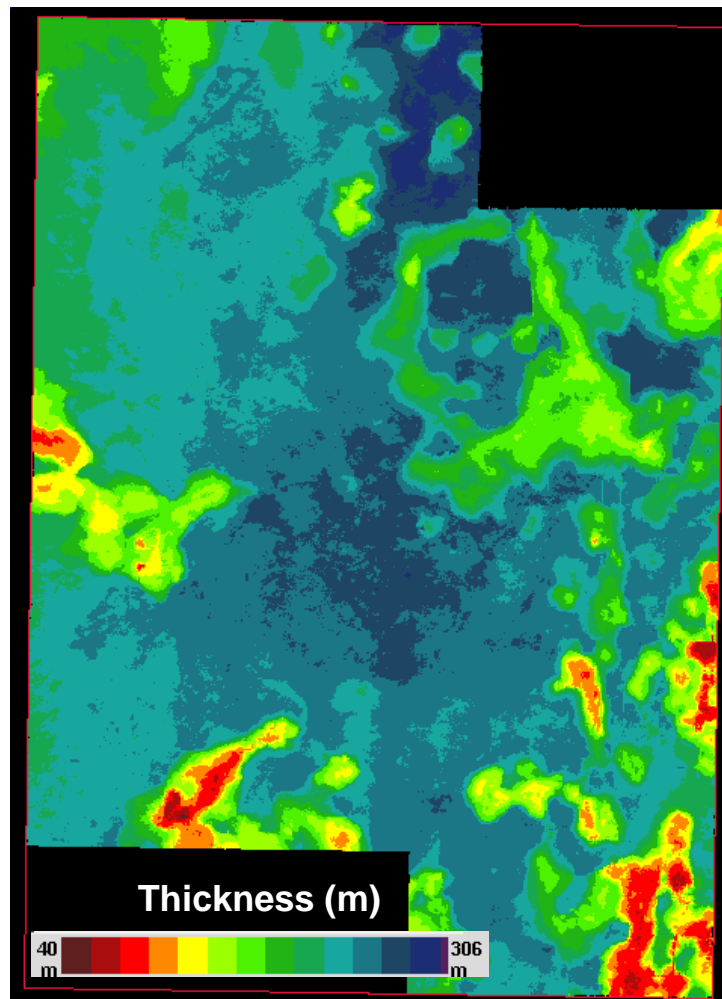


Figure 5.16 N-S section through the potential westward spill channel of the dome above the CO<sub>2</sub> injection site. Note the signal disturbances (incl. push-down) at the top Utsira Sand level linked to the presence of seismic anomalies (due to shallow gas?) above. These disturbances have severe adverse effects during interpretation of the precise position of the reservoir top. Position of line, see line B on Figure 5.14.

#### Thickness of the Utsira Sand / Storage volume

The thickness of the Utsira Sand in the area of the 3D seismic survey ST98M11 varies from ca. 50 m to slightly over 300 m (Figure 5.17). Considerable local variations are due to the presence of mud mounds at the base and corresponding depressions of the top Utsira Sand above. The thickness outside the areas affected by mud mobilisation at the base ranges mainly from 240 to 270 m. The total volume of the Utsira Sand in the survey area is  $1.485 \cdot 10^{11} \text{ m}^3$ , i.e. 148.5 km<sup>3</sup>.



*Figure 5.17 Thickness of the Utsira Sand as calculated from depth converted maps of the top and base Utsira Sand in seismic survey ST98M11. Comparison with Figure 5.6 shows that the thickness is largely determined by the topography of the base Utsira Sand.*

The volume of traps below the top Utsira Sand has been determined using the secondary hydrocarbon migration simulator SEMI. For a description of the methodology, refer to Zweigel et al. (2000a). For the calculations of the total trap volume presented here, the grid used for case U-4 in Zweigel et al. (2000a) has been used. This grid is based on a 3D autotrack-interpretation of the top Utsira Sand, slightly smoothed, depth converted using the velocities provided in Table 5.1 and resampled at a cell spacing of 50 m \* 50 m. We assumed a porosity of 30 % (Chapter 6.1.1) and a N/G ratio (including drainage effectivity) of 0.85 (Chapter 6.1.2). For the simulations, CO<sub>2</sub> was ‘injected’ at all grid points, providing upward migrating CO<sub>2</sub> in excess such that it could fill all available traps up to their spill point.

The total calculated volume of all traps below the top Utsira Sand that are fully contained within the 3D survey, amounts to ca.  $1.35 \cdot 10^8$  cubic meters. The positions of traps and the maximum column height are indicated in Figure 5.18a. Drainage areas for these traps are shown in Figure 5.18b. Note that the small drainage areas at the margin

of the survey are artefacts – many of them are probably linked to each other outside the interpreted area. A major result is that a very large area of the survey belongs to one single drainage area, with an outlet at its northern boundary.

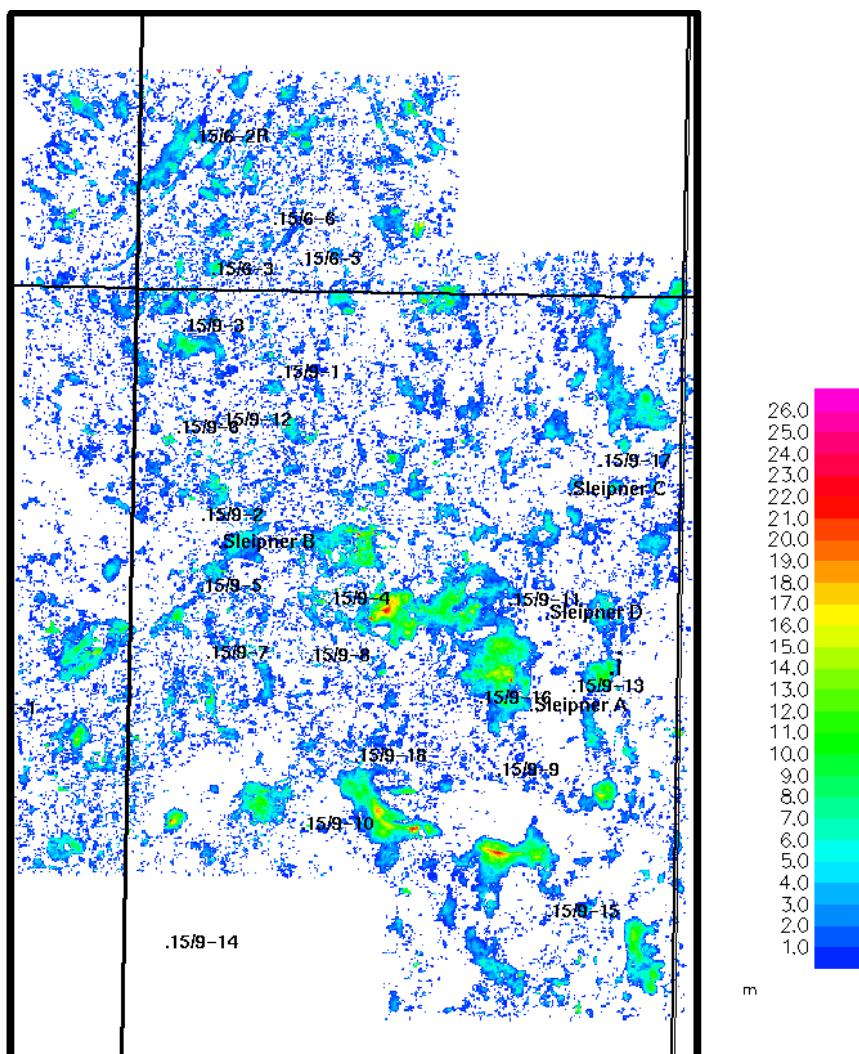


Figure 5.18 (a) Structurally controlled maximum column heights (in m) in traps below top Utsira Sand. Calculated employing the secondary hydrocarbon migration simulator SEMI.  
NEXT PAGE: (b) Corresponding drainage areas. Traps are shown in purple. Thick lines show outlines of areas that drain through the same outlet at the margin of the studied area. Note that a large part of the studied area belongs to a single drainage area. Many, if not all, of the small drainage areas are artefacts that will be linked with each other outside the study area.

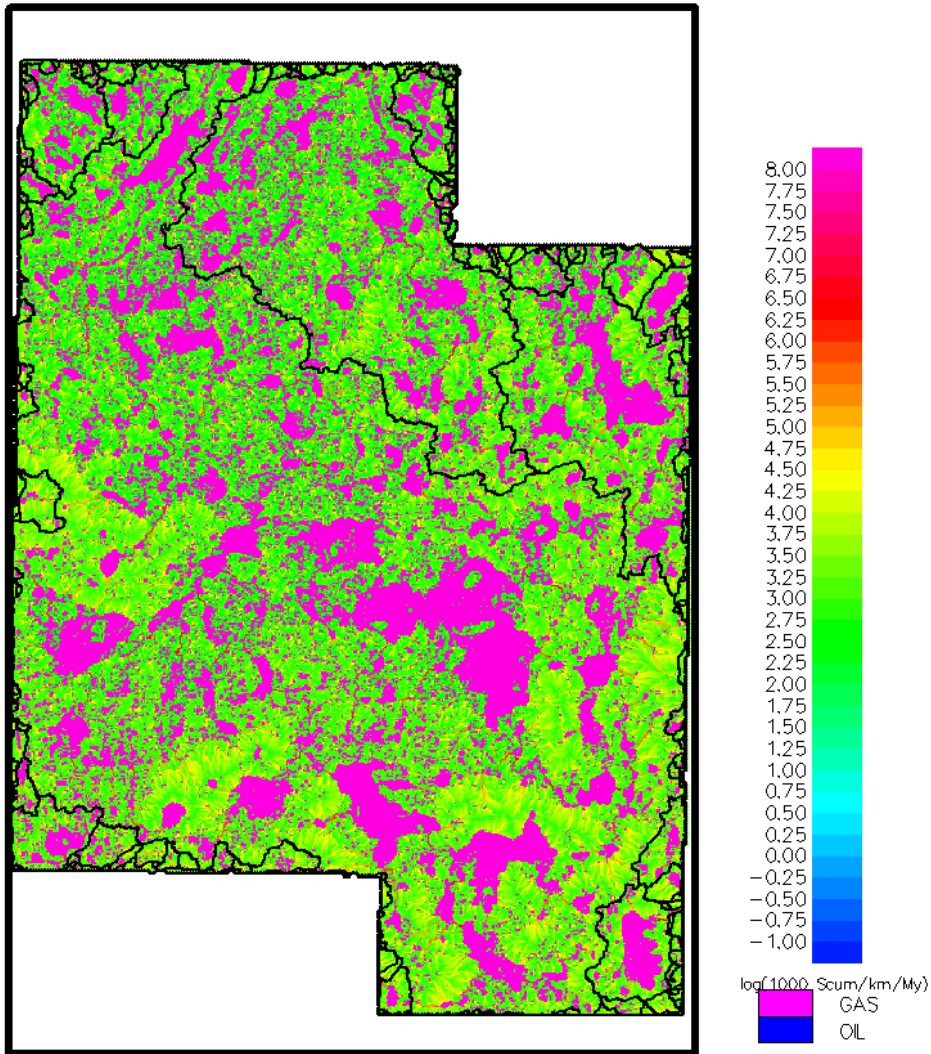


Figure 5.18 Continued from previous page.

### 5.3 Sand wedge in the cap rock

In the eastern half of the area covered by the 3D seismic survey ST98M11, low gamma ray measurements and other wire-line log data indicate the presence of a sand body within the lowermost part of the Nordland Shales (Figure 5.2; Figure 5.19). For a discussion of its assignment to the Nordland Shale and not to the Utsira Sand proper, refer to Lothe & Zweigel (1999).

This sand body is separated by a shale layer of ca. 5 m thickness from the underlying Utsira Sands. It has a wedge shape, disappearing westward in the central area of the survey (Figure 5.20), and it thickens towards east. According to well data it reaches a maximum thickness of approx. 25 m in the eastern parts of block 15/9 and in block 16/7 (location: see Figure 3.1). Seismics indicates a local thickness of up to 55 m at the eastern margin of the survey in an area where no well control exists. The top of the wedge constitutes a strong reflector closely above the top Utsira Sand reflector. It was therefore possible to map the approximate extent of the wedge by mapping the amplitudes in a time window above the top Utsira Sand (Figure 5.21).

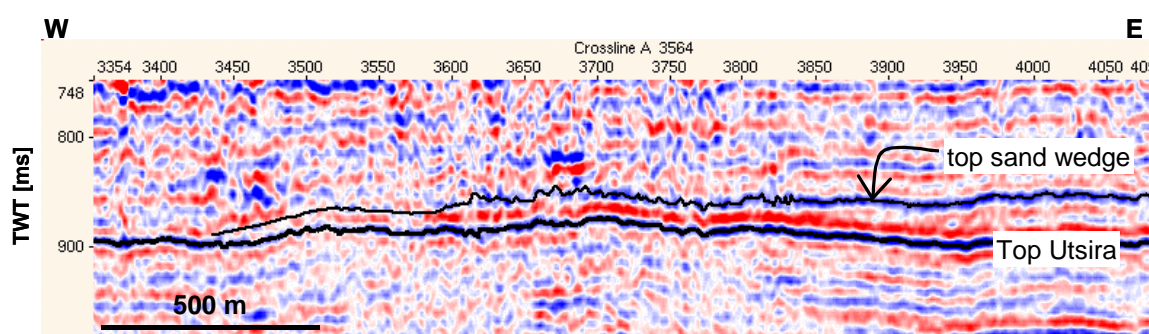


Figure 5.19 Crossline 3564 illustrating appearance of a sand wedge above top Utsira in seismic data.

Since the thickness of the sand wedge is in parts close to or even below usual seismic resolution, and since disturbed seismic signals hampered interpretation of the wedge top in some areas (see below), it was at first constructed based on a combination (Figure 5.22) of (a) sand wedge thickness in wells, (b) the western limit of strong amplitudes above the top Utsira Sand, (c) the topography of the top Utsira Sand, and (d) local information about the western wedge termination from a small number of interpreted seismic sections. This constructed wedge top (Figure 5.23) was used as a first approximation in CO<sub>2</sub> migration simulations (Zweigel et al. 2000a).

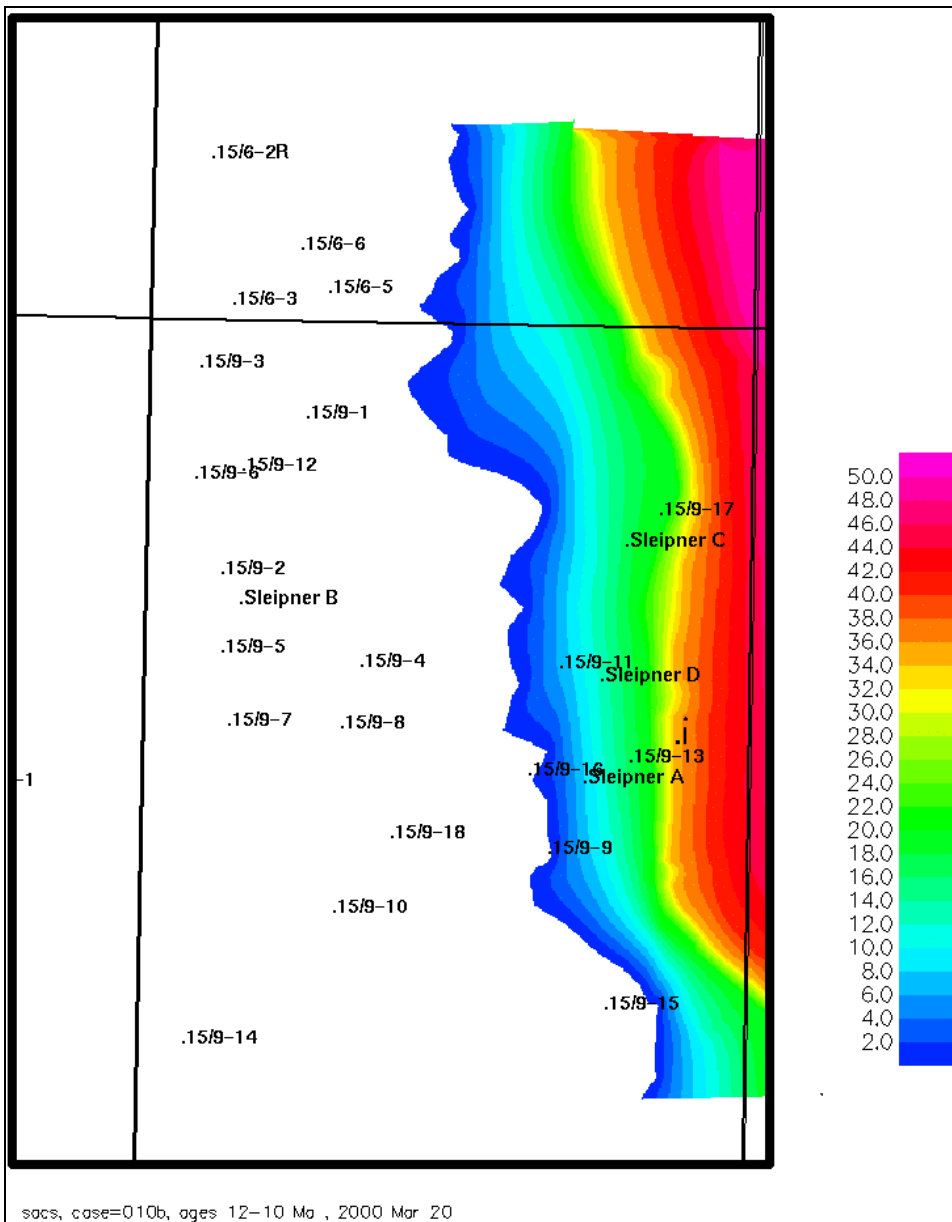


Figure 5.20 Thickness of the sand wedge in the shales above top Utsira constructed from the tip line in the west (from seismic data) and thickness data from wire-line logs in the east.

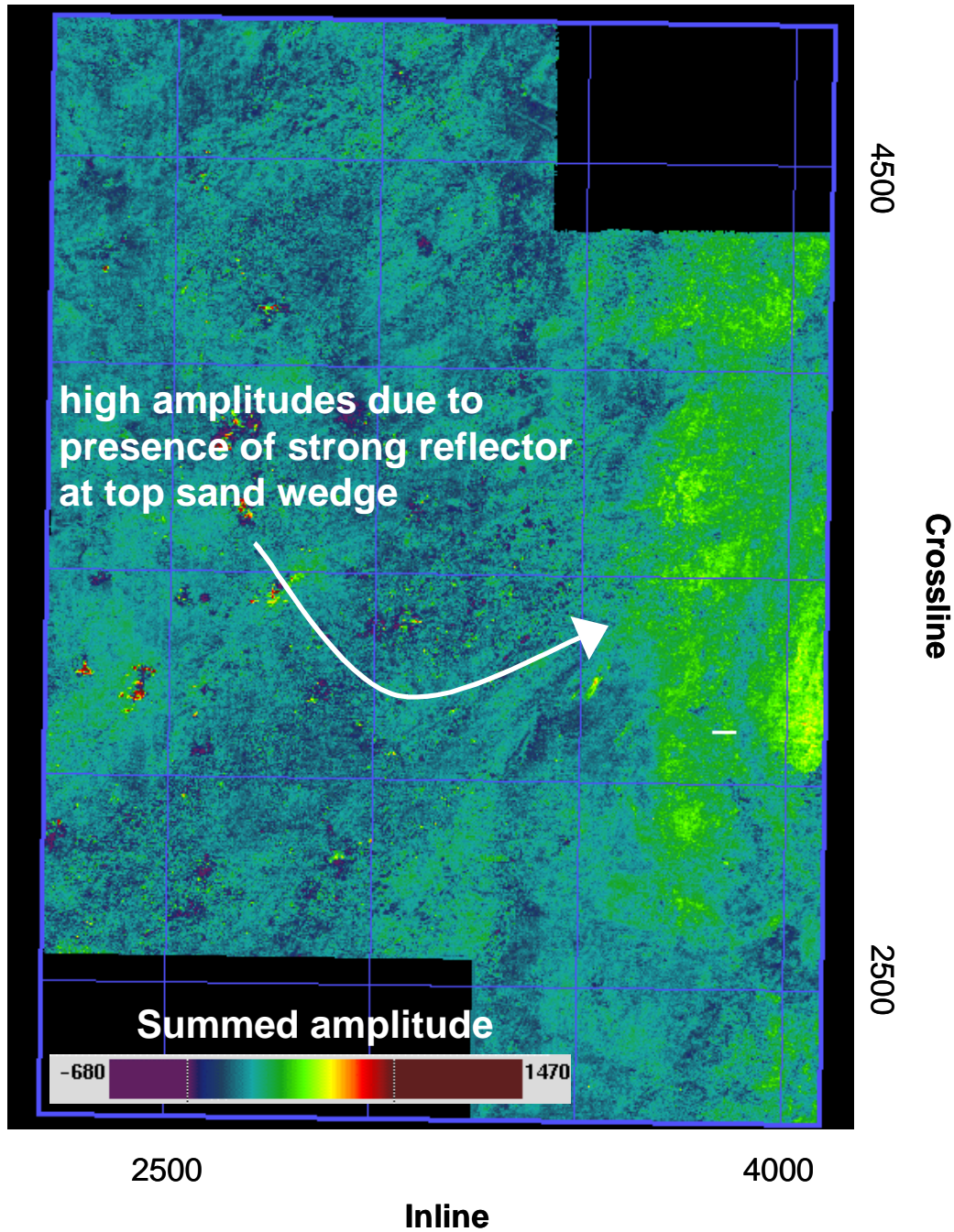


Figure 5.21 Mean seismic amplitude in a 5 ms thick layer ranging from 20 to 15 ms above top Utsira. The areal extent of elevated amplitudes corresponds roughly to the extent of the sand wedge. The amplitudes are probably due to the reflection at the lithological contact shale above sand at the top of the sand wedge.

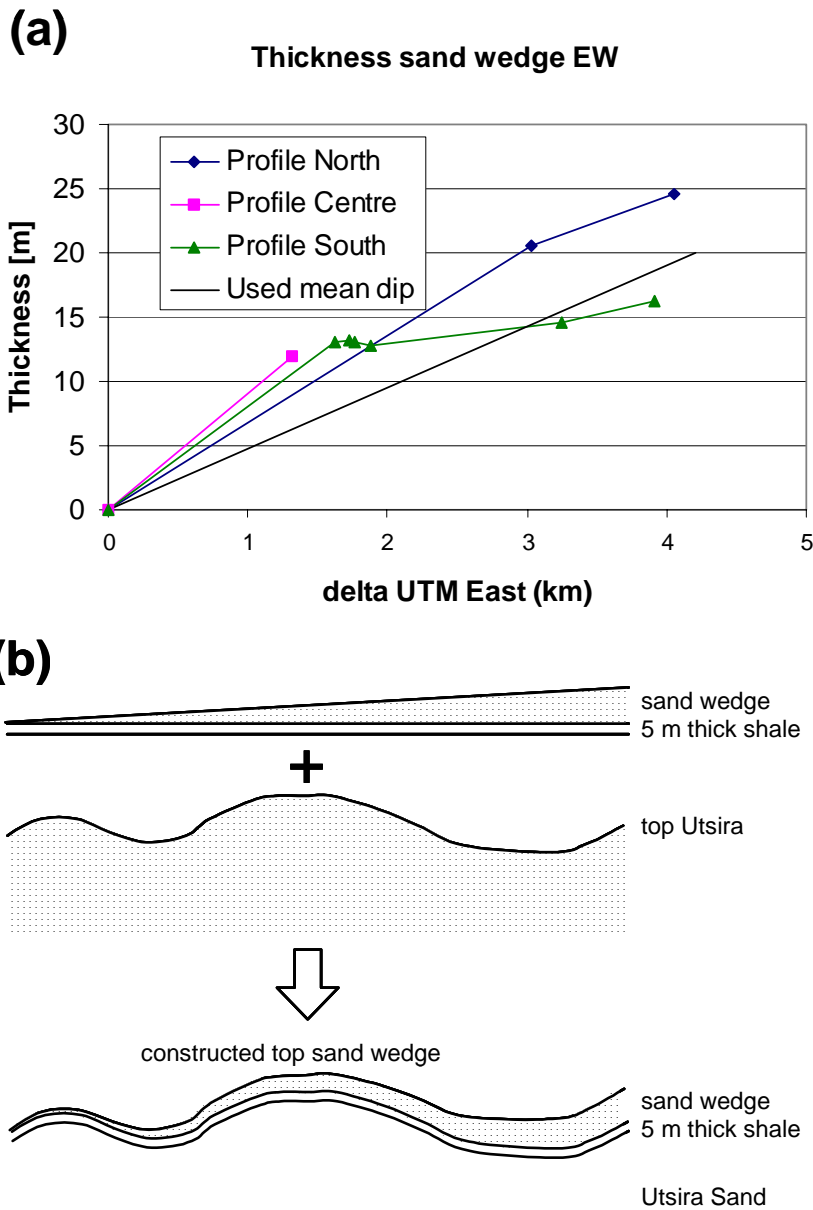
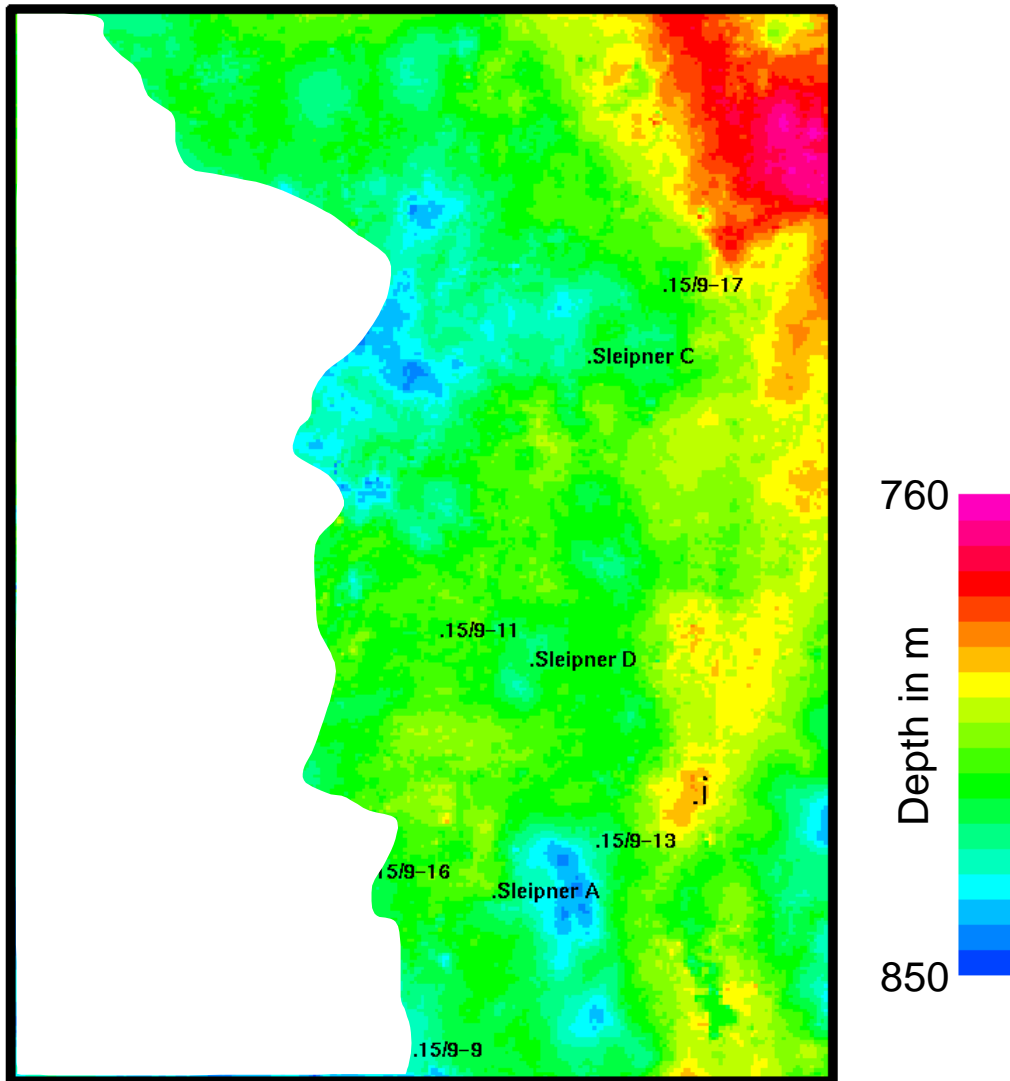


Figure 5.22 (a) Determination of the average thickness gradient of the sand wedge based on the east-west distance of wells from the position of the tip line in the west. Note that tip line used here was based on amplitude anomalies and is further east than tip line according to seismic interpretation. The real thickness gradient may, therefore be lower. (b) Construction principle for the depth to top sand wedge in the initial model, based on sand wedge thickness from wire-line logs.



*Figure 5.23 Depth (in m) to the constructed (see Figure 5.22) top of the intra-Nordland Shale sand wedge. Well positions are for orientation.*

Detailed inspection of the seismic data revealed, however, that the wedge could be traced a considerable distance further west than the western limit of strong reflections above the top Utsira Sand. It was therefore necessary to map its extent directly (Figure 5.24, [Appendix 3](#)).

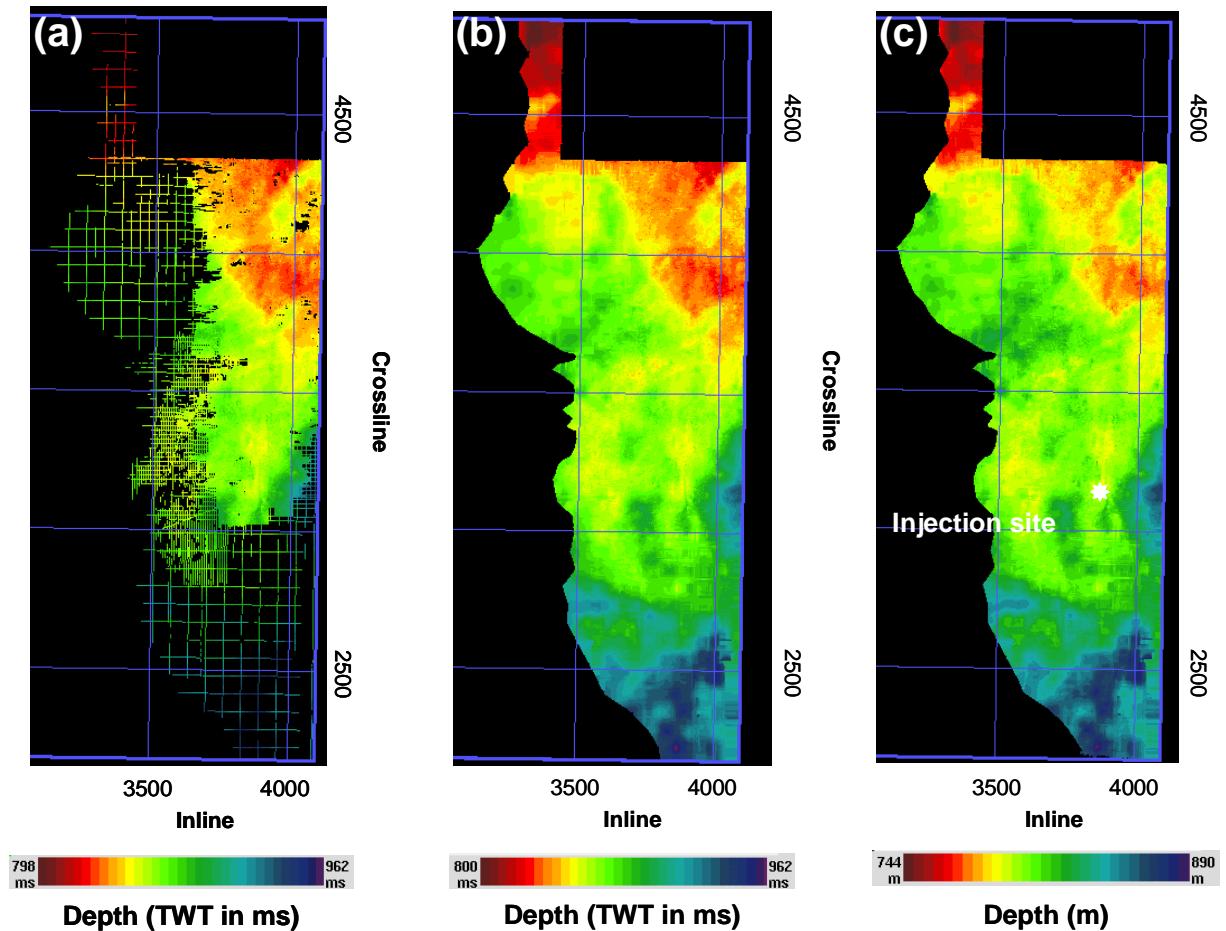


Figure 5.24 The intra-Nordland Shale sand wedge as interpreted from seismic data in survey ST98M11: (a) interpreted line pattern; (b) topography in TWT (m); and (c) topography depth converted (in m).

The mapped top of the intra-Nordland Shale sand wedge is nearly parallel to the top Utsira Sand, with the difference of an additional westward dip component of the top sand wedge. This difference in dip is the expression of in the mean ca. 3 m eastward wedge thickening over a distance of 1 km and amounts to ca.  $0.17^\circ$  (values determined from seismics). Migration modelling (Zweigel et al. 2000a) shows that this small dip difference has a decisive influence on the migration pattern in the Sleipner case.

Seismic tracing of the top sand wedge was in some areas difficult due to signal disturbances (Figure 5.25). TWT accuracy in these areas is therefore low, with TWT uncertainty in the range of up to  $\pm 10$  ms (corresponding to ca.  $\pm 10$  m). Such uncertainties have a considerable influence on migration modelling. CO<sub>2</sub> migration within the sand wedge modelled in Zweigel et al. 2000a is, however, largely outside the areas of low data quality.

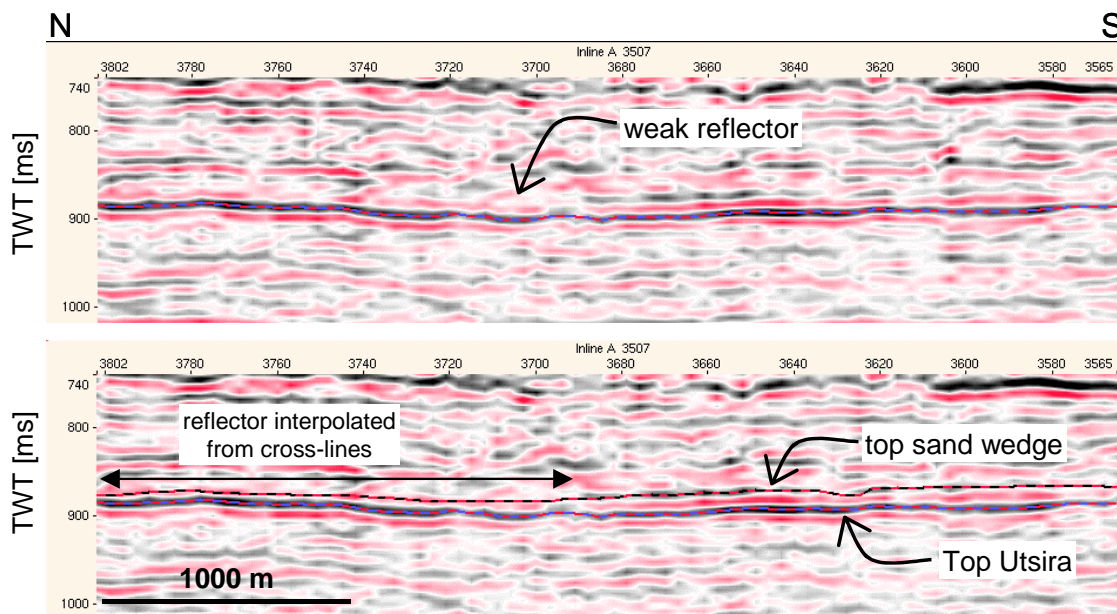


Figure 5.25 Inline 3507 illustrating the difficulties to trace top sand wedge on individual lines as a consequence of signal disturbances. Interpretation However, correlation on a network of lines enabled areal mapping of the reflector.

The total volume of the sand wedge has been calculated as the volume between the top sand wedge and a layer 5 m above the top Utsira Sand (the 5 m correspond to the mean thickness of the shale layer beneath the sand wedge). Its volume amounts to  $4.496 \cdot 10^9 \text{ m}^3$ , i.e.  $4.5 \text{ km}^3$ .

## 5.4 Reservoir internal barrier horizons

### 5.4.1 Geometry of reservoir-internal shale layers

Wire-line logs show several peaks within the Utsira Sands. These peaks are especially evident on gamma-ray logs, but are clearly visible on neutron density and sonic logs, too, as well as on some induction and resistivity logs (Figure 5.4, Figure 5.26). Glauconite has been reported to be present within the Utsira Formation (e.g. Isaksen & Tonstad 1989, Rundberg & Smalley 1989) and might be a cause for high gamma-ray values. However, most gamma-ray peaks correspond to peaks in other wire-line logs which should not respond to increased glauconite contents in otherwise constant lithology. Hence, the peaks are likely to represent shale layers. Some gamma ray peaks do not show the correspondence of peaks in other logs (arrows in Figure 5.26) and they may accordingly be due to other reasons, e.g. caused by the presence of glauconite.

The layers are usually thin, with an average thickness of slightly more than a metre (Figure 5.27). The arithmetic mean for shale thicknesses in 5 selected wells is 1.3 m, and the median (being probably more representative for an asymmetric, one-side limited distribution) is 1.1 m.

# 15/9-8

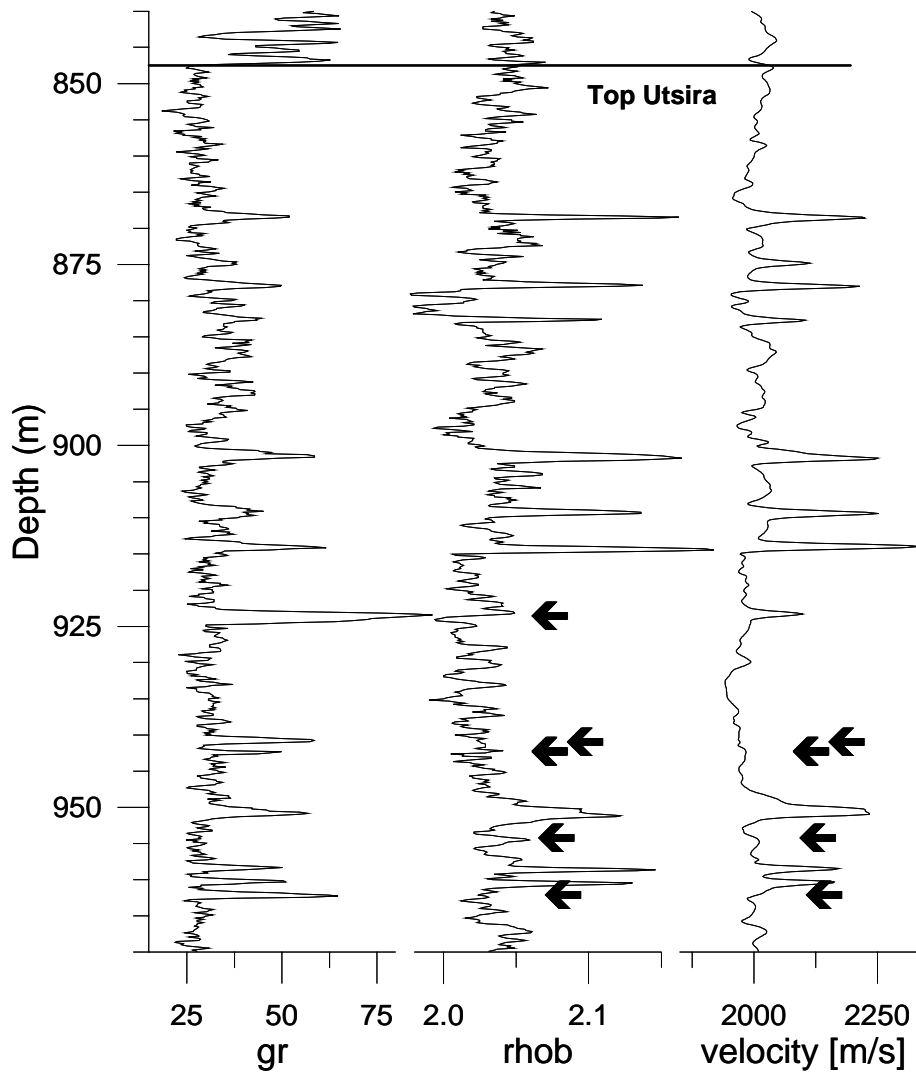


Figure 5.26 Wire-line-log data from a part of the Utsira Sand in well 15/9-8 showing 'shale peaks' in the gamma ray log and the corresponding signals in the density log and sonic log (expressed as velocity here). Most gamma ray peaks correspond to increased density and velocity and the top and the base of the corresponding shale (?) layers correspond accordingly to positive and negative reflection coefficients, respectively. Note, however, that some of the gamma ray peaks do not have corresponding peaks in the density and/or velocity logs, and vice versa (arrows).

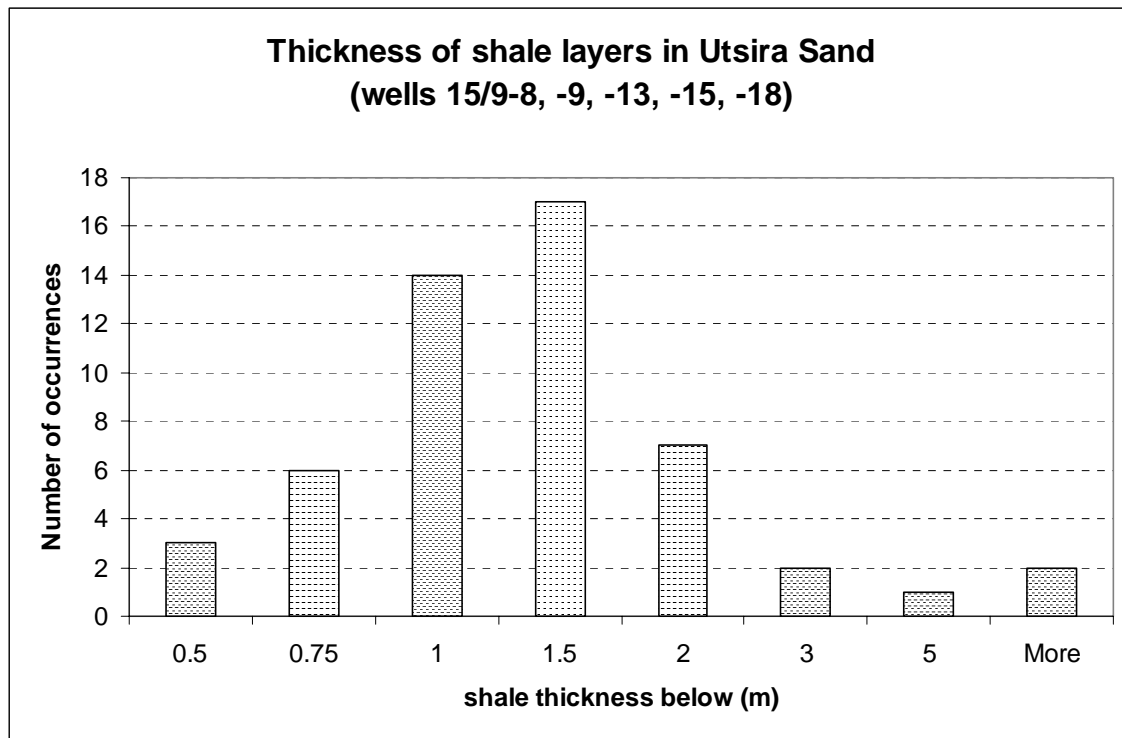


Figure 5.27 Histogram of intra-Utsira shale layer thicknesses from a representative well selection. Thickness determinations are based on application of the first derivative method to gamma ray data (see [Appendix 1](#)). Note that most shale layers are ca. 1 m in thickness.

Those gamma-ray peaks interpreted as shale layers, have higher densities and higher velocities than the surrounding sand (Figure 5.26, Table 5.2), yielding a positive and a negative reflection coefficient at their top and base, respectively. Many of these peaks seem to be correlatable to (weak) reflectors within the Utsira Sand.

Table 5.2 Mean density and acoustic velocity (from neutron density and sonic logs, respectively) from wells with suitable data quality in the Sleipner area.

well:	SAND		SHALE	
	V (m/s)	Rho (g/m3)	V (m/s)	Rho (g/m3)
15/9-9	2000	2.05	2250	ca. 2.15
15/9-18	2080	2.08	2320	2.2
15/9-15	2070	2.05	2250	2.1
15/9-7	2100	2.05	2350	2.2
15/9-6	2100	2.02	2280	2.15
15/9-8	1960	2.05	2250	2.15

Tracing of some of these reflectors in the 3D seismic survey was attempted. This was, however, hampered by the often weak amplitudes of the reflectors, by signal disturbances (weakened signals or strong multiples) due to amplitude anomalies (gas accumulations?) above, and by the probable presence of a sea floor multiple of the strong top Utsira Sand reflector.

Tracing of some of the reflectors was possible with confidence over several kilometres laterally (Figure 5.28, Figure 5.29), in spite of difficulties to correlate individual gamma-ray peaks between wells at distances of several km (Lothe & Zweigel 1999; see also Figure 5.2). We interpret the clay layers accordingly to be continuous and of regional extent. They may, however, exhibit local discontinuities, either due to localised erosion or by faulting (see e.g. Chapter 5.4.2).

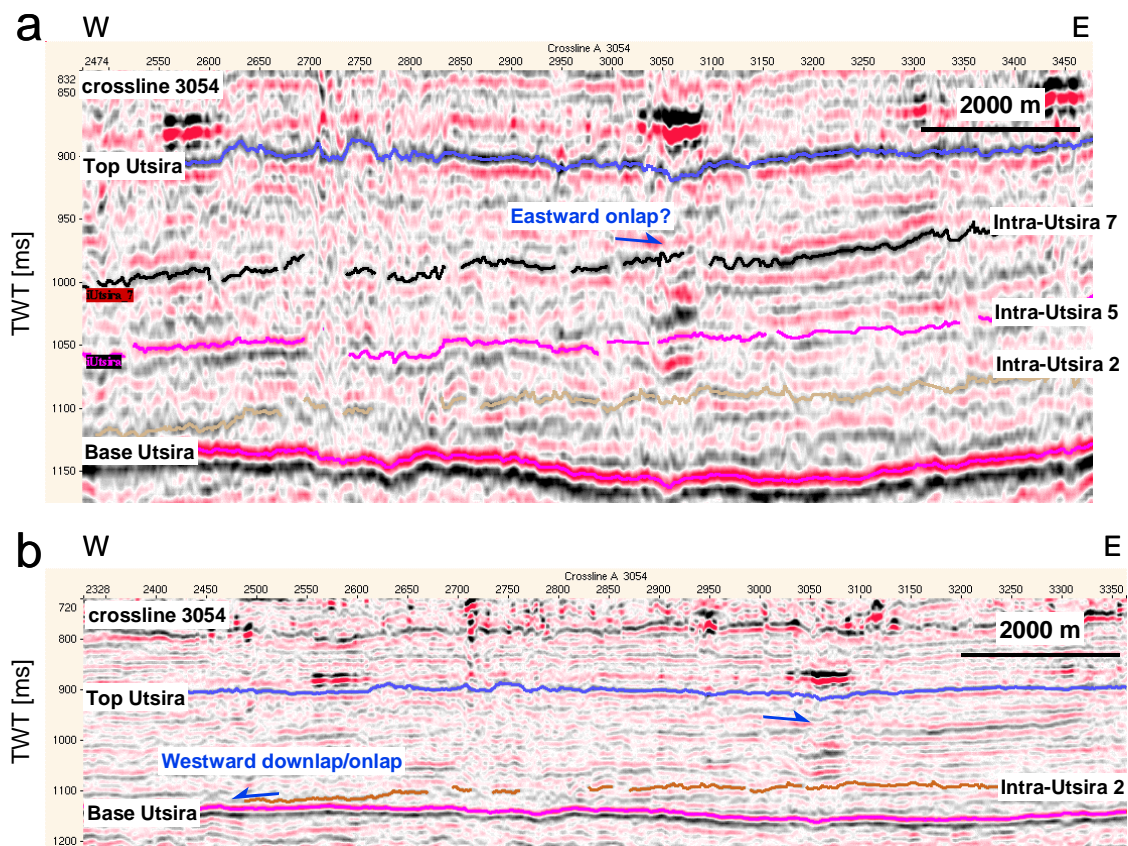


Figure 5.28 Seismic sections showing the major three intra-Utsira reflectors traced in the present study. Continuous tracing was not always possible on single lines due to weak reflections and signal disturbances. However, correlation through crossing and parallel lines permitted continued tracing. Note that all intra-Utsira reflectors have a tendency to approach the base Utsira Sand in a westward direction.

Figure 5.28 and Figure 5.29 show that all three traced intra-Utsira horizons approach the base Utsira Sand in a westward direction. This is especially evident for the lowermost of these horizons, intra-Utsira 2. The thickness of the interval between intra-Utsira 5 and intra-Utsira 2 may, however, increase slightly towards west.

Westward tapering of the lowermost part of the Utsira Sand may signify a sediment source in the east during deposition of this interval. Eastward thinning of the upper part of the Utsira Sand and indications for possible eastward onlap of internal reflectors (Figure 5.28) may suggest a western source during the later stages of Utsira Sand deposition. They would, on the other hand, be in accordance with an eastern sediment source, too, in which case the eastward onlaps would indicate the basinward onset of deposition.

The time lapse seismic survey acquired in autumn 1999 (ST9906) shows strong amplitudes in several nearly horizontal layers above the injection site (Figure 5.30). These amplitude ‘anomalies’ are most likely due to the presence of CO<sub>2</sub> in discrete layers, which would confirm predictions (Lothe & Zweigel 1999) that the intra-Utsira shale layers will have a strong influence on the (local) CO<sub>2</sub>-migration pattern, deviating gravity-driven vertical flow into layer-parallel horizontal flow. The lateral extent of individual supposed CO<sub>2</sub>-accumulations of up to ca. 1.8 km indicates the minimum lateral extent of some of the intra-Utsira shale layers. Leakage through them to higher levels within the Utsira Sand shows, moreover, that they are not entirely tight, confirming previous predictions (Lothe & Zweigel 1999).

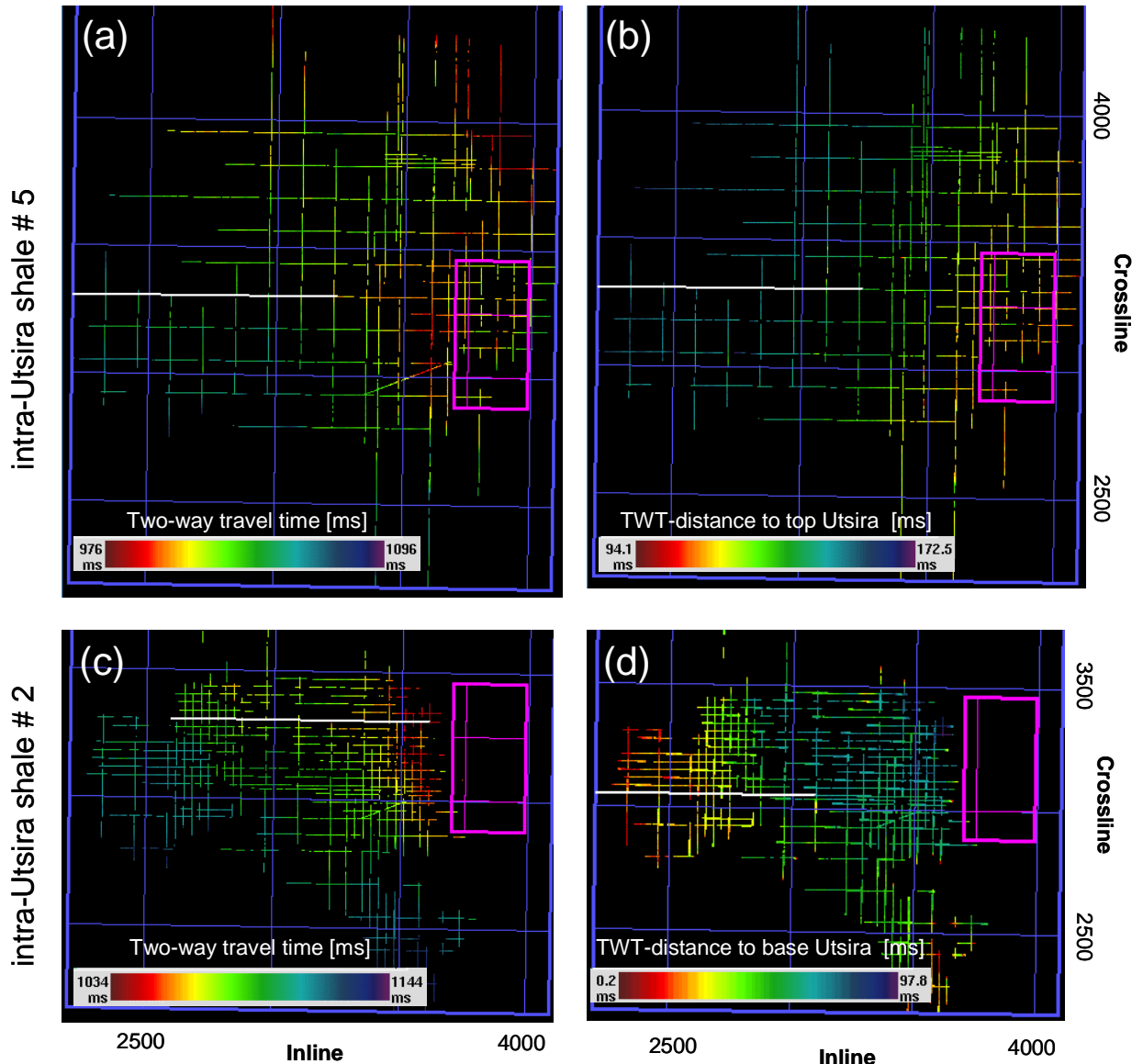
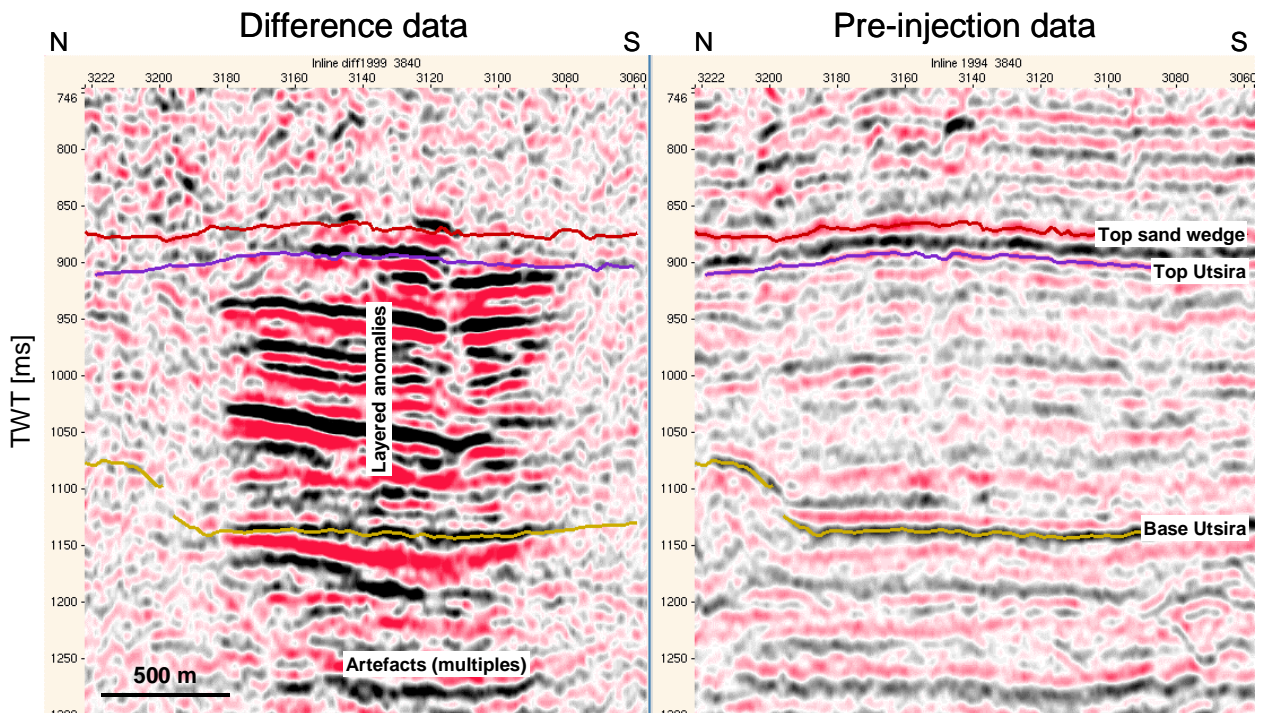


Figure 5.29 (a), and (b): TWT-depth to two major intra-Utsira reflectors in map view. Note westward deepening of these horizons. (c): Vertical TWT-distance (isotime) between top Utsira and intra-Utsira reflector '5' illustrating westward thickening of the Utsira interval above intra-Utsira 5. (d): Vertical TWT-distance (isotime) between intra-Utsira reflector '2' and base Utsira illustrating westward thinning of the Utsira interval below intra-Utsira 2.

Intra-Utsira reflections in the lower part of the Utsira Sand show usually horizontal onlap or downlap onto the surface of mud edifices (Figure 5.3). Downlap is especially common above the central parts of these edifices. We interpret the downlaps as having been rotated due to stronger compaction of the mud edifices as compared to the surrounding Utsira Sand (Figure 5.8). We consider it likely that most of them originally were horizontal onlaps.



*Figure 5.30 Representative section (inline 3840 in ST98M11 coordinates) from difference cube of time-lapse seismic survey ST9906 shot in autumn 1999, i.e. after approx. 3 years of CO<sub>2</sub>-injection, and corresponding section from reprocessed survey ST98M11. Strong amplitudes in approximately horizontal layers within the Utsira Sand (left figure) were not present in the pre-injection survey (right figure) and are most likely caused by layered accumulations of CO<sub>2</sub>. Note the presence of strong amplitudes above the top Utsira in the difference cube; this indicates migration of CO<sub>2</sub> into the sand wedge.*

Intra-Utsira reflections in the upper part of the Utsira Sand show almost always depressions above mud edifices (as does the top Utsira Sand; single exception, see Figure 5.13), which we – again – interpret as pronounced subsidence due to preferred compaction of the underlying mud sediments (Figure 5.8). In several cases, the upper part of the Utsira Sand thickens over mud edifices, and reflectors exist which are limited to the depressions and which onlap towards the margins of the depressions (Figure 5.31). They indicate that the depressions existed already during deposition of the upper parts of the Utsira Sand and that they constituted preferred deposition sites. This implies further that the locations of the mud edifices changed at least in some cases from positive relief (hills) during deposition of the lower part of the Utsira Sand to negative relief (depressions) already during deposition of the upper part of the Utsira Sand.

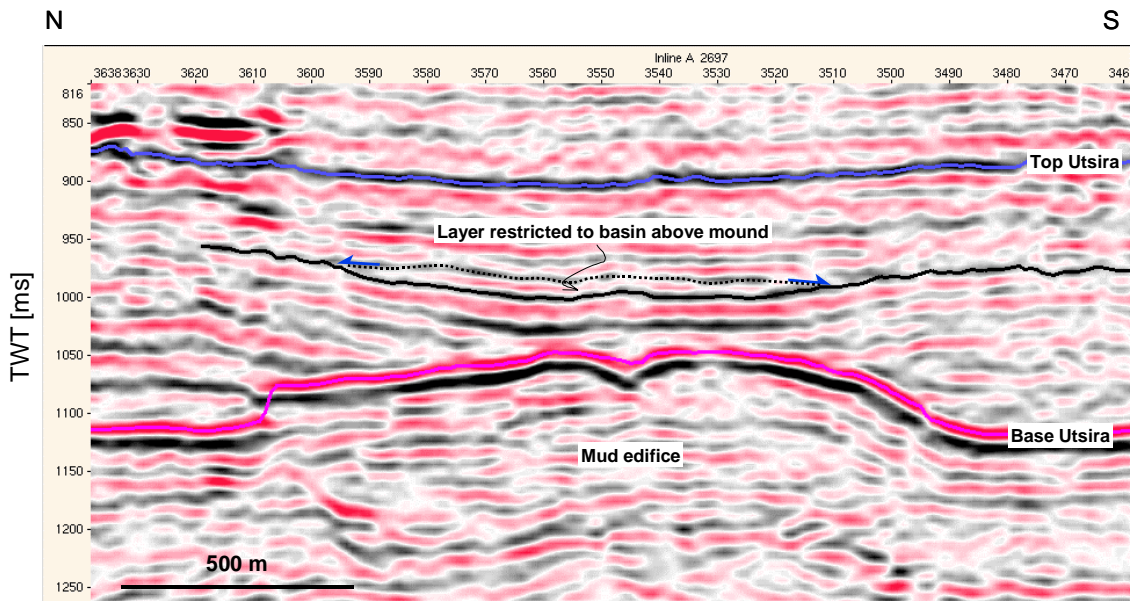


Figure 5.31 Thickening of upper parts of the Utsira Sand above a mud edifice. A reflector in the thickened part terminates by onlap onto an underlying reflector. It indicates the presence of a layer whose occurrence is limited to the area above the edifice, and the existence of a local depression during deposition of the layer (Figure 5.8). Inline 2697 from survey ST98M11.

#### 5.4.2 Deformation of reservoir-internal shale layers

Differential subsidence due to strong compaction of the mound material causes deformation of the sequence above (Figure 5.31, Figure 5.8). We investigated if this deformation may induce faulting and fracturing of potential barrier horizons, such as the intra-Utsira shale layers.

The amount of deformation has been determined based on the assumption that simple shear along vertical planes was the responsible deformation mechanism. This assumption was taken because the cause for the deformation was essentially laterally changing vertical movement (subsidence) magnitudes and because the sediments were – due to their unconsolidated state when becoming deformed shortly after deposition – expected not to exhibit much coherence to distribute the deformation laterally. Early deformation is evident from the formation of basins above some of the mounds (Chapter 5.4.1). The most strongly bent shale layers at the flanks of the mounds are approx. 50 ms below the reflectors forming the base of the local basins. The bent shale layers were, therefore, (taking compaction into account) ca. 60 m bsf when the basins on top of the mounds existed, i.e. when most of the bending had probably already happened.

The strain determination was carried out by measuring the strongest dips of intra-Utsira shale layers in the neighbourhood of mud edifices and assuming that the layers were horizontal prior to deformation (Figure 5.32). The dips were mainly below 6°, but ranged up to 10°. The maximum value of 10° corresponds to +1.5% longitudinal strain along the layer, whereas most layers experienced less than 0.6% longitudinal strain at their most strongly deformed parts. We rate these small strain amounts as not likely to have induced much faulting of the shale layers, especially since they were most likely still in an unconsolidated, highly ductile state.

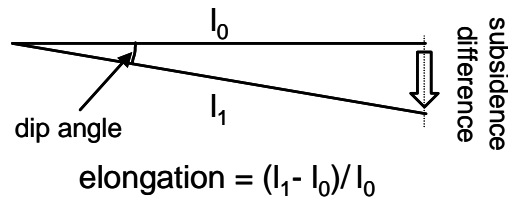


Figure 5.32 Schematic illustration of the calculation principle to determine strain (elongation) of intra-Utsira shale layers.

## 6. Reservoir properties

### 6.1 Reservoir parameters from logs and samples

Reservoir parameters of relevance for the interpretation of CO<sub>2</sub> monitoring data and for prediction of the future CO<sub>2</sub> distribution are especially porosity, Net/Gross ratio, and permeability. Ideally, the distribution of these parameters in 3D should be known. Available data, however, is merely punctual (scarce samples) or 1-dimensional (from wire-line logs) and extrapolation is necessary based on lateral homogeneity vs. heterogeneity as evident from wire-line log data or based on depositional models. Permeability measurements are not reported here. Those carried out at SINTEF are documented in Lindeberg et al. 2000a.

#### 6.1.1 Porosity

Porosity has been determined based on samples and on wire-line log data, and the results have been compared with published porosity data for comparable lithologies.

Sample based porosity determinations have been carried out by modal analysis of thin sections prepared from samples taken from the Utsira core in well 15/9-A23. Analysis of three samples from the core segment 1080 – 1081 m MD (i.e. ca. 906.0 to 906.6 m TVD) yielded 27 to 31 % porosity.

Lindeberg et al. (2000a) present porosity measurements from Utsira core segments that yield an average porosity of 38.8 %.

Wire-line log neutron density data were used to calculate porosities by the formula

$$\Phi = (\rho_{\text{grain}} - \rho_{\text{bulk}}) * 100 / (\rho_{\text{grain}} - \rho_{\text{fluid}}),$$

where  $\Phi$  is porosity (in %),  $\rho_{\text{grain}}$  is density of the grains (taken 2.65 g/cm<sup>3</sup> for sand and 2.7 g/cm<sup>3</sup> for shales),  $\rho_{\text{bulk}}$  is the bulk density as determined from density logs, and  $\rho_{\text{fluid}}$  is the density of the pore fluid (taken 1.1 g/cm<sup>3</sup>). Results for the boreholes in block 15/9 with suitable logs (density log available, few cavings) are shown in Table 6.1.

The porosities determined by three different methods show a considerable spread, ranging from 27 % to 41 %. The highest values are from neutron density log data and may be overestimations, since no shale corrections (accounting for the hydrogen in clay minerals) have been applied. The lowest values are from modal analysis, which we expected to provide rather too high values because the preparation procedure (including freezing of the sample and intrusion of the unfrozen, loose sample by epoxy) could have loosened the fabric and separated the grains from each other. On the other hand, modal analysis does not take microporosity account, which, however, we expect to be low due to the quartz-dominated, well sorted, well-rounded, and uncemented character of the samples.

We compared the resulting data with published compaction trends, i.e. porosity vs. depth curves. A problem with many of these curves is that they are based on data from hydrocarbon-production intervals, which are usually at considerable depth (often > 1500m). These data are then extrapolated to shallower depths where, however, non-

linear compaction processes may act. Brueckmann (1989) and Huang & Gradstein (1990) investigated data from shallower depths, and their results are listed along with those of Sclater & Christie (1980) in Table 6.2.

*Table 6.1 Mean porosity values for Utsira Sand and intra-Utsira clay layers determined from wire-line log neutron density data. The density values (in g/cm<sup>3</sup>) for the clay layers are the mean of the tips of the shale peaks. No shale correction was applied, and the calculated porosities (in %) especially for the shales may, therefore, rather be upper bounds.*

Well	UTSIRA SD.		SHALES in UTSIRA	
	Bulk density	Porosity	Bulk density	Porosity
15/9-9	2.05	39	2.15	34
15/9-18	2.08	37	2.2	31
15/9-15	2.05	39	2.1	38
15/9-7	2.05	39	2.2	31
15/9-6	2.02	41	2.15	34
15/9-8	2.05	39	2.15	34
	Average:			34

*Table 6.2 Porosity values for sands at ca. 800 m depth according to published porosity-depth trends.*

Sclater & Christie 1980	39 %
Brueckmann 1989	30 % (sand), 44 % (silty sand)
Huang & Gradstein 1990	41 % (mean), range from 25 % to 55 %

As Table 6.2 shows, published data show an even larger spread of porosity values. We tend to favour higher values (35 % to 40 %) as reflecting the Utsira Sand porosity for the following reasons:

- (i) the sand is very friable, indicating that it is almost not consolidated. We would expect a substantial porosity reduction to be accompanied by consolidation.
- (ii) Microscopic inspection of the grains shows only minor indications for deformation or shape changes of the grains during compaction (Figure 6.1). The amount of compaction should accordingly be low.

Values in the range 35 % to 40 % may, therefore, be preferable for reservoir simulations aiming at a simulation of the present CO<sub>2</sub> distribution. However, risk assessments, e.g. determinations of maximum migration distances, should include a ‘worst case’ porosity estimate of ca. 30 %.

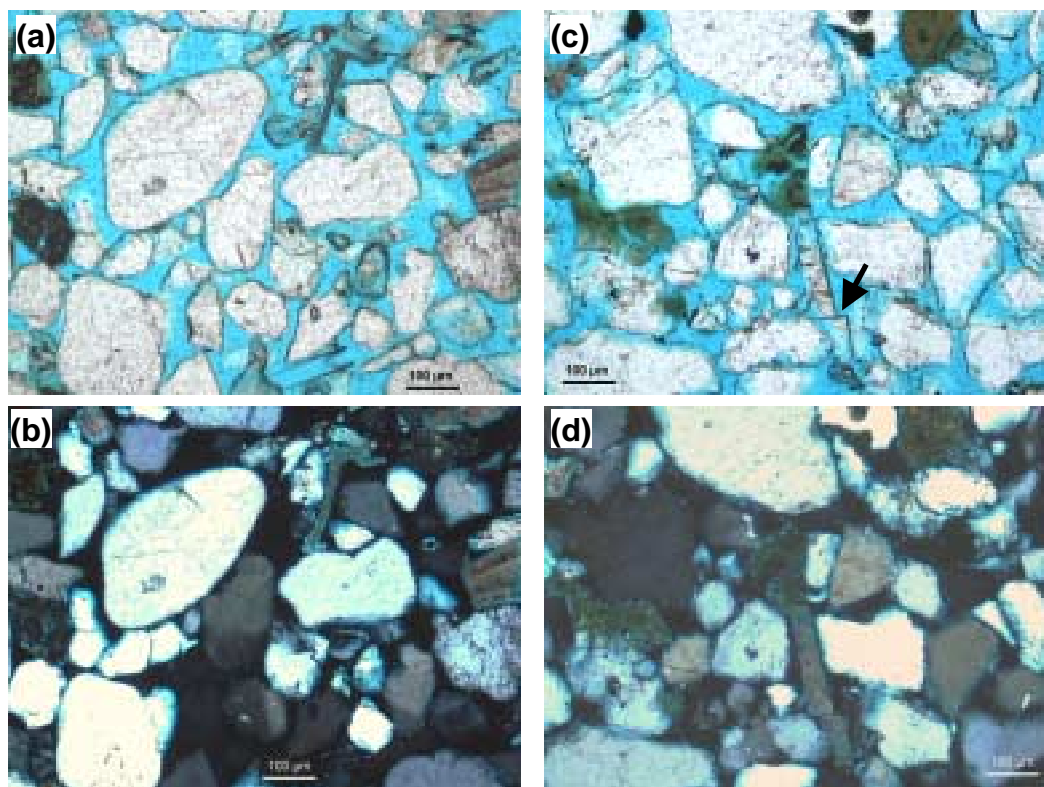


*Figure 6.1 Photomicrographs of samples from Utsira Sand in well 15/9-A23. (a) and (b) from 1080.04 m MD, (c) and (d) from 1080.70 m MD. (a) and (c) with parallel and (b) and (d) with crossed Nichols. Arrow in (b) points to broken mineral. Note scarcity of grain contacts and of fractures in grains. Quartz grains are only slightly undulous with crossed Nichols.*

### 6.1.2 Net/Gross ratio

The Net/Gross ratio is a rather loosely defined parameter. In a strict definition, it characterises the ratio between the thickness of potential reservoir rocks and the thickness of the whole reservoir unit. Defined such, the N/G ratio for the Utsira Sand (up to the base of the shale layer beneath the sand wedge) in the Sleipner area is in the order of 0.90 to 0.97 (Table 6.3). However, the gravity-driven CO<sub>2</sub> will probably mainly occupy the upper few metres of the Utsira Sand and/or the sand wedge. The N/G ratio for the whole Utsira Sand package is therefore of low importance in the present case. The uppermost interval of interest (up to ca. 15 m) does in many cases not contain shales at all, implying in many wells a N/G ratio of 1.0

*Table 6.3 Net/gross ratios for the Utsira Sand in the Sleipner area calculated from shale layer thicknesses ([Appendix 1](#)) in 5 selected wells. These values express only the ratio of sands to total unit thickness as evident from wire-line logs. They do not contain estimations of how much of the pore space will be swept.*

<b>Well</b>	<b>Summed shale thickness (m)</b>	<b>Total thickness of Utsira Sand (m)</b>	<b>Net/gross ratio</b>
15/9-8	15.70	255.00	0.94
15/9-9	7.62	236.48	0.97
15/9-13	14.48	184.95	0.92
15/9-15	25.30	244.54	0.90
15/9-18	10.68	239.98	0.96

## 6.2 Observations on seismic data

### 6.2.1 Amplitude anomalies within and at the top of the sand units

Scanning through seismic lines of cube ST98M11 showed that areas of locally elevated seismic amplitudes (positive and/or negative) are present within and at the top of the Utsira Sand and rarely at the top of the sand wedge. The areal distribution of these amplitude anomalies was mapped and each of the anomalies was inspected.

#### *Amplitude anomalies at the top of the Utsira Sand*

The map of the amplitude at the top Utsira Sand (Figure 6.2) shows that pronounced anomalies exist that are ca. 4 to 5 times as strong as the usual amplitude at top Utsira. They are of negative amplitude, i.e. the strength of the (negative) reflection at the contact shale-sand increased. This could be caused by the presence of gas in the pore space of the Utsira Sand. Amplitude anomalies occur only in the western half of the survey area, with a concentration in the northwestern corner (Figure 6.3).

All these anomalies are in topographic high positions: in domes and anticlines (Figure 6.4a). This would concur with an interpretation as gas accumulations. However, they are not always in the highest positions indicated by seismics. A cross section parallel to the large anomaly at the northern margin of the survey area (Figure 6.4b) shows that the anomaly covers only part of the anticline, and a south-westward continuation of the anomaly would be expected from the topography of the anticline. Similarly, a cross-section across this anomaly (Figure 6.4c) illustrates that relatively deep part of the anticline possess an anomaly whereas the shallower marginal parts in the east and west have regular amplitudes. The anomaly close to the centre of the survey (Figure 6.4d) exhibits two 'wings' within the lower part of the Nordland Shale. They might indicate the migration of gas into the lowermost parts of the cap rock.

*Figure 6.2 ON NEXT PAGE: Seismic amplitude anomalies at the top Utsira Sand. Comparison with Figure 5.12 shows that most of them are at the tops of domes and anticlines. White line on left figure indicates location of Figure 6.4d. White rectangle on left figure corresponds to area of Figure 6.3. Grey outline on right figure shows margin of maximum extent of modelled CO<sub>2</sub> migration below top Utsira and thick grey line corresponds to predicted migration pathway if more than 20 Million tons CO<sub>2</sub> would be injected; stippled outline shows margin of trapped CO<sub>2</sub> when migrating within the sand wedge (Zweigel et al. 2000a).*

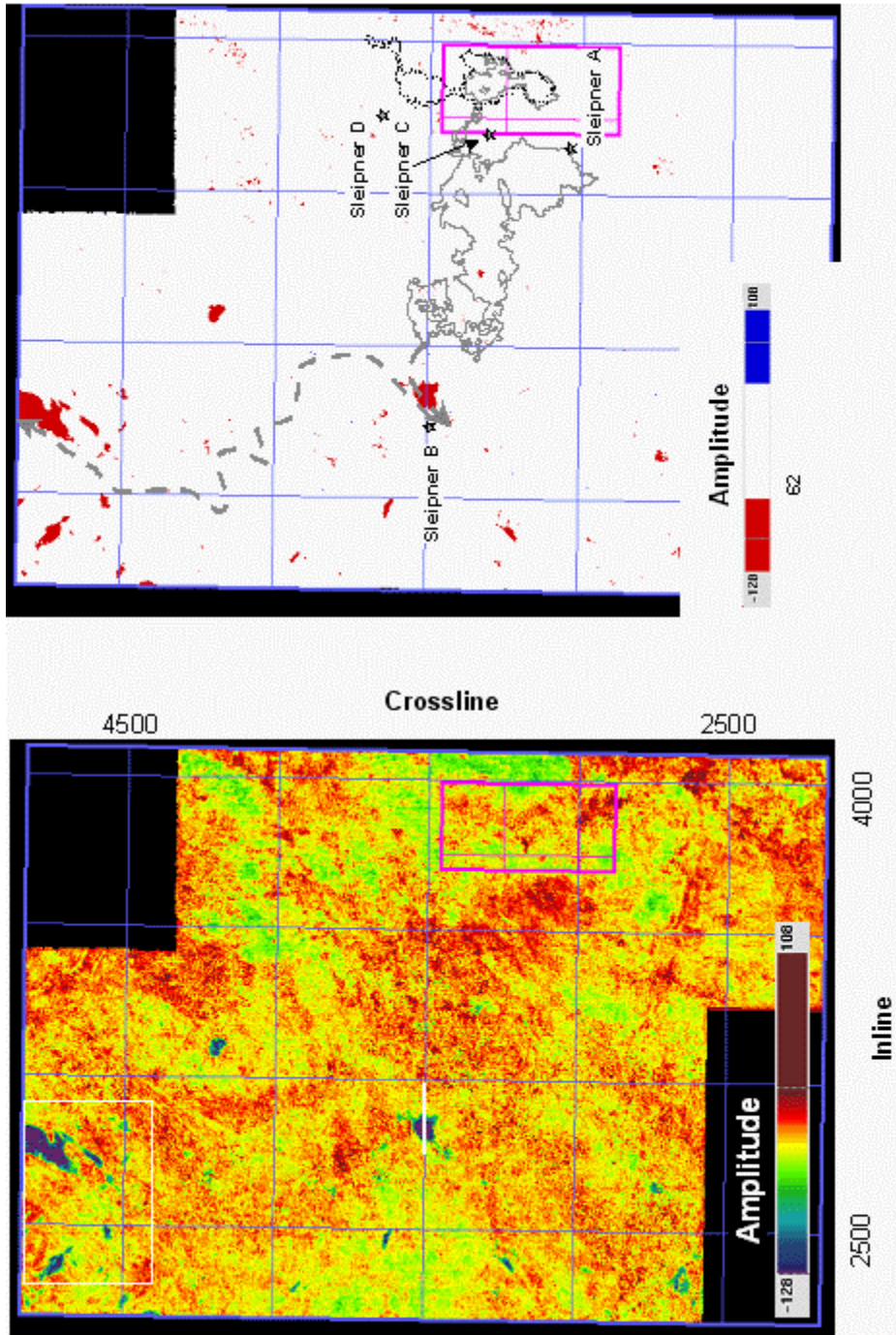


Figure 6.1 Figure caption on previous page.

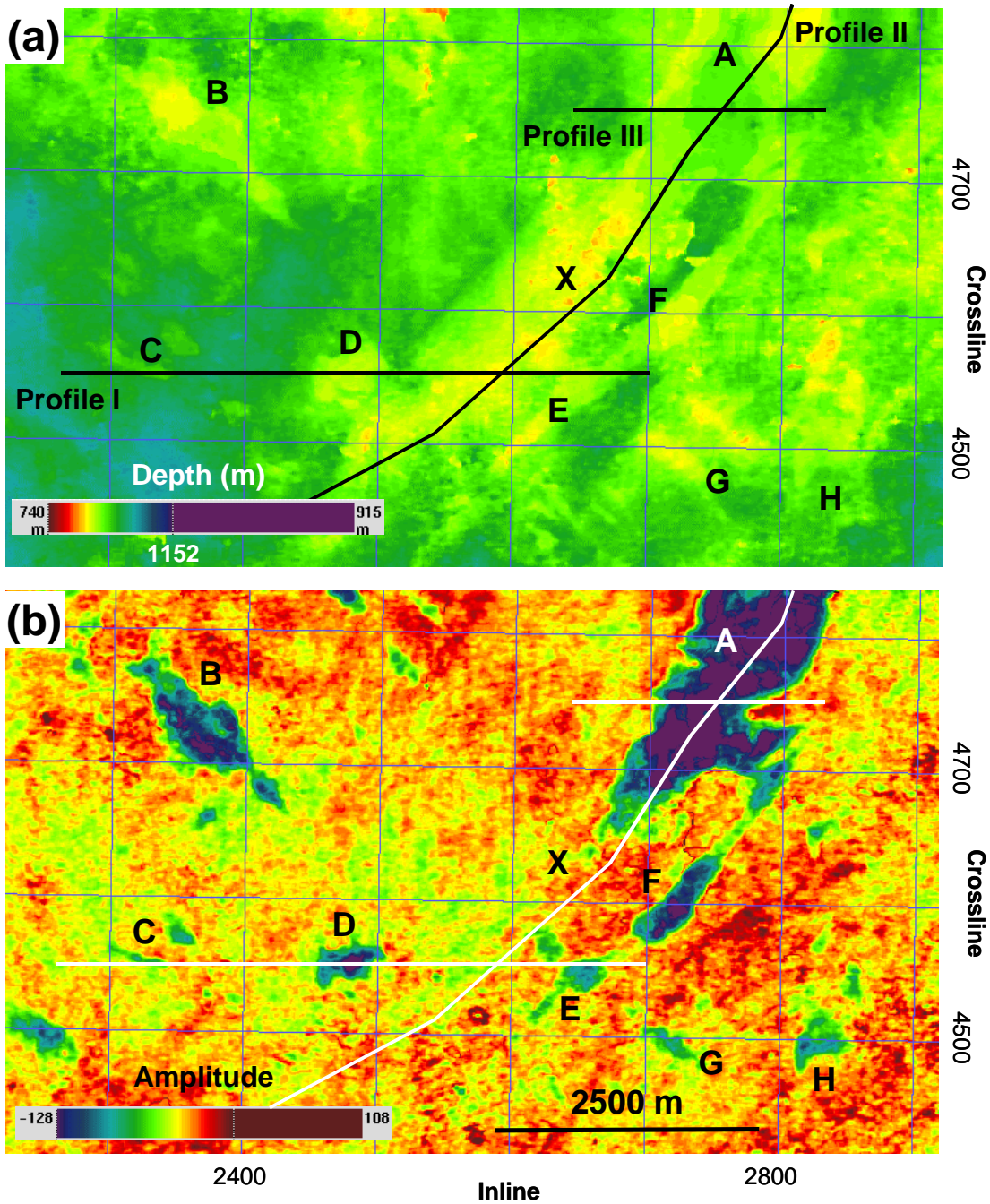


Figure 6.3 Detailed maps of the northwestern part of the study area, illustrating the relationship between (a) top Utsira Sand topography and (b) seismic amplitude anomalies at this level. Letters denote individual anomalies. Note that no anomaly corresponds to the major anticline at 'X'. Profile I, II, and III: Figure 6.4a, Figure 6.4b, and Figure 6.4c, respectively.

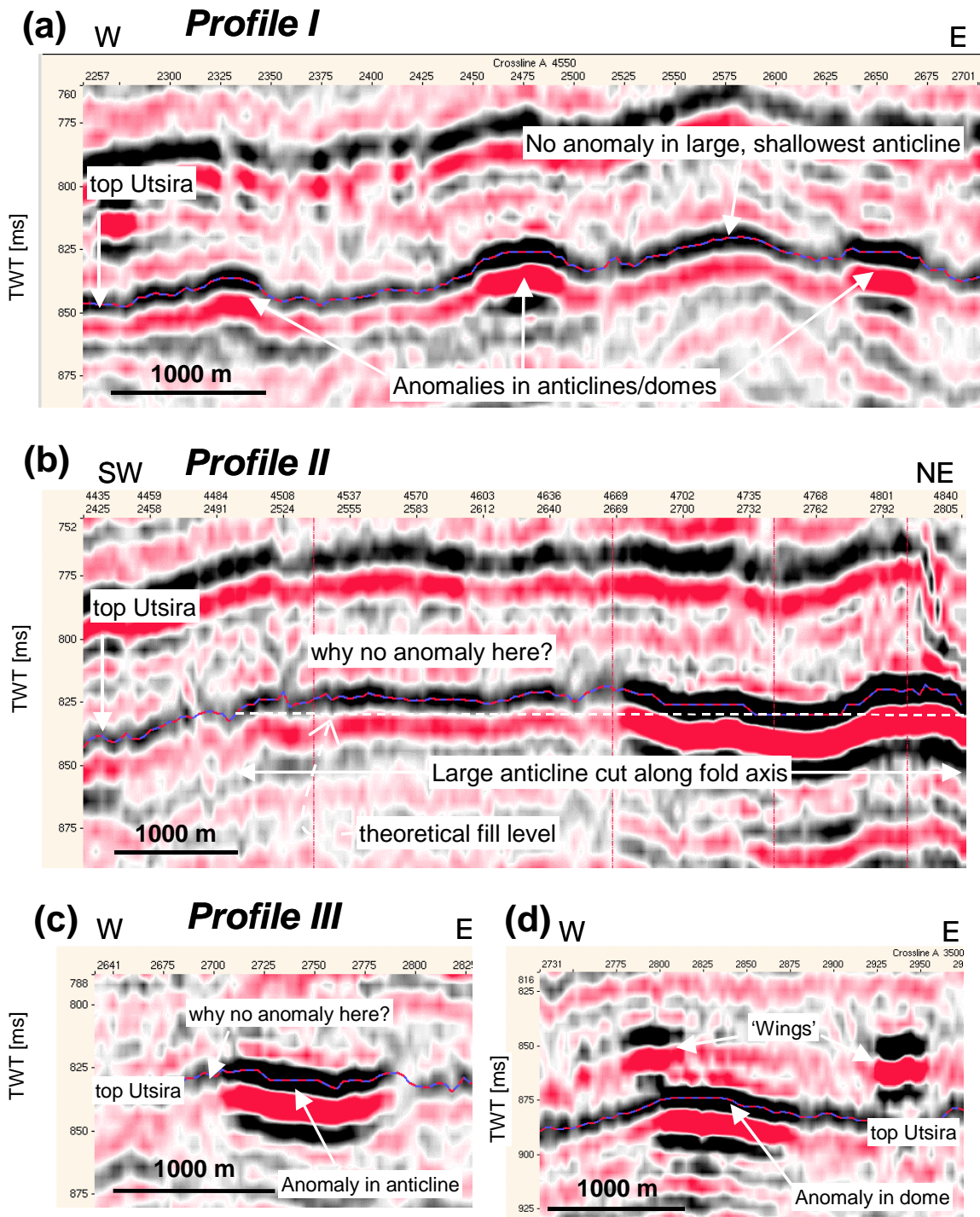
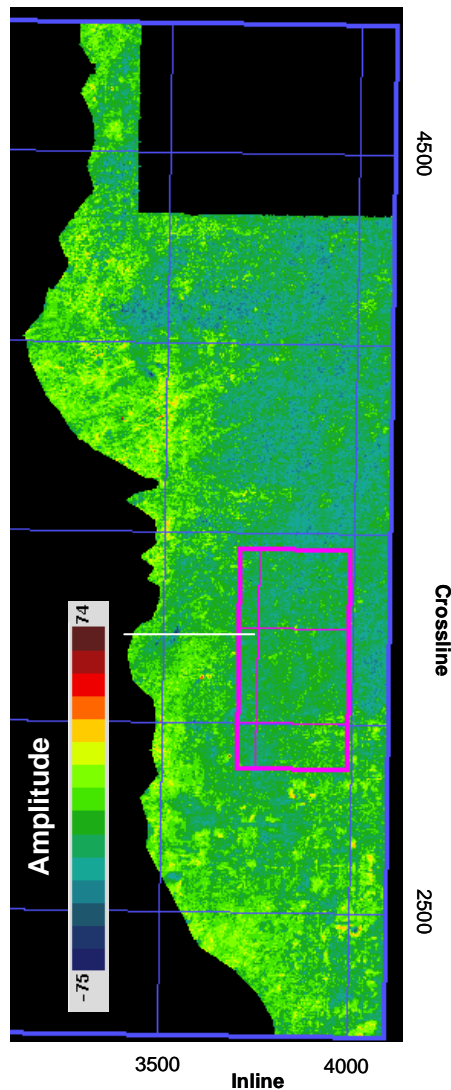


Figure 6.4 Profiles through seismic amplitude anomalies at top Utsira Sand level. Position of profiles: see Figure and Figure 6.3.

*Amplitude anomalies at the top of the sand wedge*

The top of the sand wedge (and the volume of the sand wedge) exhibits only slight amplitude anomalies (Figure 6.5). Positive amplitude values in the western part are probably negative interference effects (see Appendix B in Zweigel et al. 2000); where the sand wedge is very thin, the reflections from the top and the base cancel each other. One strong negative anomaly is present close to the western tipline of the sand wedge (Figure 6.6). This anomaly might correspond to a local gas accumulation.



*Figure 6.5 Amplitude at the top sand wedge. Note that positive amplitude values in the west are probably due to negative interference effects where the sand wedge tapers out. White line: position of Figure 6.6.*

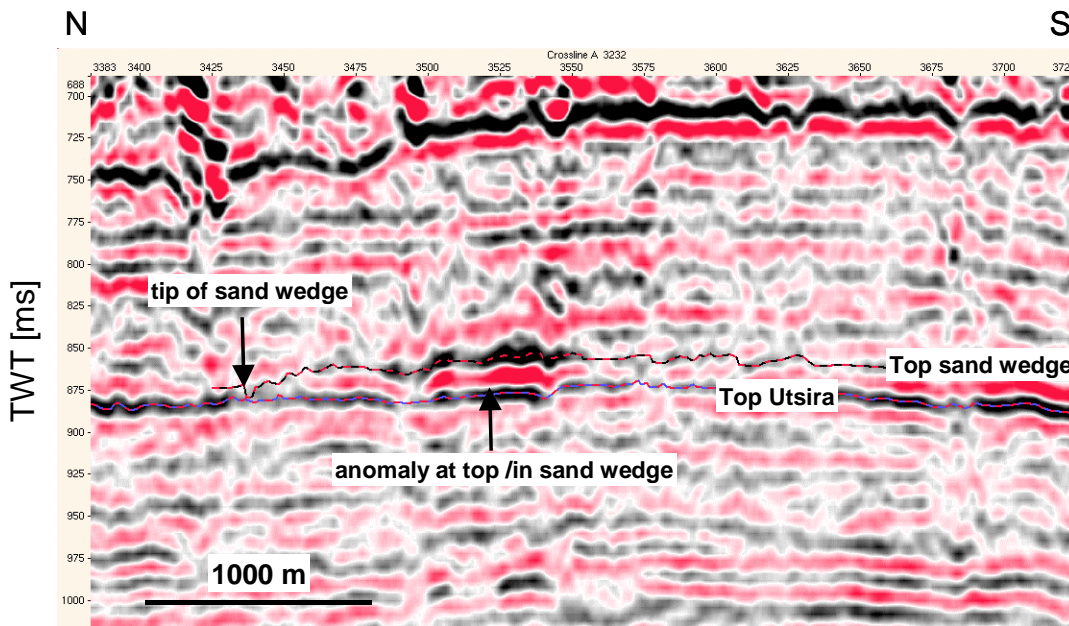


Figure 6.6 The single, strong amplitude anomaly at top sand wedge in cross section. Crossline 3232, position: see Figure 6.5

#### Amplitude anomalies within the Utsira Sand

Numerous localised amplitude anomalies are present in the Utsira Sand (Figure 6.7). Each of them has been inspected and is described in [Appendix 2](#). Many of the mapped anomalies seem to be multiples of anomalies higher up (Figure 6.8a), e.g. at the top Utsira (see above), or within the lower Pliocene (Zweigel 2000). All the others are linked to mud edifices underneath or directly besides (example see Figure 6.8, full documentation in [Appendix 2](#)). There is no clear structural preference of the anomalies, i.e. they do not preferentially occur in structural highs - rather the contrary, since intra-Utsira reflectors are often in structurally low positions above mud edifices. So far, the reason(s) for the existence of the anomalies are not known. Possibly, tuning effects due to thin, localised shale layers associated with the mud edifices might be one of the reasons.

Figure 6.7 On NEXT PAGE: Average amplitude magnitude in Utsira Sand (see [Appendix 2](#) for details). Grey outline on right figure shows margin of maximum extent of modelled CO<sub>2</sub> migration below top Utsira and thick grey line corresponds to predicted migration pathway if more than 20 Million tons CO<sub>2</sub> would be injected; stippled outline shows margin of trapped CO<sub>2</sub> when migrating within the sand wedge (Zweigel et al. 2000a). Numbers refer to anomalies presented in [Appendix 2](#).

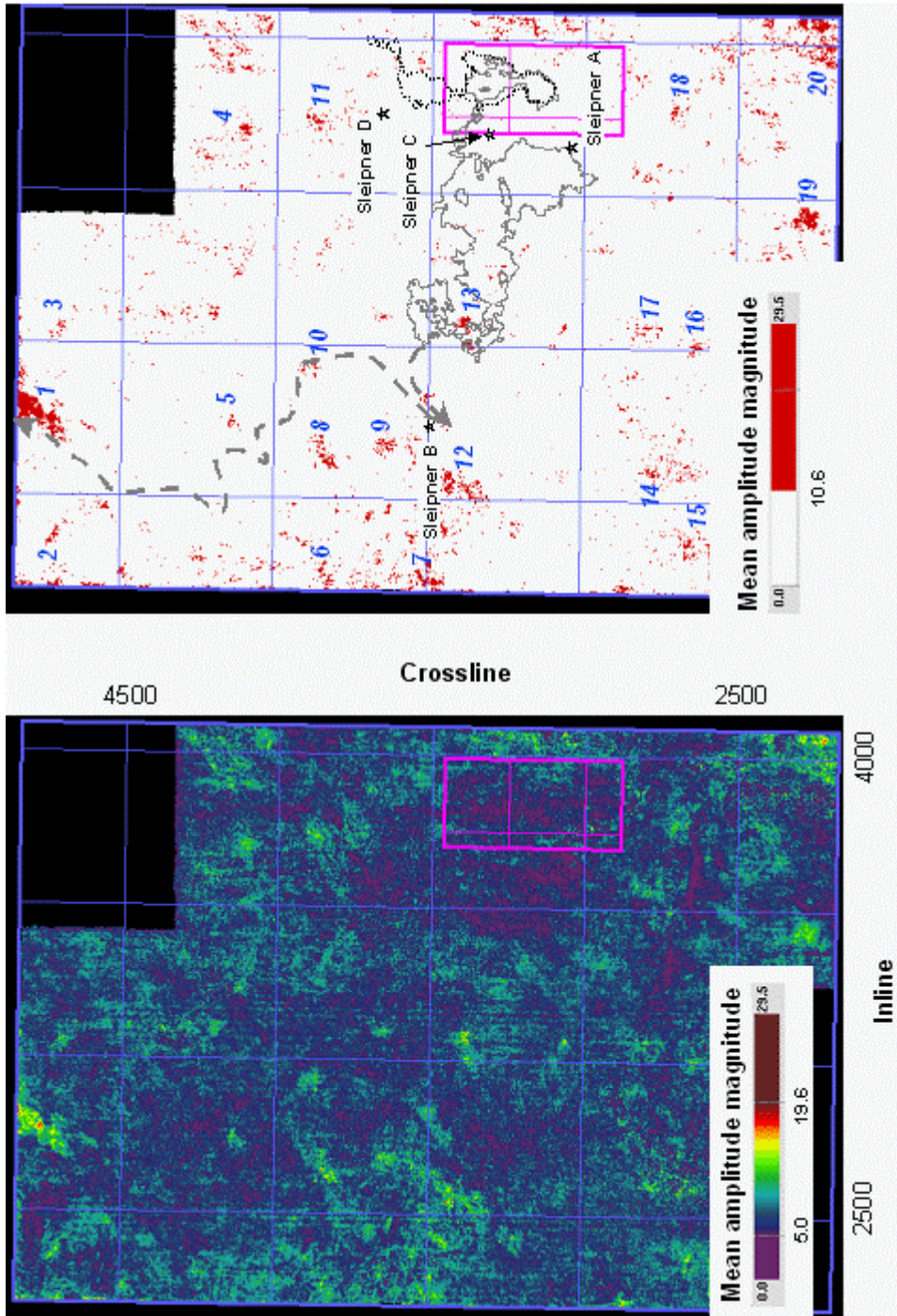


Figure 6.6 Figure caption on previous page.

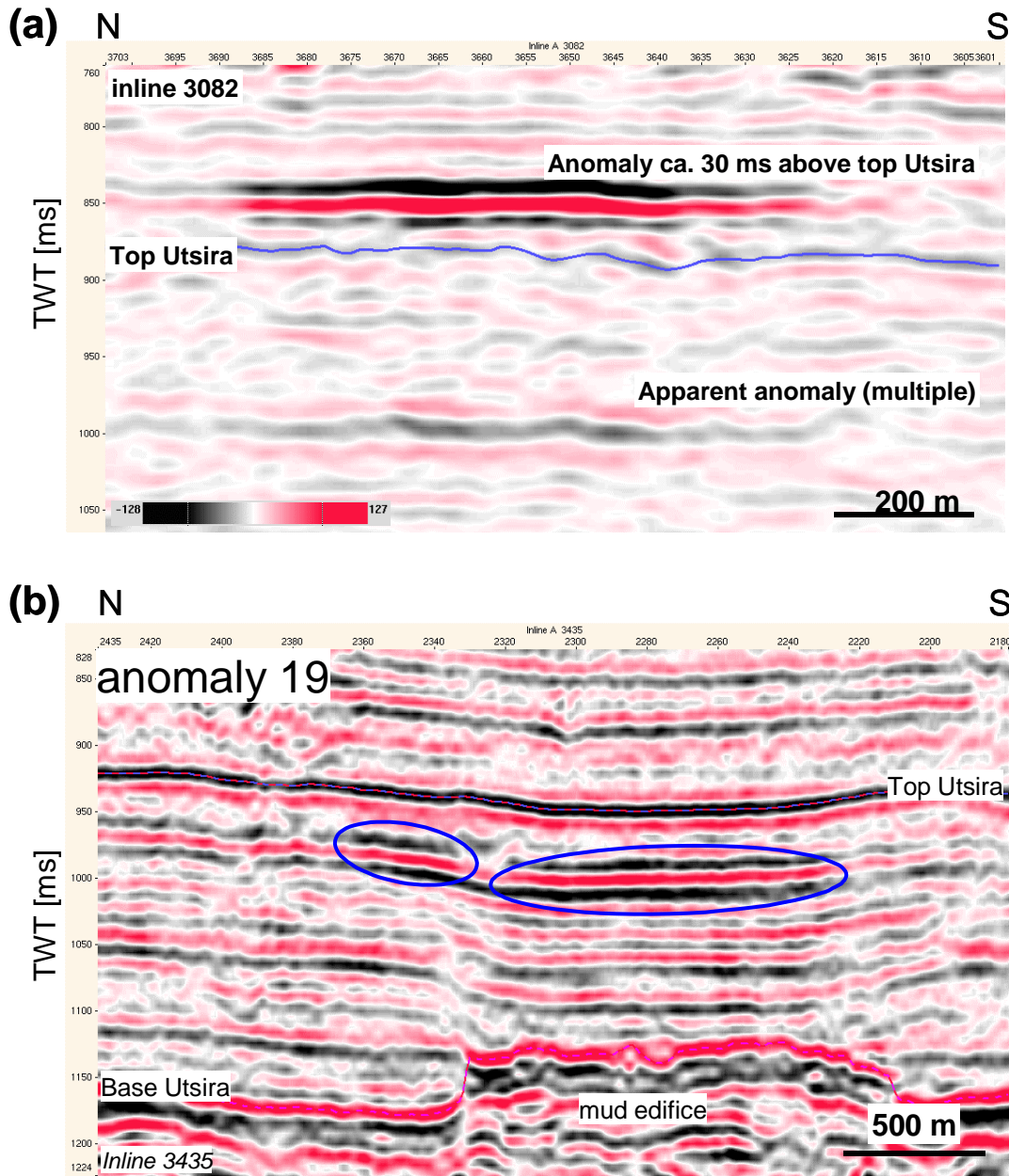


Figure 6.8 Representative examples for amplitude anomalies in the Utsira Sand. (a) Artificial anomaly caused by a multiple of a real anomaly in the Nordland Shales. (b) Real anomalies spatially linked to a mud edifice underneath.

### 6.2.2 Sand wedge heterogeneity

The sand wedge in the lower part of the Nordland Shale (Figure 5.19) contains narrow, elongate, sinuous features that are visible mainly in the thickness map (Figure 5.24d, Figure 6.9). They correspond to a locally thicker sand unit (Figure 6.10). These features were difficult to observe on TWT and depth maps of the top sand wedge because the topography caused by subsidence anomalies is much stronger than the local thickness difference of the channel-shaped features.

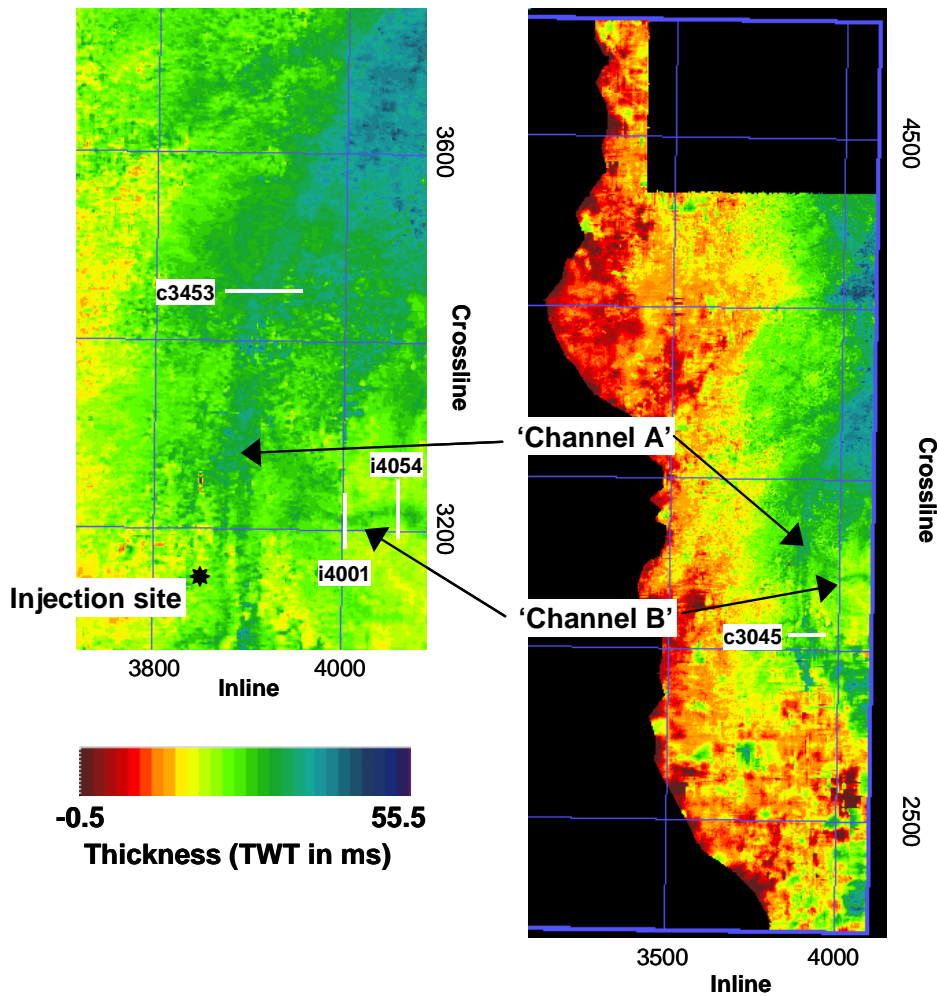


Figure 6.9 Thickness (in ms TWT) of the sand wedge in the lower part of the Nordland Shale. Thickness calculated by subtracting 5 ms (corresponding to thickness of shale layer beneath sand wedge) from difference between depth to top Utsira and depth to top sand wedge. Map on left side shows area with channel structures enlarged. White lines are positions of seismic sections shown in Figure 6.10.

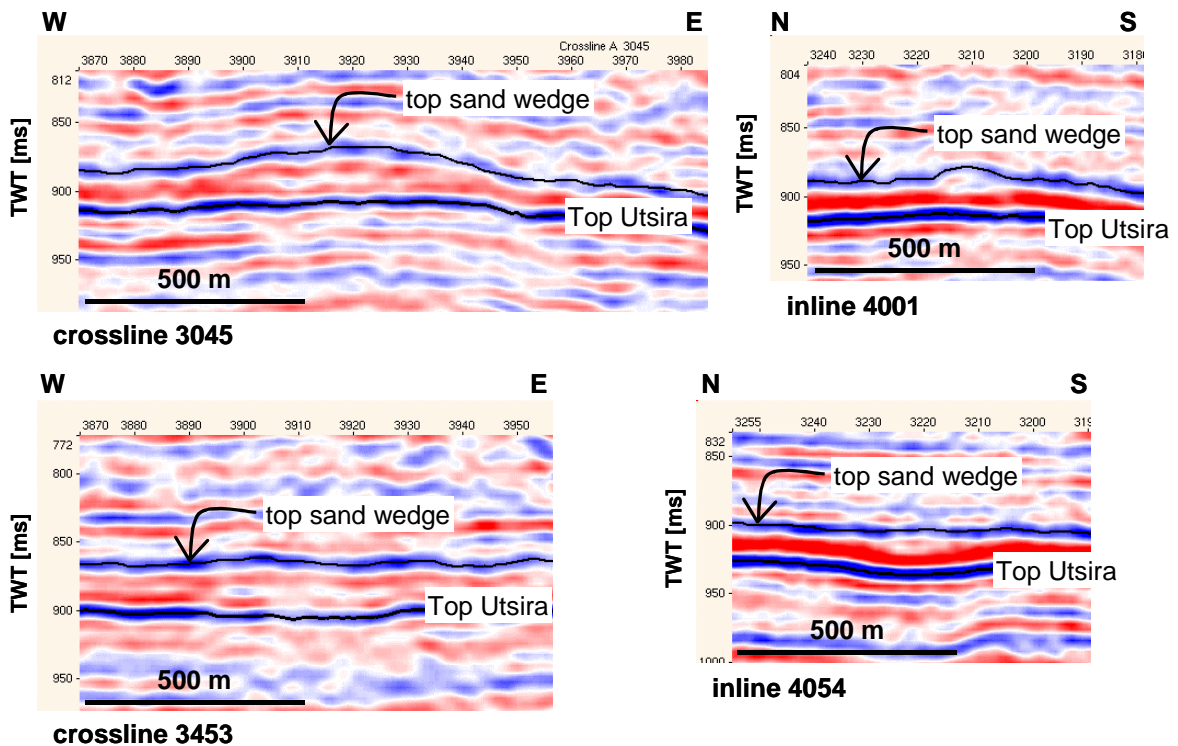


Figure 6.10 Seismic sections showing channels in the sand wedge. Positions: see Figure 6.9

The detailed cross-section geometry of the sinuous features is not resolved on seismic sections in survey ST98M11. We interpret them, however, due to their shape in map view and because they are thicker as the surrounding, as channels. In some sections, they correspond to a deeper base of the sand wedge (e.g. crossline 3453 and inline 4054 in Figure 6.10) in others to an elevated top (other examples in Figure 6.10). Especially the elevated tops do not imply that the channels were positive topographic features during deposition, but may rather be a result of subsequent compaction, during which the sands became less reduced in thickness than the adjacent shales (compare e.g. with the case in the Alba Field, Mattingly & Bretthauer 1992).

The channels pass now over topographic highs of both, the top sand wedge and the top Utsira Sand (Figure 6.11). If they really are channels, they can not have crossed ‘hills’ during their activity. This implies that a considerable part of present day structuring of the top Utsira and top sand wedge is post-depositional (compare this with the localised deposition above mud edifices). If channel B (Figure 6.11) is a tributary channel to channel A, as it looks now, the topography during its activity must have differed from the present day topography, otherwise it would apparently have flown upward.

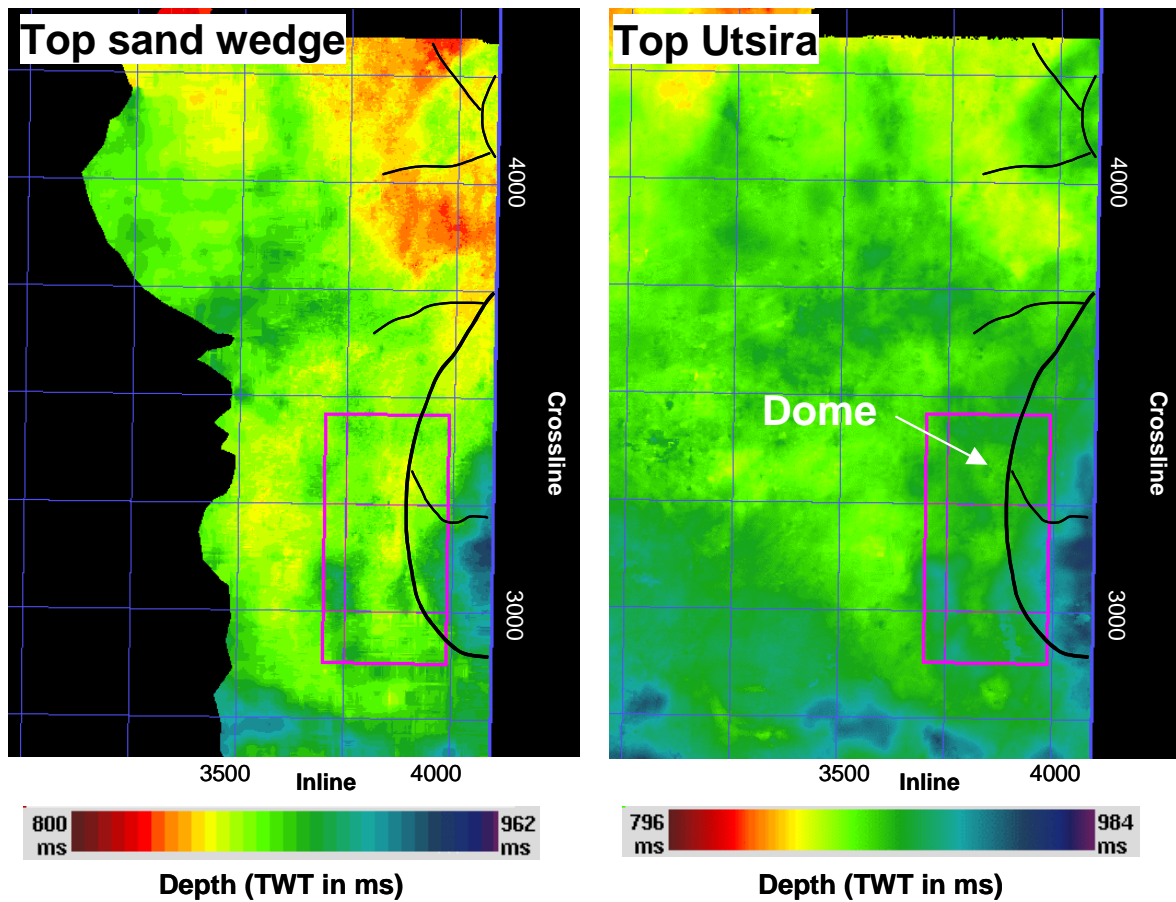


Figure 6.11 Relationship of channel-like features in the intra-Nordland shale sand wedge to the topography of the top Utsira Sand and of the top sand wedge. Note that the ‘channels’ seem not to follow present topographic depressions of these horizons, and potential flow along the ‘channels’ may have occurred up-dip the present horizon topography. This might indicate either that the features are no channels or that the present topography has been created after deposition of the sand wedge.

## 7. Discussion

### 7.1 Available storage volume

The total volume of the Utsira Sand in the survey area is  $148.5 \text{ km}^3$ , which corresponds to a total pore volume of  $44.55 \text{ km}^3$  taking a porosity of 30%. Calculations presented in Chapter 5.2 yielded a storage volume in traps at the top Utsira Sand of  $0.135 \text{ km}^3$  for the area of survey ST98M11. This means that if all existing traps in the survey area would be filled to spill point, only 0.3 % of the available pore space in the whole Utsira Sand would be occupied. However, a significant proportion (ca. 1/3) of the trap pore volume is present as small, localised traps (Figure 5.18) that will not be reached when injecting through a small number of wells.

Note that the calculated proportion values will not change when the mean porosity value is changed because the porosity is used as a factor both in total pore volume and trap pore volume calculation. A change in the sweep efficiency value (0.85 was used here for the trap pore volume; see Chapter 7.2) will, however, affect the percentages.

Previously carried out migration modelling for the Sleipner CO<sub>2</sub> injection case predicted a main migration path from the dome above the injection site into the adjacent dome to the north, then through the western outlet of the northern dome towards west into the large dome, afterwards filling of a complex array of domes and anticlines, and finally migration northwards from the western end of the array until the northern margin of the seismic survey (Figure 7.1; Zweigel et al. 2000a). The calculated storage volume of all traps reached on this path would amount to ca.  $0.05 \text{ km}^3$ , i.e. this path corresponds to ca. 37 % of the theoretically available storage volume contained in traps in the area of the investigated 3D survey (Figure 5.18a) and to ca. 0.11% of the total pore volume in the survey area.

The total trap pore space volume in the survey area for the combined cases of migration and storage beneath top Utsira and top sand wedge and injection at the present injection site amounts to ca.  $0.058 \text{ km}^3$  (Zweigel et al. 2000a). The combined total pore volume in the Utsira Sand and the sand wedge is approx.  $45.9 \text{ km}^3$  (at 30 % porosity), i.e. ca. 0.12 % of the total pore volume will be used.

The ongoing Sleipner injection project intends to inject ca. 20 Mill. metric tons (i.e. ca.  $0.03 \text{ km}^3$ ) CO<sub>2</sub> into the Utsira Sand; this corresponds to ca. 22 % of the available storage volume in traps within the studied area. Some of the theoretically available volume is represented by small traps, some of which might even be seismic interpretation artefacts. There exist, however, some large trap structures, especially in the south and south-west of Sleipner A, that might be used for CO<sub>2</sub> storage in the future. The drainage area map (Figure 5.18b) indicates that these traps would ultimately spill into the same trap system that will probably be filled by the ongoing injection, and they would, thus, ultimately spill towards north. A quantification of the volume of these additional individual traps and a simulation of the probable spill pattern has not been carried out here but should be done prior to using these structures for storage.

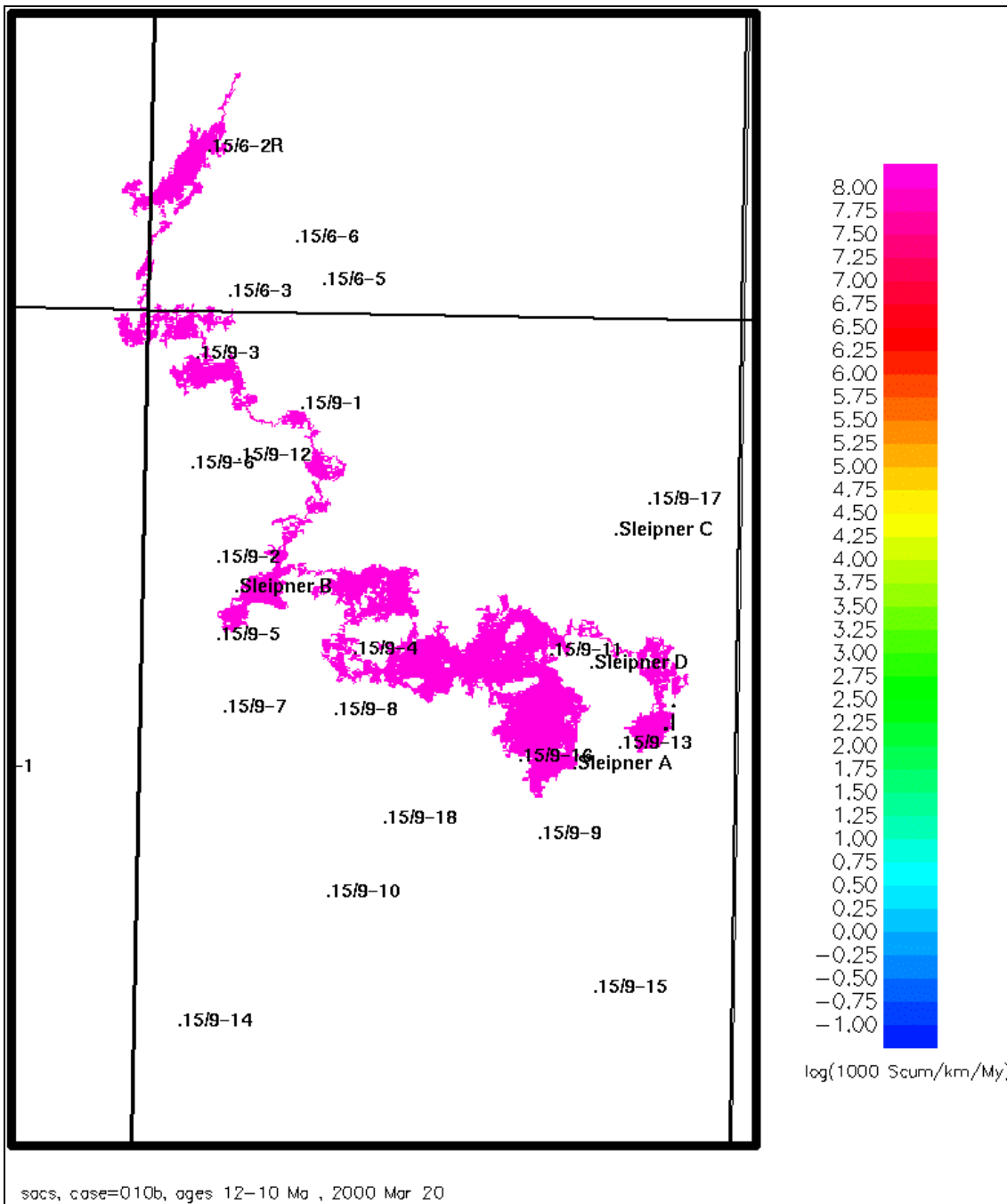


Figure 7.1 Spill path of injected CO<sub>2</sub> from the present injection site. The total storage volume along this spill path is more than 50 Mill. m<sup>3</sup>. Case U-4 (extended) of Zweigel et al. (2000a).

The determined percentage values for that proportion of the aquifer pore space which is contained within traps (0.3%) or which can be reached by an optimally placed well as in the present Sleipner injection case (up to 0.12 %), are similar to the mean value (3% trapped volume \* 4% sweep efficiency = 0.12%) assumed in Holloway et al. (1996) for calculation of the storage potential when storage in traps would be required. It is,

however, much lower than previously published estimates for the storage efficiency of saline aquifers in general. Holloway et al. (1996) assume proportions between 2 % and 6% (based on simulation results of Van der Meer, 1995) when estimating the storage capacity in the case that no traps would be required. The area of survey ST98M11 is in a relatively flat part of the top Utsira (in many other areas it has considerable regional dip, see e.g. Chadwick et al. 2000), far from potential spill points at the lateral margins of the depositional area of the Utsira Sand, and in an area where local structuring of the top into anticlines and domes is relatively strong (providing abundance of traps and relatively large trap heights).

On the other hand, storage efficiency as calculated here, depends mainly on the ratio between trap volume (strongly dependent on trap height) and reservoir thickness. Since reservoir thickness of the Utsira Sand is lower in most areas outside the studied area (Chadwick et al. 2000), storage efficiency may be higher there.

Given the presence of plausible causes for both, lower and higher storage efficiency outside the studied area, whose effects may cancel each other, we rate the low storage efficiency values determined here as a representative estimate. Our results do, therefore, confirm the estimated total storage volume in traps for the case of the Utsira Sand (Holloway et al. 1996).

## 7.2 Sweep efficiency

A major parameter of interest for reservoir simulations is drainage efficiency, i.e. how much of the pore space (porosity) in the CO<sub>2</sub>-accumulation zone will become occupied by CO<sub>2</sub>, and how much will still contain formation water. The drainage efficiency depends on the microscopic scale on the local CO<sub>2</sub>-saturation level (saturation efficiency) and on the larger scale on the flow pattern of CO<sub>2</sub> in response to material inhomogeneity (sweep efficiency).

Capillary pressure experiments (Lindeberg et al. 2000a) show that only a small fraction of water (< 5%) will remain in the pores in the main, upper parts of CO<sub>2</sub> accumulations. There will, however, be a transition zone of approx. 5 m thickness at the base of these accumulations, in which CO<sub>2</sub> saturation increases from 0 to > 95% (E. Lindeberg, pers. comm.). The mean saturation efficiency for the CO<sub>2</sub> column at a point will, therefore, vary depending on the thickness of the accumulation: thin accumulations will be dominated by the transition zone and will have low mean saturation efficiency, whereas thicker accumulations will have high saturation efficiency. This implies that the topography of barrier horizons plays a key role to define the saturation efficiency (and consequently the available space for CO<sub>2</sub>) of the trap underneath.

Traps with relatively flat tops will have a lower storage volume (due to lower mean saturation efficiency) than traps with steeper tops, even though both traps might contain the same pore volume. The sensitivity of storage volume on reservoir top topography will be especially strong in the case of relatively flat traps (as in the Utsira case), where large parts of the trap pore space are in the saturation transition zone.

Sweep efficiency, on the other hand, depends largely on the distribution of permeability within a reservoir unit (e.g., Tchelepi and Orr 1994). This is especially the case when a strong viscosity contrast exists between the two pore-filling fluids (as for CO<sub>2</sub> and water), which will cause viscous fingering (Homsy 1987). High-permeable volumes (e.g. coarse-grained channel fill) will then be swept preferentially, leaving low permeable volumes (e.g. silty parts) undrained. A quantitative assessment of the sweep efficiency in the Sleipner case is not yet possible.

Wire-line logs of the Utsira Sand (Figure 5.2) show relatively little variability in reservoir properties of the sands themselves. This may signify little heterogeneity and therefore high sweep efficiency. On the other hand, the sand wedge exhibits features that might be indicative for a channel (Figure 6.9 and Figure 6.10), which could be associated with considerable heterogeneity of lithology and reservoir parameters. Similar features may exist in the Utsira Sand where they are much more difficult to observe. Detection of such potential features in the Utsira Sand would require extensive and detailed mapping of intra-Utsira reflectors, which was not possible within the frame of the present project.

Seismic amplitude anomalies at the top Utsira Sand are usually at trap structures (Figure 6.2, Figure 6.3, and Figure 6.4). However, they are in several cases not in the topographically highest position of the structures which may - if the anomalies are due to the presence of gas - imply heterogeneity of the Utsira Sand. This heterogeneity would favour gas accumulation in certain parts of the area, whereas others would not be invaded and/or would have a much lower gas saturation. Given this interpretation, an inhomogeneous migration and distribution of CO<sub>2</sub> could be expected, too. However, the reflector topography in TWT needs not necessarily to represent the real topography of the top Utsira at depth at an accuracy precise enough to allow structural interpretation at a resolution of ca. +/- 5 m, as demanded here.

### 7.3 Seal efficacy

If the seismic amplitude anomalies at the top Utsira Sand (Figure 6.2) and at the top sand wedge (Figure 6.5) correspond to gas accumulations, these gas accumulations are very restricted in occurrence. The depth map of the top Utsira (Figure 5.12) exhibits several large domal and anticlinal structures that constitute potential traps (Figure 5.18). Assuming upward migration of gas (and/or oil) since the Pliocene, e.g. due to leakage from the Sleipner East and Sleipner West reservoirs beneath, accumulations of gas (and/or oil) would be expected in the trap structures (similarly for the top sand wedge). Such accumulations are indicated by seismics only for a few minor traps, and they are not known from drilling reports.

This lack of abundant gas accumulations in Utsira Sand and sand wedge traps may indicate the absence of upward gas migration at present and possibly during the last few million years. This interpretation is, however, in contrast to the presence of potentially gas-related amplitude anomalies (Zweigel 2000) and related gas-shows in the overburden of the Sleipner CO<sub>2</sub> reservoir system. If the gas in the overburden were of

thermogenic origin, the lack of gas at the top Utsira would imply a lack of adequate storage capability of the seal-reservoir couple Nordland Shale above Utsira Sand/sand wedge. This topic will be further analyzed in a forthcoming report covering the Nordland Shale.

## 8. Outlook/ Open questions

Work on the reservoir geology of the CO<sub>2</sub> storage system in the Sleipner area has already improved our understanding. These improvements are evident when considering successful predictions based on the updated geological model, as., e.g., the seismic monitoring feasibility study (Lindeberg et al. 1999) or reservoir simulations that predicted the CO<sub>2</sub> distribution within the Utsira Sand (Lindeberg et al. 2000a and 2000b). Further, the geological model was used as input for reservoir simulations aiming to ‘mimic’ the pattern observed in time-lapse seismics (Lindeberg et al. 2000b, Van der Meer et al. 2000).

A number of questions, however, remain open; the answers to some of which may have considerable impact on our ability to correctly predict the future fate of injected CO<sub>2</sub>.

- How important is reservoir heterogeneity? Given the lack of suitable direct information (no outcrop, scarce core samples), the answer may be based on predictions drawing on the choice of a depositional model/environment. Then, analogue examples may be consulted and the effects of reservoir heterogeneity may be estimated by geostatistical modelling or depositional modelling.
- The extent of the sand wedge towards east and the existence of potential migration pathways out of the sand wedge could not be assessed. Hopefully, ongoing work within the regional part of the SACS Reservoir Geology Task will provide further information about this part of the reservoir system.
- Will the cap rock be able to retain the CO<sub>2</sub> within the Utsira Sand and the sand wedge? A further evaluation of this question will be the topic of a separate report addressing a number of cap-rock related topics. Conclusions seem, though, to require analyses of cap rock samples.

This report documents the main results of the SACS activities aiming directly at an understanding of the reservoir. Ongoing work on the regional scale and on interpretation of the time-lapse seismic data will, however, most likely provide further data characterising the reservoir. These results should then be used to update simulations of the behaviour and distribution of CO<sub>2</sub> in the underground.

## 9. Quoted references

- Arts, R., 2000: SACS Internal report, Note on the seismic data. NITG-TNO report NITG 00-237-B, 15 pp., restricted. ([www-link](#))
- Arts, R.J.; Zweigel, P.; & Lothe, A.E. 2000: Reservoir geology of the Utsira Sand in the Southern Viking Graben area – a site for potential CO<sub>2</sub> storage.-62<sup>nd</sup> EAGE 2000 conference, Glasgow, B-20, 4p. ([www-link](#))
- Baklid, A.; Korbøl, R.; & Owren, G. 1996: Sleipner Vest CO<sub>2</sub> disposal, CO<sub>2</sub> injection into a shallow underground aquifer. Paper presented on the 1996 SPE Annual technical Conference and Exhibition, Denver, Colorado, USA, SPE paper 36600, 1-9.
- Brueckmann, W., 1989: Typische Kompaktionsabläufe mariner Sedimente und ihre Modifikation in einem rezenten Akkretionskeil (Barbados Ridge). Tuebinger Geowissenschaftliche Abhandlungen, A5, 1-135.
- Cartwright, J.A. & Lonergan, L., 1996: Volumetric contraction during the compaction of mudrocks: a mechanism for the development of regional-scale polygonal fault systems. *Basin Research*, 8, 183-193.
- Chadwick, R.A., Holloway, S., Kirby, G.A., Gregersen, U., & Johannessen, P.N. 2000: The Utsira Sand, Central North Sea - An assessment of its potential for regional CO<sub>2</sub> disposal. 5<sup>th</sup> International Conference on Greenhouse Gas Control Technologies, Cairns (Australia), August 2000. ([www-link](#))
- Davies, R., Cartwright, J., & Rana, J., 1999: Giant hummocks in deep-water marine sediments: Evidence for large-scale differential compaction and density inversion during early burial. *Geology*, 27, 907-910.
- Deegan, C.E. & Scull, B.J. 1977: A standard lithostratigraphic nomenclature for the Central and Northern North Sea, Report 77/25, 1, Institute of Geological Science, London, Oljedirektoratet, Stavanger.
- Eidvin, T., Riis, F. and Rundberg, Y., 1999: Upper Cainozoic stratigraphy in the central North Sea (Ekofisk and Sleipner fields). *Norsk Geologisk Tidsskrift*, 79, 97-128.
- Gregersen, U.; Michelsen, O.; & Sørensen, J.C. 1997: Stratigraphy and facies distribution of the Utsira Formation and the Pliocene sequences in the northern North Sea. *Marine and Petroleum Geology*, 14, 893-914.
- Gregersen, U.; Johannessen, P.N.; Møller, J.J.; Kristensen, L.; Christensen, N.P.; Holloway, S.; Chadwick, A.; Kirby, G.; Lindeberg, E.; & Zweigel, P. 1998: Saline Aquifer CO<sub>2</sub> Storage S.A.C.S Phase Zero 1998. Internal report. GEUS (DK), BGS (UK), IKU (N).
- Heggland, R. 1997: Detection of gas migration from a deep source by use of exploration 3D seismic data. *Marine Geology* 137, 41-47.
- Holloway, S.; Arts, R.; Chadwick, R.A.; Gregersen, U.; Johannessen, P.N.; Kirby, G.A.; Kristensen, L.; Lothe, A.E.; Pearce, J.M.; & Zweigel, P. 2000: Saline Aquifer CO<sub>2</sub> Storage. Final report. Work Area 1 – Geology. British Geological Survey Report WH/2000/21C. 28 p. Confidential. ([www-link](#))
- Homsy, G.M., 1987: Viscous fingering in porous media. *Annual Reviews of Fluid Mechanics*, 19, 271ff.
- Huang, Z. & Gradstein, F.M., 1990: Depth-porosity relationship from deep sea sediments. *Scientific Drilling*, 1, 157-162.
- Isaksen, D. & Tonstad, K. 1989: A revised Cretaceous and Tertiary lithostratigraphic nomenclature for the Norwegian North Sea, NPD Bulletin 5, Oljedirektoratet, Stavanger.

- Jordt, H. Faleide, J.I.; & Bjørlykke, K. 1996: 3-D seismic mapping of Neogene sedimentation and clay diapirism in block 35/8 northern North Sea, in: Jordt, H.: The Cenozoic geological evolution of the central and northern North Sea based on seismic sequence stratigraphy, PhD thesis, University of Oslo.
- Lindeberg, E. & Wessel-Berg, D., 1997: Vertical convection in an aquifer column under a gas cap of CO<sub>2</sub>. *Energy Convers. Mgmt.*, 38, Suppl., S229-S234.
- Lindeberg, E.; Causse, E.; & Ghaderi, A. 1999: Evaluation of to what extent CO<sub>2</sub> accumulations in the Utsira formations are possible to quantify by seismic by August 1999. SINTEF Petroleum Research report 54.5148.00/01/99, 13p. Restricted. ([www-link](#))
- Lindeberg, E.; van der Meer, B.; Moen, A.; Wessel-Berg, D.; & Ghaderi, A. 2000a: Saline Aquifer CO<sub>2</sub> Storage (SACS): Final report Task 2: Fluid and core properties and reservoir simulation. Confidential report, 43pp. ([www-link](#))
- Lindeberg, E., Zweigel, P., Bergmo, P., Ghaderi, A., & Lothe, A. 2000b: Prediction of CO<sub>2</sub> dispersal pattern improved by geology and reservoir simulation and verified by time lapse seismic. 5<sup>th</sup> International Conference on Greenhouse Gas Control Technologies, Cairns (Australia), August 2000. ([www-link](#))
- Lothe, A.E. & Zweigel, P., 1999: Saline Aquifer CO<sub>2</sub> Storage (SACS). Informal annual report 1999 of SINTEF Petroleum Research's results in work area 1 'Reservoir Geology'. SINTEF Petroleum Research report 23.4300.00/03/99, 54 p. Restricted. ([www-link](#))
- Løseth, H., Wensaas, L., Gading, M. & Vik, E., 1999a: Vertical migration as a driving mechanism for mud diapirism in the Hordaland Group. In: I.J.Martinsen & T.Dreyer (eds); *Sedimentary Environments offshore Norway; Palaeozoic to Recent*. Extended abstracts. Norwegian Petroleum Society/NPF, 227- 230.
- Mattingly, G.A. & Bretthauer, H.H., 1992: The Alba field; a middle Eocene deep water channel system in the UK North Sea. In Halbouty, M. T. (Ed.): *Giant oil and gas fields of the decade 1878-1988*, AAPG Memoir, 54, 78-88.
- Odonne, F., Ménard, I., Massonat, G.J., & Rolando, J.-P. 1999: Abnormal reverse faulting above a depleting reservoir. *Geology*, 27, 111-114.
- Rundberg, Y. & Nystuen, J.P., 1999: Large scale slumping, sliding and soft sediment deformation of Oligocene strata in the Northern North Sea and Møre Basin; A giant collapse in response to tectonic uplift. *Norsk Geologisk Forening Vintermøte 1999*, Stavanger, Abstract Volume (Geonytt), 88-89.
- Rundberg, Y. & Smalley, P.C., 1989: High Resolution Dating of Cenozoic Sediments from Northern North Sea Using <sup>87</sup>Sr/<sup>86</sup>Sr Stratigraphy. *American Association of Petroleum Geologists Bulletin*, 73, 298-308.
- Sclater & Christie (1980)
- Tchelepi, H.A. & Orr, F.M., Jr., 1994: Interaction of viscous fingering, permeability heterogeneity, and gravity segregation in three dimensions. *Soc. Pet. Eng. Res Eng.*, 9(4), 266-271.
- Van der Meer, L.G.H., 1995:
- Van der Meer, L.G.H., Arts, R.A., & Paterson, L., 2000: Prediction of migration of CO<sub>2</sub> after injection in a saline aquifer: reservoir history matching of a 4D seismic image with a compositional gas/water model. 5<sup>th</sup> International Conference on Greenhouse Gas Control Technologies, Cairns (Australia), August 2000.
- Zweigel, P. 2000: Seismic anomaly maps. File on internal SACS project web pages. [http://www.iku.sintef.no/projects/IK23430000/internal/other\\_reports/Seismic\\_anomaly\\_maps\\_\(SINTEF\\_Nov00\).pdf](http://www.iku.sintef.no/projects/IK23430000/internal/other_reports/Seismic_anomaly_maps_(SINTEF_Nov00).pdf)

Zweigel, P., Hamborg, M., Arts, R., Lothe, A., Sylta, Ø., & Tømmerås, 2000: Simulation of migration of injected CO<sub>2</sub> in the Sleipner case by means of a secondary migration modelling tool – A contribution to the Saline Aquifer CO<sub>2</sub> Storage project (SACS). SINTEF Petroleum Research report (CD) 23.4285.00/01/00, 63 p., 6 app., confidential. ([www-link](#))

Zweigel, P., Hamborg, M., Arts, R., Lothe A., & Tømmerås, A. 2000: Prediction of migration of CO<sub>2</sub> injected into an underground depository: Reservoir geology and migration modelling in the Sleipner case (North Sea). 5<sup>th</sup> International Conference on Greenhouse Gas Control Technologies, Cairns (Australia), August 2000. ([www-link](#))

## Appendix 1 Determination of intra-Utsira shale layer thicknesses

The thickness of shale layers within the Utsira Sands has been determined for five representative wells. The determination is based on gamma-ray wire-line logs because these logs portray the shales best. However, since each data-point of the log corresponds to a combined effect of rock properties within a certain radius from the logging tool, a definition of the base and top of the shale layers is not straightforward. A common approach is, to use the extremes of the first derivative of the gamma ray versus depth as an indication for the margin of the shale layer ([Figure A1-1](#)).

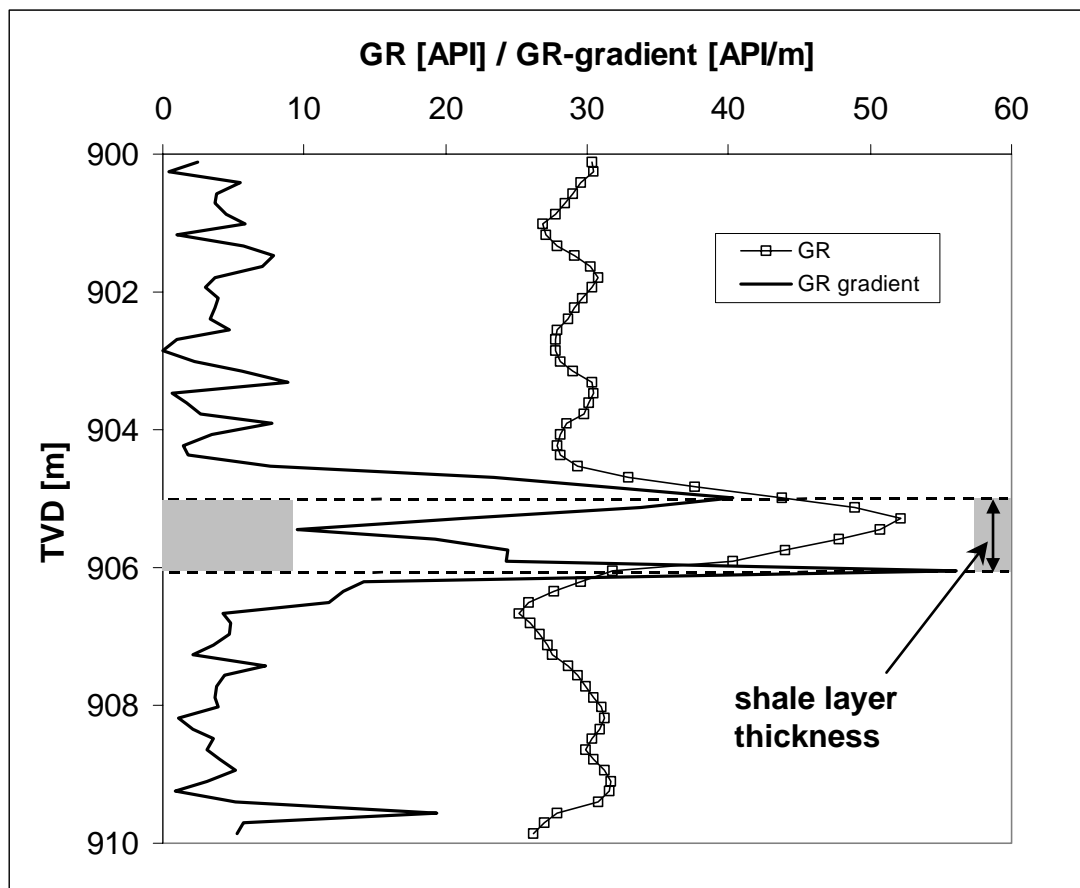


Figure A1-1 Part of gamma-ray (GR) log in well 15/9-18, illustrating procedure of definition of top and base of intra-Utsira shale layers.

Since the gamma ray values always represent a ‘mean’ of a moving window, thin shale layers with thicknesses close to the radius sampled by the GR tool (usually ca. 30 cm) may have a reduced effect on GR measurements and, thus, be associated with reduced gamma ray values. We checked this by plotting determined layer thicknesses against GR maximum values of the GR peaks ([Figure A1-2a](#)). The baseline, i.e. the GR values outside the shale peaks, showed some variation. We calculated therefore an ‘effective gamma ray value’, subtracting the baseline from the shale peaks. Layer thicknesses plotted against effective GR values are shown in [Figure A1-2b](#). The plots show that no

systematic relationship between the determined thickness of shale layers and their maximum gamma ray values exists.

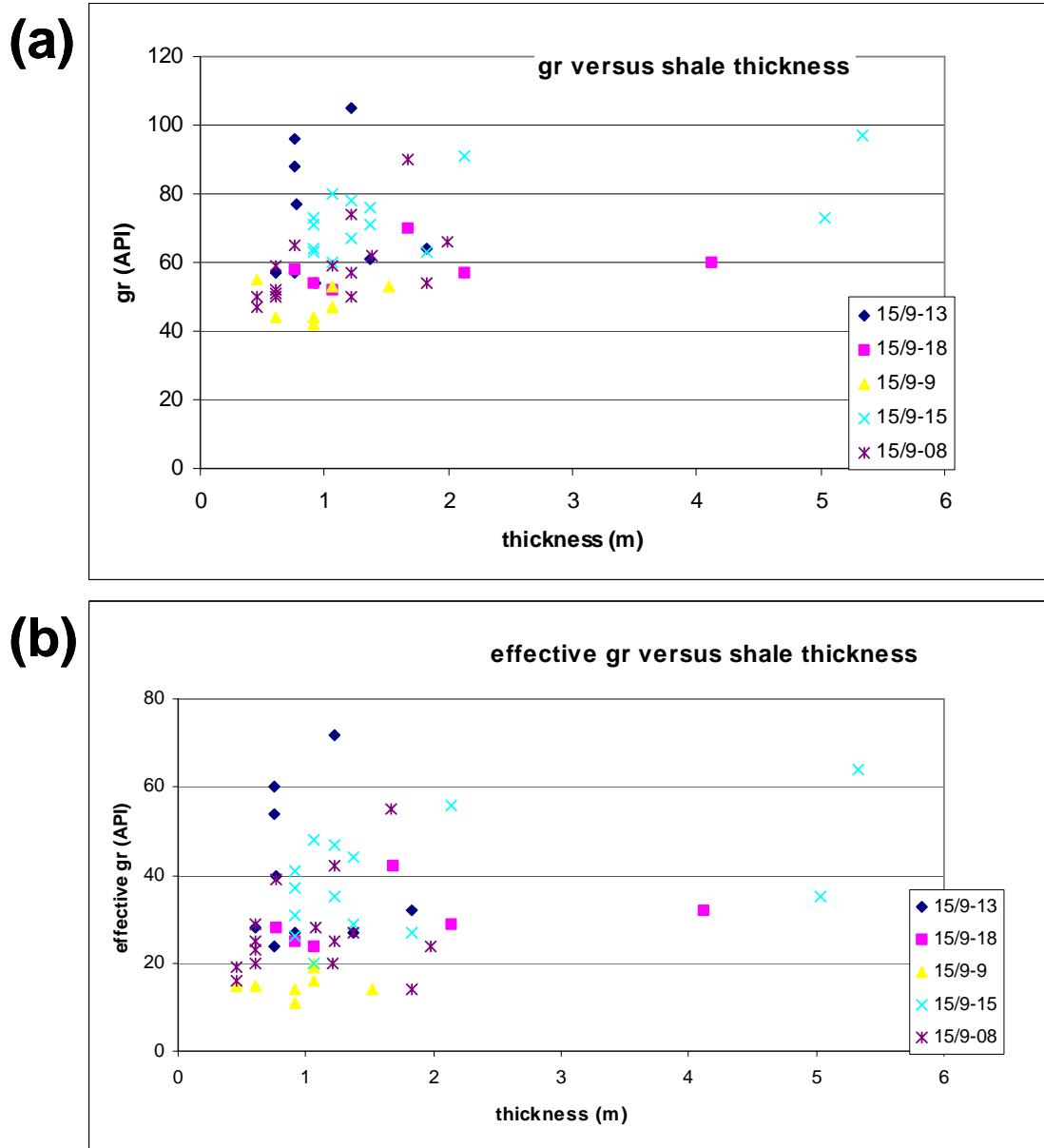


Figure A1-2 (a) Maximum gamma-ray values and (b) maximum effective gamma-ray values at shale peaks within the Utsira Sand plotted vs. determined shale layer thickness.

## Appendix 2      Amplitude anomalies in the Utsira Sand

The average amplitude magnitude of the Utsira Sand interval was calculated by summing absolute values of amplitudes from 30 ms below the Top Utsira to 10 ms above the base Utsira, and dividing the sum by the thickness (in number of samples). The upper 30 ms of the Utsira Sand were excluded because they are dominated by amplitude variations at the Top Utsira (potentially shallow gas accumulations at the top). The lower 10 ms were excluded because they are affected by the strength of the Base Utsira reflector which may rather reflect lateral acoustic property changes in the underlying shales.

The average amplitude magnitude of this interval is shown in Figure 6.7. Major anomalies are marked and numbered on the map, and these anomalies are explained in [Table A2-1](#). Examples of anomalies are shown in Figure 6.8. Those anomalies which we do not interpret as artefacts, are shown in [Figure A2-1](#).

*Table A2-1      Major amplitude anomalies in the interval between 30 ms below Top Utsira and 10 ms above Base Utsira. Numbers refer to [Figure A2-1](#).*

<b>Nr.</b>	<b>Description</b>
1	Multiple of anomaly at Top Utsira
2	Multiple of anomaly at Top Utsira
3	Multiple of anomaly in lower Pliocene
4	Anomaly exists above, at Top Utsira. TWT-distance is approx. 55ms --> multiple??
5	Multiple of anomaly in lower Pliocene
6	Above mud edifice. Amplitudes of upper anomaly are not higher than at many other places in Utsira. Possibly effect of reduced Utsira thickness above mud edifice.
7	At margin of mud edifice.
8	Multiple of anomaly in lower Pliocene
9	Multiple of anomaly in lower Pliocene
10	Multiple of anomaly in lower Pliocene
11	Above mud edifice.
12	Multiple of anomaly in lower Pliocene
13	Multiple of anomaly in lower Pliocene
14	Multiple of anomaly in lower Pliocene
15	Multiple of anomaly at Top Utsira
16	Above/at margin of mud edifice.
17	Above mud edifice.
18	At margin of, and partly above, mud edifice. Top Utsira and top sand wedge above --> may be multiple.
19	Above mud edifice. Strong anomaly.
20	Above mud edifice. Partly due to wrong base Utsira interpretation (too deep position of interpretation causes base Utsira reflector to be included in calculation of average amplitude strength).

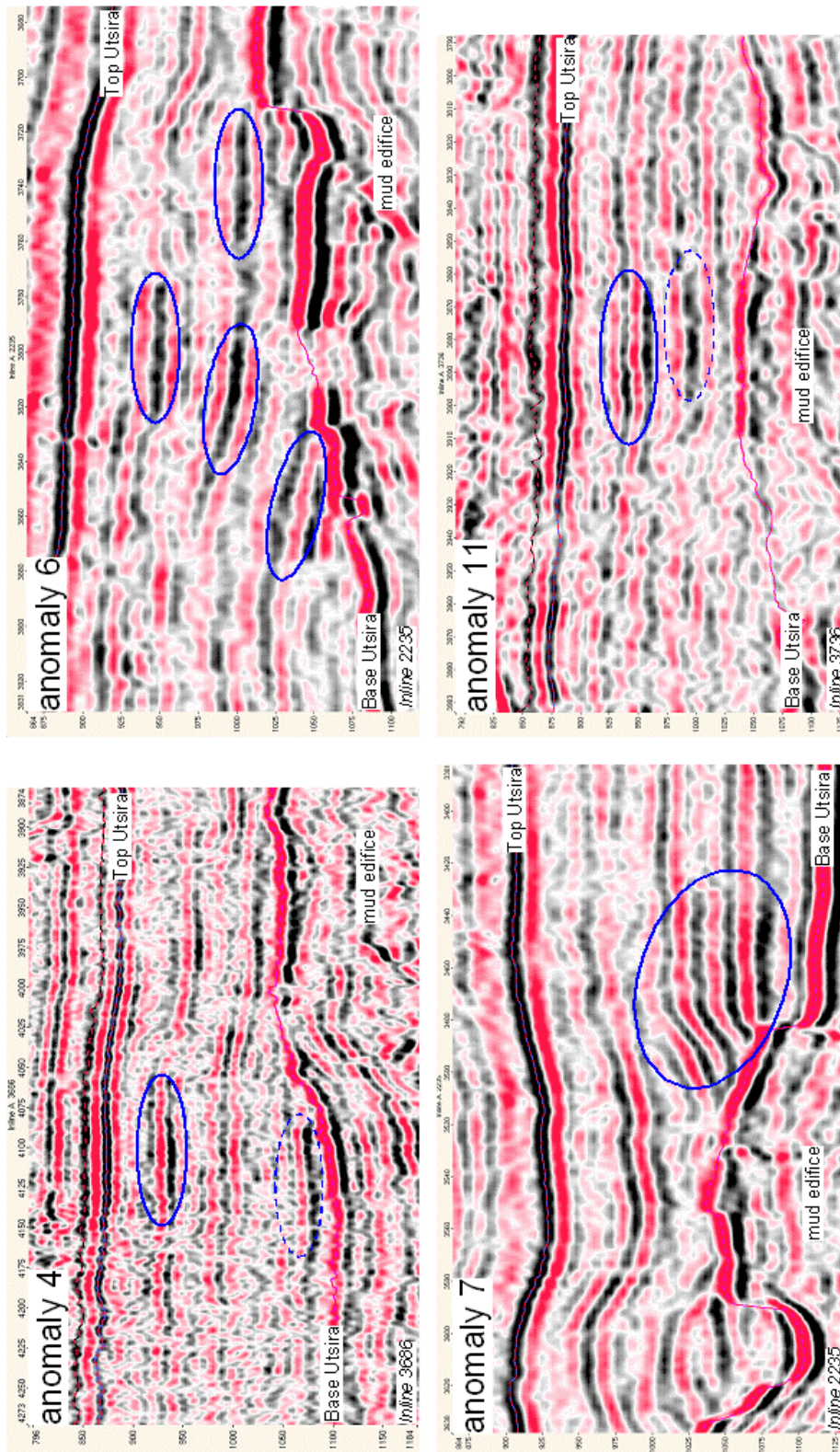


Figure A2-1 Seismic sections through amplitude anomalies within the Utsira Sand which were not interpreted as multiples of anomalies above.

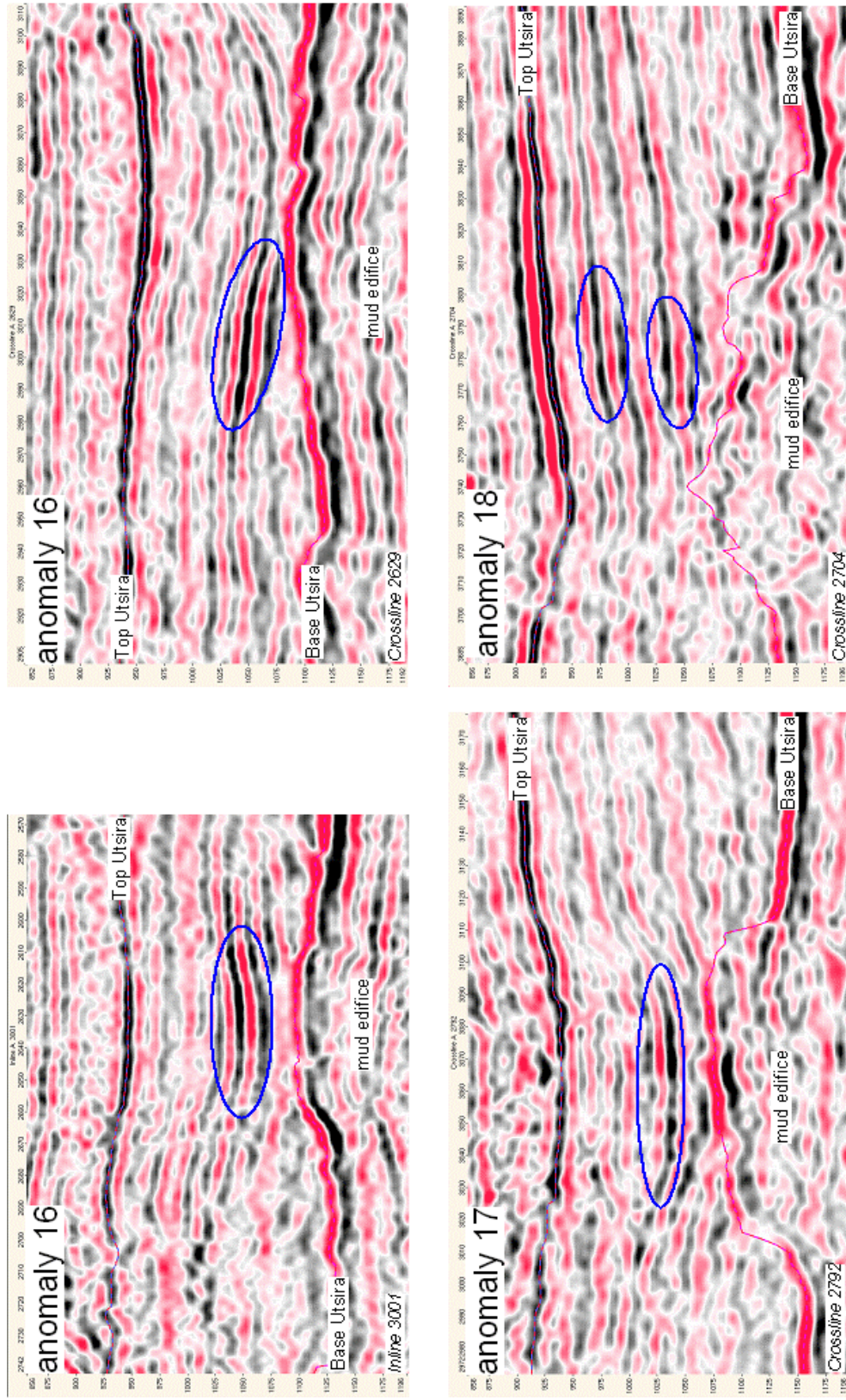


Figure A2-1 Continued.

### **Appendix 3            Horizon grids in 3D view**

This appendix contains 3D visualisations of the three key horizons interpreted.

Running of the visualisations requires installation of the free software GLView Express which can be downloaded from <http://www.ceetron.com/>

For viewing the horizons in 3D, start GLView Express and open the files

Top\_Sandwedge.vtf

Top\_Utsira.vtf

Base\_Utsira.vtf